A NEW METHOD FOR HISTORY MATCHING AND FORECASTING SHALE GAS/OIL RESERVOIR PRODUCTION PERFORMANCE WITH DUAL AND TRIPLE POROSITY MODELS

A Thesis

by

ORKHAN SAMANDARLI

Submitted to the Office of Graduate Studies of
Texas A&M University
in partial fulfillment of the requirements for the degree of

MASTER OF SCIENCE

August 2011

Major Subject: Petroleum Engineering

A NEW METHOD FOR HISTORY MATCHING AND FORECASTING SHALE GAS/OIL RESERVOIR PRODUCTION PERFORMANCE WITH DUAL AND TRIPLE POROSITY MODELS

A Thesis

by

ORKHAN SAMANDARLI

Submitted to the Office of Graduate Studies of
Texas A&M University
in partial fulfillment of the requirements for the degree of

MASTER OF SCIENCE

Approved by:

Co-Chairs of Committee,	Robert A. Wattenbarger
	Bryan Maggard
Committee Member,	Emil Straube
Head of Department,	Stephen A. Holditch

August 2011

Major Subject: Petroleum Engineering

ABSTRACT

A New Method for History Matching and Forecasting Shale Gas/Oil Reservoir Production Performance with Dual and Triple Porosity Models.

(August 2011)

Orkhan Samandarli, B.Sc., Middle East Technical University

Co-Chairs of Advisory Committee: Dr. Robert A. Wattenbarger
Dr. Bryan Maggard

Different methods have been proposed for history matching production of shale gas/oil wells which are drilled horizontally and usually hydraulically fractured with multiple stages. These methods are simulation, analytical models, and empirical equations. It has been well known that among the methods listed above, analytical models are more favorable in application to field data for two reasons. First, analytical solutions are faster than simulation, and second, they are more rigorous than empirical equations.

Production behavior of horizontally drilled shale gas/oil wells has never been completely matched with the models which are described in this thesis. For shale gas wells, correction due to adsorption is explained with derived equations. The algorithm which is used for history matching and forecasting is explained in detail with a computer program as an implementation of it that is written in Excel's VBA. As an objective of this research, robust method is presented with a computer program which is applied to field data.

The method presented in this thesis is applied to analyze the production performance of gas wells from Barnett, Woodford, and Fayetteville shales. It is shown that the method works well to understand reservoir description and predict future performance of shale gas wells. Moreover, synthetic shale oil well also was used to validate application of the method to oil wells.

Given the huge unconventional resource potential and increasing energy demand in the world, the method described in this thesis will be the “game changing” technology to understand the reservoir properties and make future predictions in short period of time.

DEDICATION

I dedicate my work to my parents, Yashar and Masuma, for their support and encouragement throughout my life, for raising me and helping me during my education. I also want to dedicate my work to my brother, Tural, for helping me all the time as an elder brother and for his good deeds toward me.

I also dedicate my work to my country, Azerbaijan, where the first oil well was drilled in the world.

ACKNOWLEDGEMENTS

All praises to Almighty Allah for his mercies and blessings that he gave over the years which made me stronger.

I want to acknowledge and express my sincere appreciation to my advisor, Dr. Robert A. Wattenbarger, for his guidance, ideas, and valuable contributions to this work. Dr. Wattenbarger spent endless hours with me, encouraging and guiding me during this research. Whatever I achieved in my Master of Science degree I owe to him. I was honored to work under his supervision. At this point, words are not enough to express my gratitude and appreciation to Dr. Wattenbarger.

I want to acknowledge my co-chair, Dr. Bryan Maggard and my committee member, Dr. Emil Straube for being on my advisory committee and the advice given on producing this thesis.

I want to acknowledge Dr. David Schechter for his encouragement and support during the first year of my Master of Science degree. He never hesitated to spend time with me to solve any type of problem that I encountered during my work.

I also want to acknowledge all professors and instructors, with department head, Dr. Steve Holditch, at the top of the list for valuable courses that are taught at Texas A&M University.

I also want to acknowledge my colleagues in the Reservoir Modeling Consortium: Hasan Al-Ahmadi, Hassan Hamam, Anas Almarzooq, Pahala Sinurat,

Salman Mengal, Haider Abdullal, Ammar Agnia, Wahaj Khan, Ahmad Alkouh, and Vartit Tivayanonda for their intellectual discussions and friendship.

TABLE OF CONTENTS

CHAPTER Page

CHAPTER Page

LIST OF FIGURES

FIGURE Page

FIGURE Page

FIGURE Page

FIGURE Page

FIGURE Page

LIST OF TABLES

CHAPTER I

INTRODUCTION

Production from shale gas reservoirs in US doubled from 1.2 Tscf to 3.1 Tscf from 2007 to 2009. According to Energy Information Administration, gas production coming from shale gas contributed to approximately 14% of gross production in United States. Now, with increase in oil price it is expected that same boom will occur in shale oil, too. This is not a surprise with current technology that industry employs; even ultra-low permeability rocks such as shales can serve as a source of fuel.

Shale gas/oil is considered to be one kind of unconventional resource. Unconventional shale deposits are difficult to characterize overall, but in general are lower in resource concentration, more dispersed over large areas, and require well stimulation or some other extraction or conversion technology. The shale acts as both the source and the reservoir for the fluid.

Interest in shale gas started with discovery of Barnett play where amount of resources in place was huge compared to conventional reservoirs. Wells were drilled vertically till early 2000's when first horizontal well was drilled in Barnett. With the increase of advance in hydraulic fracturing technology, production from shale attracted attention of many investors. Nowadays, many shale gas/oil reservoirs are being explored and over ten thousand of shale gas/oil wells have been drilled in United States.

This thesis follows the style of *SPE Journal.*

Along with the economic success comes the complexity of understanding and modeling gas/oil production from the horizontal wells with multistage hydraulic fractures. Two main reservoir engineering practices are often used in the industry – history matching and forecasting. Both are important in reservoir engineering and management. By history matching production of a shale gas/oil well we can get an idea about the quality of the fracturing job, quality and the size of reservoir. Forecasting is used to calculate the annual reserves.

Different authors have proposed different methods to handle history matching and forecasting of shale gas wells. Some of them use simulation (Cipolla 2009, Freeman et al. 2009), some use analytical models, (Bello and Wattenbarger 2008, 2009, 2010) and some use empirical models (Ilk 2010, Valko 2009). Lee and Sidle (2010) explained advantages and disadvantages of simulation, analytic, and empirical models in forecasting. According to their work, empirical models are easy to apply for thousands of wells in a short period of time and accurate enough to estimate annual reserves.

1.1 Motivation

Motivation for this work was derived by huge interest in exploring shale gas/oil reservoir not only in US but all over the world in recent years. It is important to appreciate the reserves that can be added by unconventional resources to the global energy demand. The amount of shale gas/oil in terms of reserves is incredibly huge yet the challenge is to understand their performance during exploitation so that, production technology can be improved in the future wells.

1.2 Objectives

Objective of this research was to develop new methods for better understanding of production from shale gas/oil wells. Linear Dual Porosity proposed by El-Banbi (1998) was used in modeling the horizontally drilled shale gas/oil well with multiple hydraulic fractures. Analytical solutions are employed to history match and forecast the production from shale gas/oil wells. The advantage of having analytical model as a tool is the simple fact that they are as rigorous as simulation but faster, and as fast as empirical model but much more rigorous.

1.3 Organization of the Thesis

This thesis is divided into seven chapters. Organization of the thesis was developed in following way.

Chapter I is introduction of the thesis and consists of objectives motivation and description of thesis parts.

In Chapter II brief description of literature review is outlined. Theoretical information is given about Dual Porosity models, Triple Porosity models, linear flow in hydraulically fractured shale reservoirs, history matching and forecasting of shale reservoirs.

Chapter III gives information about linear Dual Porosity model. Model assumptions, asymptotic equations for transient flow regimes, different regions, and important parameter group affecting different regions are discussed in detail.

Chapter IV discusses important assumptions, asymptotic equations for transient flow regimes, different regions, and important parameters group affecting each region in linear Triple Porosity model.

Chapter V describes history matching with linear Dual Porosity model with synthetic examples as validation for derived equations and algorithm. Equations for gas and oil are outlined in detail. Correction for adsorbed gas and changing gas properties are explained for shale gas well matching. Synthetic wells generated in CMG's IMEX and GEM simulators were used to validate the accuracy and usefulness of the proposed method. A method for variable drawdown matching is explained with synthetic well example. Comparison is done between variable drawdown and constant drawdown matching.

Chapter VI shows application of linear Dual Porosity model on shale gas wells. Shale gas wells from Barnett, Fayetteville, and Woodford plays were used in history matching and forecasting with Dual Porosity model.

Chapter VII discusses conclusions and recommendations.

CHAPTER II

LITERATURE REVIEW

2.1 Dual Porosity Systems

Dual Porosity systems are usually used to represent naturally fractured reservoirs. However, it can be used to model any type of reservoir where there are two different storage systems. Warren and Root (1963) showed that "non-homogeneous" reservoirs can be represented by two dimensionless parameters; omega and lambda, where omega is the measure of flow capacitance of the secondary porosity system and lambda is related to the scale of heterogeneity that presents in the system. In typical dual porosity reservoirs the primary porosity system (matrix) mostly contributes to the storage of the fluid and has no impact on the flow capacity (Fig. 2.1). On the other hand, secondary porosity system (fractures) does not contribute much to the storage of the fluid however, is the only medium which transmits the fluid.

By solving the continuity equation using the Laplace Transformation proposed by Van Everdingen and Hurst (1949), Warren and Root (1963) showed the solution to the problem in Laplace domain and asymptotic equations for specific cases. Pseudo-steady state flow is assumed between primary and secondary porosity system in this analysis. (Warren and Root, 1963)

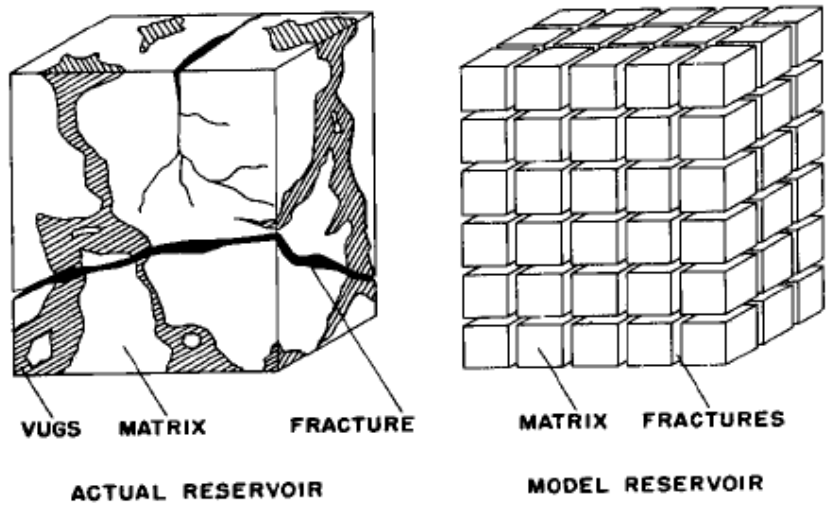

Fig. 2.1—Idealization of dual porosity system with "sugar cube" model. From Warren and Root (1963)

Another approach to the problem was proposed by Kazemi (1969). Compared to Warren and Root (1963), Kazemi (1969) assumed unsteady state flow in the matrix system which would decrease the error caused by incorrect pseudo steady state flow assumption for early time (Fig. 2.2). However, results presented by Kazemi for pressure build up and drawdown were not very different than results of Warren and Root. The only difference was in the transition period of fluid flow from fracture to matrix system.

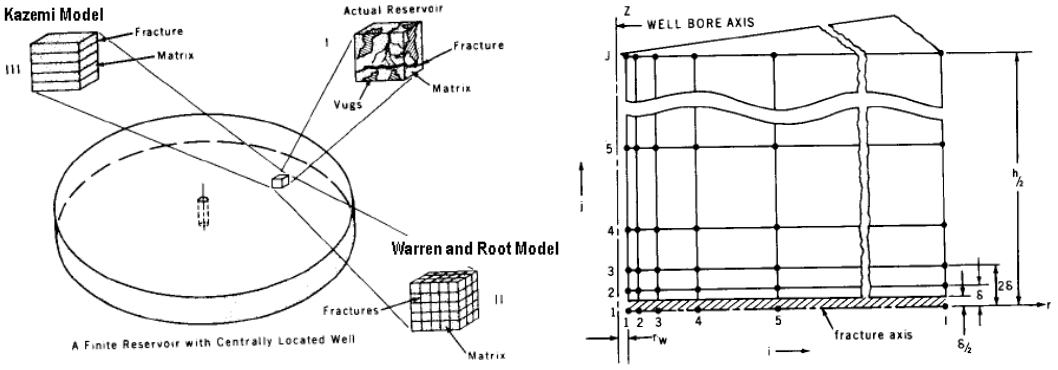

Fig. 2.2—Idealization of dual porosity system with slabs. From Kazemi (1969)

Most of the other research on modeling of the Dual Porosity systems are based on either Warren and Root (1963) or Kazemi (1969) assumptions for flow between primary and secondary porosity systems.

2.2 Triple Porosity Systems

Triple Porosity System was first introduced by Abdassah and Ershaghi (1986) to represent naturally fractured reservoirs. Motivation to find the new model to describe fracture-matrix interactions was some odd results from build up and drawdown test data which could not be described by Dual Porosity system. The main flaw of the Dual Porosity system is a uniform matrix properties assumption throughout the reservoir. According to Abdassah and Ershaghi (1986) Triple Porosity system refers to a system where there are two matrix systems with different properties besides the natural fractures. Both matrix systems were assumed to be under gradient (unsteady state) flow. Abdassah and Ershaghi (1986) proposed two models for Triple Porosity System; (1) Strata Model (Fig. 2.3) and (2) Block Model (Fig. 2.4).

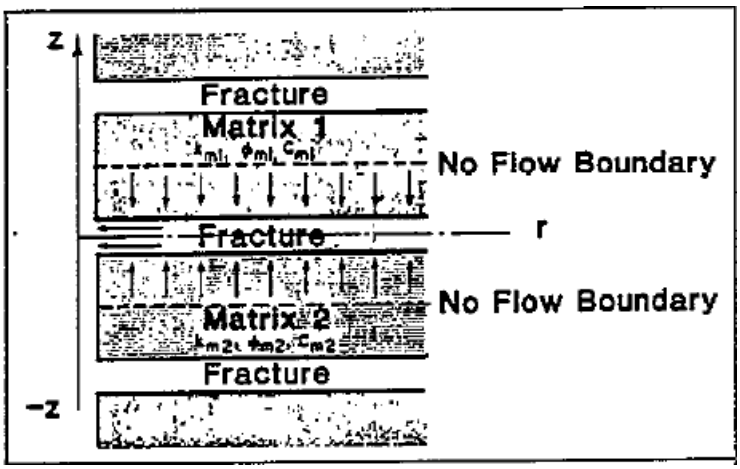

Fig. 2.3—An idealized strata model. From Abdassah and Ershaghi (1986)

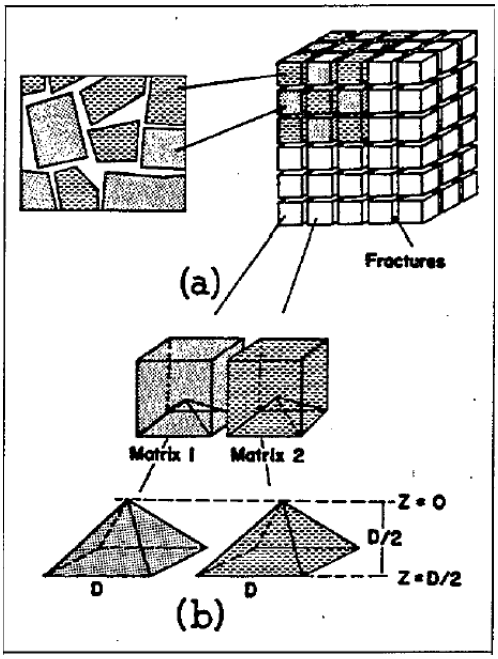

Fig. 2.4—An idealized block model. From Abdassah and Ershaghi (1986)

According to Abdassah and Ershaghi (1986) Dual Porosity model is a specific case of Triple Porosity model where two matrices have same properties. Their Triple Porosity behavior will appear if $\acute{\omega}1=\acute{\omega}2$ and $\lambda 1 \neq \lambda 2$ or $\acute{\omega}1 \neq \acute{\omega}2$ and $\lambda 1=\lambda 2$. For the case

where ώ1≠ώ2 and λ1≠λ2 Dual Porosity models should work fine because first contribution to the flow will be from matrix with higher storage capacity and lower interconnectivity, which will have negligible disruption effect to the slope.

Jalali and Ershaghi (1987) emphasized the advantages of both pseudo steady state and unsteady state flow assumption in the matrix systems by claiming the equal frequency of occurrence in the nature. Thus, for the Triple Porosity system with two distinct matrix systems they proposed three inter-porosity conditions:

1. Both Matrix systems have pseudo steady state flow
2. Both Matrix systems have unsteady state flow
3. One Matrix system has pseudo steady state, and the other has unsteady state flow

The diffusivity equation was solved for those different models and asymptotic equations were presented for variety of time ranges.

Al-Ghamdi and Ershaghi (1996) proposed new triple porosity model – Dual Fracture Model where instead of having two matrix systems they have two fracture systems: microfractures and macrofractures. According to their assumptions, it is more realistic to have two fracture systems than two matrix systems. Al-Ghamdi and Ershaghi (1996) proposed two different triple porosity models: (1) Microfractures and Matrix drain to Macrofractures separately (2) Matrix blocks feed Microfractures and Microfractures drain to either wellbore or Macrofractures. Diffusivity equations were solved in Laplace domain and approximately inverted back to real time by using Stehfest algorithm. Dimensionless parameters such as ώ1, ώ2, λ1, and λ2 were defined

differently than Abdassah and Ershaghi (1986). This work could be considered as a beginning of new modeling for naturally fractured reservoirs.

Dreier et al. (2004) proposed a Quadruple Porosity model where there are three fracture systems: megafractures, macrofractures, and microfractures. Only megafractures transport fluid to the wellbore, macrofractures and microfractures do not communicate with the well. The flow in the fractures assumed to be unsteady state however, in the matrix is pseudo steady state. Dreier et al. (2004) used regression to match well test data with proposed models.

Al-Ahmadi (2010) improved the triple porosity model proposed by Al-Ghamdi and Ershaghi (1996) by using El-Banbi (1998) solutions for linear flow in dual porosity reservoirs. He proposed four different models where various combinations of flow regimes assumed in the matrix and fracture systems.

- Model 1: Fully Transient Triple Porosity Model
- Model 2: Mixed Flow Triple Porosity Model (Pseudo steady state between matrix and microfractures, unsteady state between microfractures and macrofractures)
- Model 3: Mixed Flow Triple Porosity Model (unsteady state between matrix and microfractures, pseudo steady state between microfractures and macrofractures)
- Model 4: Fully pseudo steady state Triple Porosity Model

Al-Ahmadi (2010) showed that with Model 1 six different regions can be observed in the dimensionless rate versus time plot of constant pressure solution in

Triple Porosity model (Fig. 2.5). Those regions are alternating linear and bilinear flows ending with boundary dominated flow of the system.

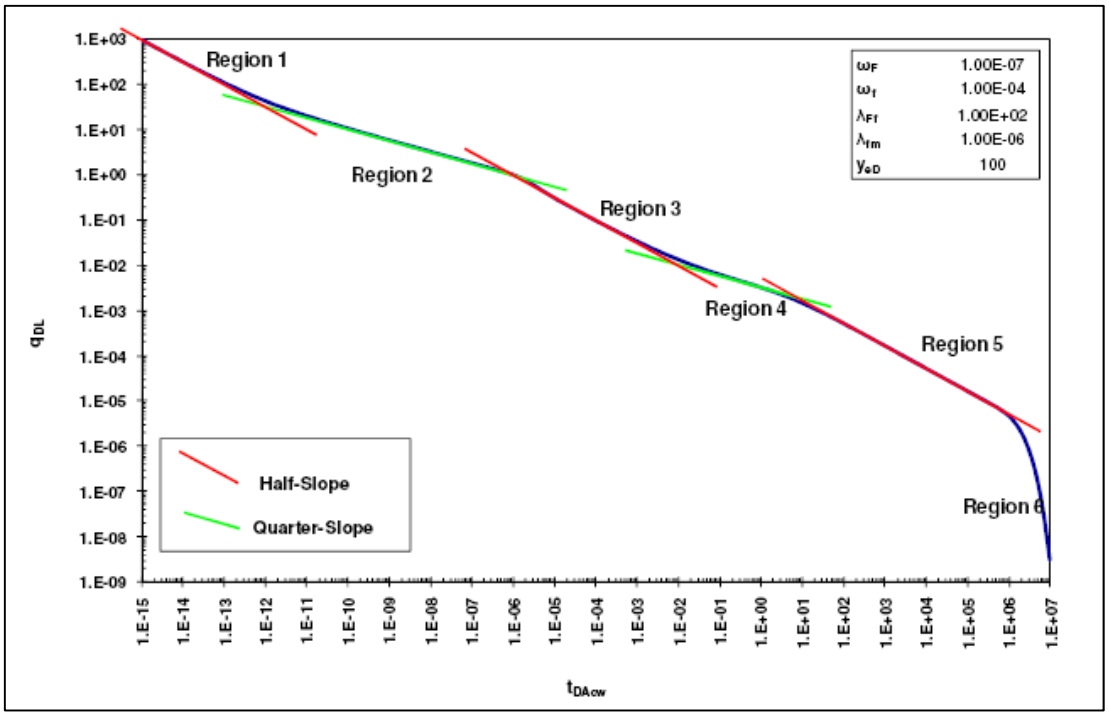

Fig. 2.5—Flow regions for Triple Porosity Model 1. From Al-Ahmadi (2010)

Al-Ahmadi (2010) also showed that regression can be used to find reservoir parameters and match the production behavior with analytical solutions. The analytic cases which were used for history matching were only for constant pressure which is not always the case in reality. The regression described in that work (Al-Ahmadi, 2010) is multi-parameter regression and the physical relations between found parameters and flow regimes was not described well to estimate the initial guess values. Considering

that regression method used in that work (Al-Ahmadi, 2010) highly sensitive to initial guesses, it will affect the success of the history matching.

2.3 Linear Flow in Hydraulically Fractured Reservoirs

According to Wattenbarger (2001), long term linear flow in tight gas reservoirs may be caused by anisotropy, naturally fractured reservoirs, linear or elongated reservoirs, high permeability streaks, and hydraulic fractures. Most of the shale gas wells drilled in US are horizontal wells with multistage hydraulic fractures. Hydraulic fractures act like high conductive medium which results in linear flow to the hydraulic factures from the formation. Bello and Wattenbarger (2008) proposed a method to analyze hydraulically fractured shale gas wells. According their model, the drainage area of the reservoir is as big as the extend of the hydraulic fracture, there is no flow from matrix to wellbore – the only flow to the wellbore is from hydraulic fractures, the matrix flows to hydraulic fractures and hydraulic fractures drain to the well, reservoir is considered as a dual porosity model where matrix is the primary source of porosity and hydraulic fractures are secondary porosity (Fig. 2.6).

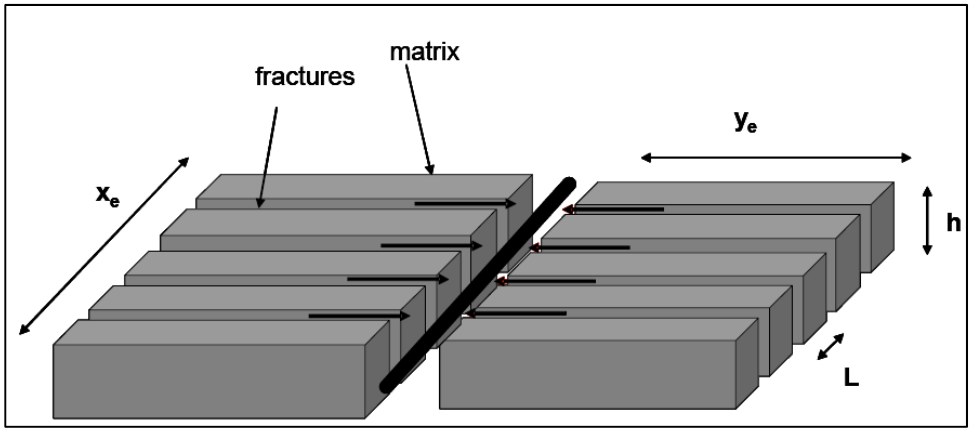

Fig. 2.6—Schematic of slab matrix linear model of hydraulically fractured well. From Bello and Wattenbarger (2010)

2.4 History Matching and Forecasting of Shale Reservoirs

Watson et al. 1990 proposed an analytical method to history match the production behavior of naturally fractured reservoirs. Although they were taking into account the gas properties change by applying normalized time (Fraim and Wattenbarger, 1987), they do not mention desorption of gas at low pressures. Moreover, their model was developed for vertical wells drilled in Devonian shale which means that analytical solutions used in their work are different than linear dual porosity model (El-Banbi, 1998).

Mattar et al. (2008) summarized both empirical and semi-analytical methods to describe the production data from shale gas wells up to date. Empirical analysis techniques discussed in their work are "power-low exponential" and "hyperbolic" rate relation with time. They also discussed the effect of wellbore geometry (vertical versus horizontal) and use of analytical solutions from hydraulically fractured vertical wells in multiply fractured horizontal wells. They observed that finite conductivity vertical fracture may result in observation of "false radial" flow. They also discussed the existence of Stimulated Reservoir Volume – Effective Drainage Area and suspected that in ultra-low permeability reservoirs fluid will flow only inside the SRV. As a simulation model they favored "compound linear flow" approach rather than using vertical well model for horizontal wells.

Bello and Wattenbarger (2008) present a mathematical model for horizontally drilled shale gas wells with multiple hydraulic fractures. The mathematical model is linear dual porosity model. This model has been checked with slab, cylinder and sphere shapes as a matrix block and proved to give the same result for linear flow if proper f(s) function is used. It was showed that area volume ratio between those shapes is 1:2:3, respectively. The main flow is considered to be the linear flow from matrix block to fractures. Therefore, cross sectional area to the flow is defined as the hydraulic fractures surface contacting the matrix. By analyzing linear flow on square root of time plot square root of permeability and cross sectional area product can be determined.

Bello and Wattenbarger (2009) presented a new solution for linear dual porosity model which would incorporate the "skin effect" – early flat region on a log-log plot of the field data. According to their work, early time behavior of horizontally drilled and multistage fractured shale gas wells should be interpreted as "skin effect" rather than bilinear flow because of linear flow convergence at early time or any completion related problem. They clearly showed that constant rate and constant pressure solutions for linear flow are different on the contrary to radial flow. Since in the field operators are trying to maintain well under constant bottomhole flowing pressure, an approximate equation is derived for constant pressure solution. The method is simple and straight forward to apply which makes it easy to use in the analysis of field data. The only region analyzed with this method is Region 4 – a transient linear flow from matrix to hydraulic fractures. The square root of permeability and cross sectional area product can be determined from this analysis.

Jordan et al. (2009) presented a model which is a quadratic equation of cumulative production and OGIP depending on rate and pressure. This method is applied with Arp's decline curve analysis to calculate OGIP in iterative manner. The method also calculates the equivalent effective permeability assuming that the well is at the center of homogenous reservoir. The flaw of the method is the fact that it is designed for vertical wells and typical linear flow in horizontally drilled shale gas wells cannot be analyzed with this method.

Freeman et al. (2009) did simulation study trying to explain flow behavior in horizontally drilled and hydraulically fractured tight/shale gas wells. According to them, analysis of ultra-low permeability reservoir with simulation is superior to analytical methods because the latter cannot take into account the adsorbed gas and change of permeability as a function of pressure. They observed compound linear flow when transient in the fractures ended and fluid is flowing from non-stimulated part to the well. They recommended not mixing this flow behavior with "boundary effects". Another recommendation was not to use analytical dual porosity models in modeling the ultra-low permeability reservoirs because they assume pseudo-steady state as an interporosity flow between matrix and fracture.

Luo et al. (2010) analyzed the flow regimes in multiply fractured horizontal wells and discussed the importance of compound linear flow (CLF). According to their work CLF slope on derivative plot depends on the ratio of fracture length to spacing and interference between neighboring wells however, it does not depend on formation

permeability. On the other hand reservoir permeability will affect the occurrence of CLF in the life of the well – low permeability will result in late occurrence (if it ever occurs).

Ilk et al. (2010) proposed a systematic workflow to analyze the production data from unconventional reservoirs. They proposed to do diagnostics, rate-time analysis and model based production analysis in systematic order as data is gathered from the well life. They proposed to use derivative function as diagnostics to understand the flow regimes and quality of production data. As a rate time analysis they recommended to use modified Arp's decline equations for unconventional reservoirs.

Medeiros et al. (2010) discussed semi-analytical solutions to horizontally drilled well in a homogeneous and dual porosity reservoirs with lateral and transverse hydraulic fractures. One of the most significant findings is the fact that hydraulic fracturing of horizontal wells might not add significant increase in production if formation is already naturally fractured. Hydraulic fractures should be designed to re-activate originally existing natural fractures rather than creating new fractures in already naturally fractured reservoir. In a very tight formation extent of drainage area may be limited to extent of hydraulic fractures.

Nobakht and Mattar (2010) described a method to analyze the production data from shale gas wells with apparent skin by using type curves. According to their work, linear flow can be masked with high apparent skin and can lead to incorrect interpretation on type curves. Therefore, normalized rate is modified by using the Bello and Wattenbarger (2009) method to take into account the skin in linear flow under

constant bottomhole pressure conditions. Although existence of skin can give erroneous results in type curves, square root of time will show the linear flow if it exists.

Nobakht et al. (2010) proposed a new method which is simple yet rigorous enough to cover theory of linear flow and boundary dominated hyperbolic decline. According to this method an analyst does not need to find fracture half-length or permeability exactly which makes it simple to apply. The only unknown appears to be the drainage area which can be used from previous wells. Once the end of linear flow is determined by Wattenbarger (2001) method, forecasting is done for boundary dominated flow part by using hyperbolic decline curve. The main assumption here is the fact that boundary dominated flow starts as soon as the linear flow ends which supports the stimulated reservoir volume (SRV) theory. In other words, drainage area of the reservoir is limited to the extent of fracture half length.

Bello and Wattenbarger (2010) presented asymptotic equations for transient flow regimes that can happen in linear dual porosity model. According to their work, the linear flow which is seen in field most of the time is the Region 4 which is transient linear flow of fluid from matrix into the hydraulic fractures. They described transient regions and presented analysis equation for each of them. They also outlined assumptions for linear dual porosity model which was initially proposed by El-Banbi (1998). In case of application to the field data, square root of permeability and cross sectional area product can be determined.

CHAPTER III

DESCRIPTION OF LINEAR DUAL POROSITY MODEL

3.1 Introduction

In this chapter important assumptions for linear Dual Porosity model are discussed briefly. Asymptotic equations proposed by Bello and Wattenbarger (2010) are shown and explanation is given for each flow region. Important parameters group affecting each region is found and shown. Both gas and oil equations are derived in filed units from dimensionless equations.

3.2 Model Assumptions

Bello and Wattenbarger (2010) presented Dual Porosity Model to describe the nature and behavior of the flow in hydraulically fractured shale gas wells (Fig. 3.1). The model is equally applicable to hydraulically fractured tight gas and shale oil wells, too where governing flow regime is transient liner flow and reservoir geometry is rectangle.

Following are major assumptions and features of Linear Dual Porosity Model.

- The drainage area of the horizontal well is a rectangular geometry called Stimulated Reservoir Volume (SRV).
- The SRV consists of network of natural and hydraulic fractures that enhances the flow fluid in low permeability reservoirs.
- Reservoir is assumed to be Dual Porosity consisting of matrix blocks and hydraulic fractures (slab model).
- The perforated length, x_e is the same as the length of the reservoir.

- Matrix blocks feed hydraulic fractures and only hydraulic fractures drain to the wellbore.
- Transient dual-porosity solutions proposed by El-Banbi (1998) are used to solve constant bottomhole flowing pressure and constant rate cases.

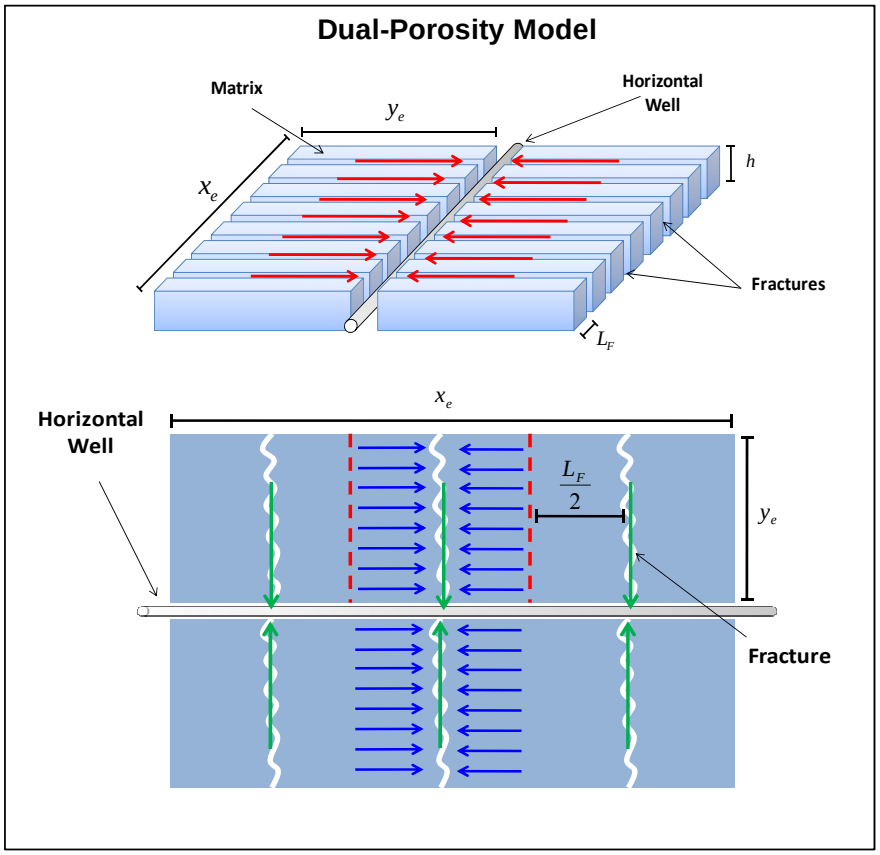

Fig. 3.1—Sketch for Dual Porosity model

3.3 Definition of Dimensionless Variables

Following are dimensionless variables which are used in modeling of linear Dual Porosity System.

$$t_{DA_{cw}} = \frac{0.00633\, k_F t}{\phi \mu c_t A_{cw}} \quad \text{..... (3.1)}$$

$$\frac{1}{q_{DL}} = \frac{k_F \sqrt{A_{cw}} \left[m(p_i) - m(p_{wf}) \right]}{1422\, q_g T} \quad \text{..... (3.2)}$$

$$\frac{1}{q_{DL}} = \frac{k_F \sqrt{A_{cw}} \left[p_i - p_{wf} \right]}{141.2 q_o B \mu} \quad \text{..... (3.3)}$$

$$\lambda = \frac{12}{L_F^2} \frac{k_m}{k_F} A_{cw} \quad \text{..... (3.4)}$$

$$\omega = \frac{\left[\phi V c_t \right]_F}{\left[\phi V c_t \right]_t} \quad \text{..... (3.5)}$$

$$y_{eD} = \frac{y_e}{\sqrt{A_{cw}}} \quad \text{..... (3.6)}$$

3.4 Asymptotic Equations

Bello and Wattenbarger (2010) presented asymptotic equations for transient flow regimes that can occur in Linear Dual Porosity Model. Most of their work is related to Region 4, which is transient linear flow from matrix to hydraulic fractures. Early flat region in the life of the well is assumed to be result of "skin effect" which caused by linear flow convergence or any type of completion problem. Occurrence of bilinear flow is ignored and apparent skin calculation is done instead. However, in some shale gas/oil wells significant periods of bilinear flow are observed as a quarter slope in log-log plot of rate versus time. Fig. 3.2 is showing five different regions that can occur in linear Dual Porosity system. Table 3.1 is the summary of asymptotic equations for each region.

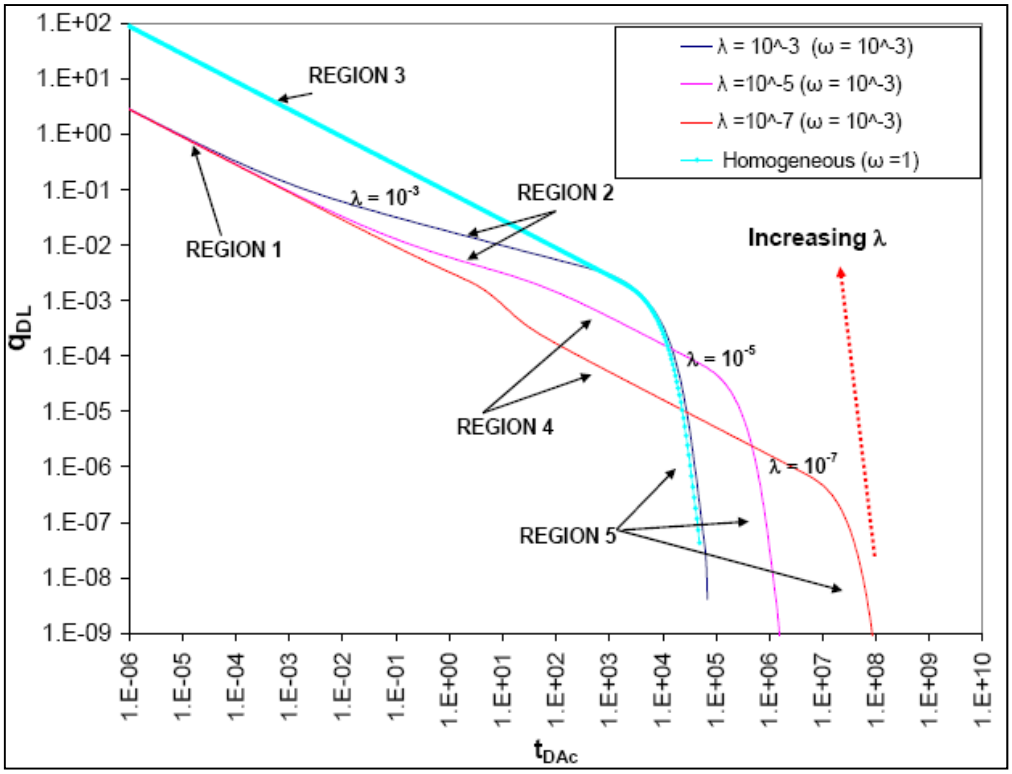

Fig. 3.2—Illustration of the five flow regions for a slab matrix dual porosity linear reservoir (y_{De} = 100); λ_{Ac} =10-3, 10-5, 10-7 for values of ω = 10-3. From (Bello and Wattenbarger, 2010)

Table 3.1—Summary of analysis equations for the constant p_{wf} inner boundary case (slab matrix, dual porosity). From (Bello and Wattenbarger, 2010)

Region	Equation
1	$q_{DL} = \frac{\sqrt{\omega}}{2\pi\sqrt{\pi}} t_D^{-1/2}$
2	$q_{DL} = \frac{\lambda^{1/4}}{10.133} t_D^{-1/4}$
3	$q_{DL} = \frac{1}{2\pi\sqrt{\pi}} t_D^{-1/2}$
4	$q_{DL} = \frac{(\lambda/3)^{1/2} y_{eD}}{2\pi\sqrt{\pi}} t_D^{-1/2}$ or $q_{DL} = \frac{1}{2\pi\sqrt{\pi}} t_D^{-1/2}$
5	----------

3.5 Important Parameter Group for each Region

According to Bello and Wattenbarger (2010), asymptotic equations can match different regions that can occur in linear Dual Porosity systems. However, beginning and the end of each region is not well known. Since the primary aim of this research is to use linear Dual Porosity model to history match the production data of shale gas/oil wells, asymptotic equations shown in Table 3.1 expanded to field units to find out important parameters which are usually unknown and need to be matched. In the following sections brief description of each region will be given first, which is followed by derived rate equation in field units for each region. Complete derivation for both oil and gas is shown in Appendix A.

3.5.1 Region 1

Region 1 is the transient linear flow from hydraulic fractures to the wellbore. Because of high permeability and low storage inside the fractures, this region usually lasts from few hours to couple of days in the field. Therefore, transient linear flow in hydraulic fractures is difficult to record in the life of the well.

$$q_g = \frac{\left[m(p_i) - m(p_{wf})\right]}{2844\pi\sqrt{\pi T}}\left[\frac{\mu}{0.00633}\right]^{1/2} A_{cw}\left\{\left[\phi V c_t\right]_F^{1/2} k_F^{1/2}\right\}\frac{1}{t^{1/2}} \quad \text{..... (3.7)}$$

$$q_o = \frac{\left[p_i - p_{wf}\right]}{282.4\pi\sqrt{\pi B}}\left[\frac{1}{0.00633\mu}\right]^{1/2} A_{cw}\left\{\left[\phi V c_t\right]_F^{1/2} k_F^{1/2}\right\}\frac{1}{t^{1/2}} \quad \text{..... (3.8)}$$

3.5.2 Region 2

This region is bilinear flow where two simultaneous transient linear flows occur, one from the matrix to the hydraulic fractures, and the other one from the hydraulic

fractures to well. Bilinear flow has been seen in shale gas wells from time to time, and duration can be significantly long. Some wells from Fayetteville, Woodford and Barnett shale are showing long period of bilinear flow approximately a month or two.

$$q_g = \frac{\left[m(p_i) - m(p_{wf})\right]}{14409.126T}\left[\frac{12\phi\mu c_t}{0.00633L_F^2}\right]^{1/4} A_{cw}\left\{k_F^{1/2}k_m^{1/4}\right\}\frac{1}{t^{1/4}} \quad \text{..... (3.9)}$$

$$q_o = \frac{\left[p_i - p_{wf}\right]}{1430.78B}\left[\frac{12\phi c_t}{0.00633L_F^2\mu^3}\right]^{1/4} A_{cw}\left\{k_F^{1/2}k_m^{1/4}\right\}\frac{1}{t^{1/4}} \quad \text{..... (3.10)}$$

3.5.3 Region 3

Region 3 is the same as linear flow in homogeneous system. This flow would occur in shale gas/oil wells before fracture job. On the other hand, permeability of shale formation is so low that fluid would not flow at economic rates in non-fractured well.

$$q_g = \frac{\left[m(p_i) - m(p_{wf})\right]}{2844\pi\sqrt{\pi T}}\left[\frac{\phi\mu c_t}{0.00633}\right]^{1/2}\left\{k_m^{1/2}A_{cm}\right\}\frac{1}{t^{1/2}} \quad \text{..... (3.11)}$$

$$q_o = \frac{\left[p_i - p_{wf}\right]}{282.4\pi\sqrt{\pi}B}\left[\frac{\phi c_t}{0.00633\mu}\right]^{1/2}\left\{k_m^{1/2}A_{cm}\right\}\frac{1}{t^{1/2}} \quad \text{..... (3.12)}$$

3.5.4 Region 4

This region is transient linear flow from the matrix to the hydraulic fractures. The half slope seen in field data corresponds to this region. Bello and Wattenbarger (2010) were analyzing this flow to calculate product of matrix permeability and fracture half length.

$$q_g = \frac{\left[m(p_i) - m(p_{wf})\right]}{2844\pi\sqrt{3\pi T}}\left[\frac{12\phi\mu c_t}{0.00633L_F^2}\right]^{1/2} A_{cw}\left\{k_m^{1/2}y_e\right\}\frac{1}{t^{1/2}} \quad \text{..... (3.13)}$$

$$q_o = \frac{[p_i - p_{wf}]}{282.4\pi\sqrt{3\pi T}}\left[\frac{12\phi c_t}{0.00633 L_F^2 \mu}\right]^{1/2} A_{cw}\left\{k_m^{1/2} y_e\right\}\frac{1}{t^{1/2}} \quad \text{..... (3.14)}$$

3.5.5 Region 5

This region is related to the boundary dominated flow of SRV or interference effects between hydraulic fractures. No asymptotic equation is derived for this region, but simulation on synthetic data indicates that if matrix linear flow occurs, the end of the half slope will depend on the value of fracture half length, that is, the longer the fracture half length, the later the curve will bend on log-log plot of rate versus time (Fig. 3.3).

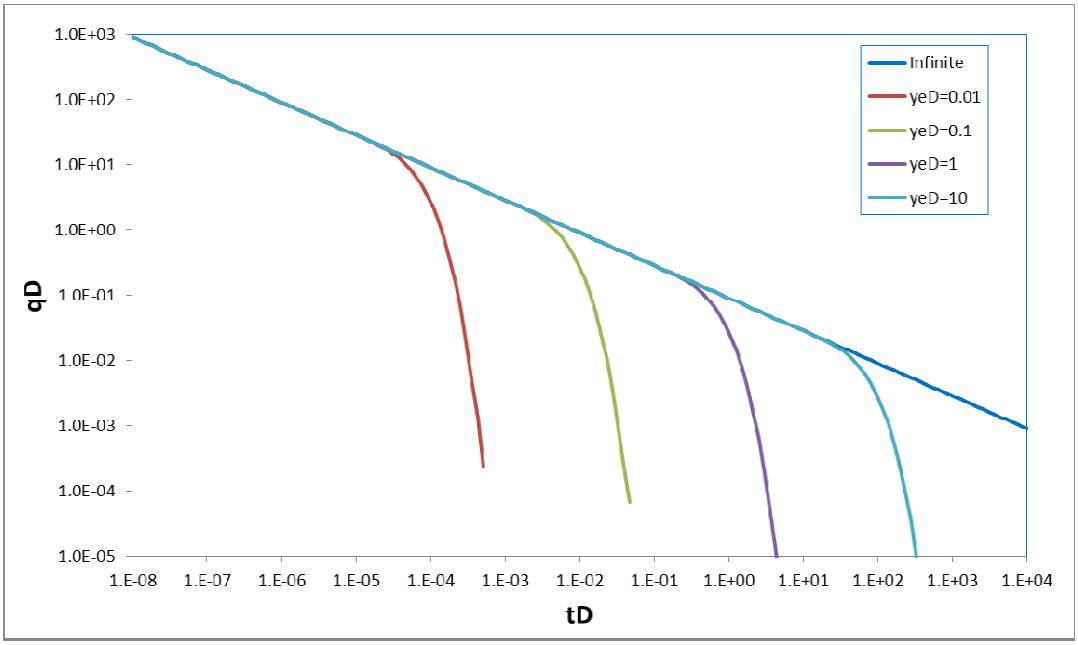

Fig. 3.3—q_{DL} vs t_{DAcw} plot. Beginning of boundary effects for different y_{eD} values in linear dual porosity model. As y_{eD} increases occurrence of boundary effects is later in time.

3.6 Chapter Summary

In this chapter important assumption and characteristics of Dual Porosity model was discussed in detail. Asymptotic equations proposed by Bello and Wattenbarger (2010) for Dual Porosity model were summarized. Important parameter group affecting each flow region in Dual Porosity model was presented. Considering that most seen flow regimes in the field data are bilinear and linear flows Dual Porosity is suitable model to describe production performance of shale gas/oil wells.

CHAPTER IV

DESCRIPTION OF LINEAR TRIPLE POROSITY MODEL

4.1 Introduction

In this chapter linear Triple Porosity model is described in detail. Twelve different regions are identified for Model 1 proposed by (Al-Ahmadi, 2010). Asymptotic equations and important parameter groups are derived for each region. Description and conditions to occur for each region are outlined in detail.

4.2 Model Assumptions

Linear Triple Porosity model used in this research was adapted from Al-Ahmadi (2010) (Fig. 4.1). Following are the assumptions for mathematical model.

- Triple-porosity system made up of matrix, less permeable micro-fractures and more permeable macro-fractures.
- Each medium is assumed to be ideally isotropic.
- Matrix blocks idealized as slabs.
- Flow is sequential from medium to other; from matrix to micro-fractures, from micro-fractures to macro-fractures, and only macro-fractures drain to the well.
- Drainage area is as big as extent of macro-fractures and length of the horizontal well.
- The interporosity flow condition assumed between macro-fractures and micro-fractures, micro-fractures and matrix is unsteady state flow.

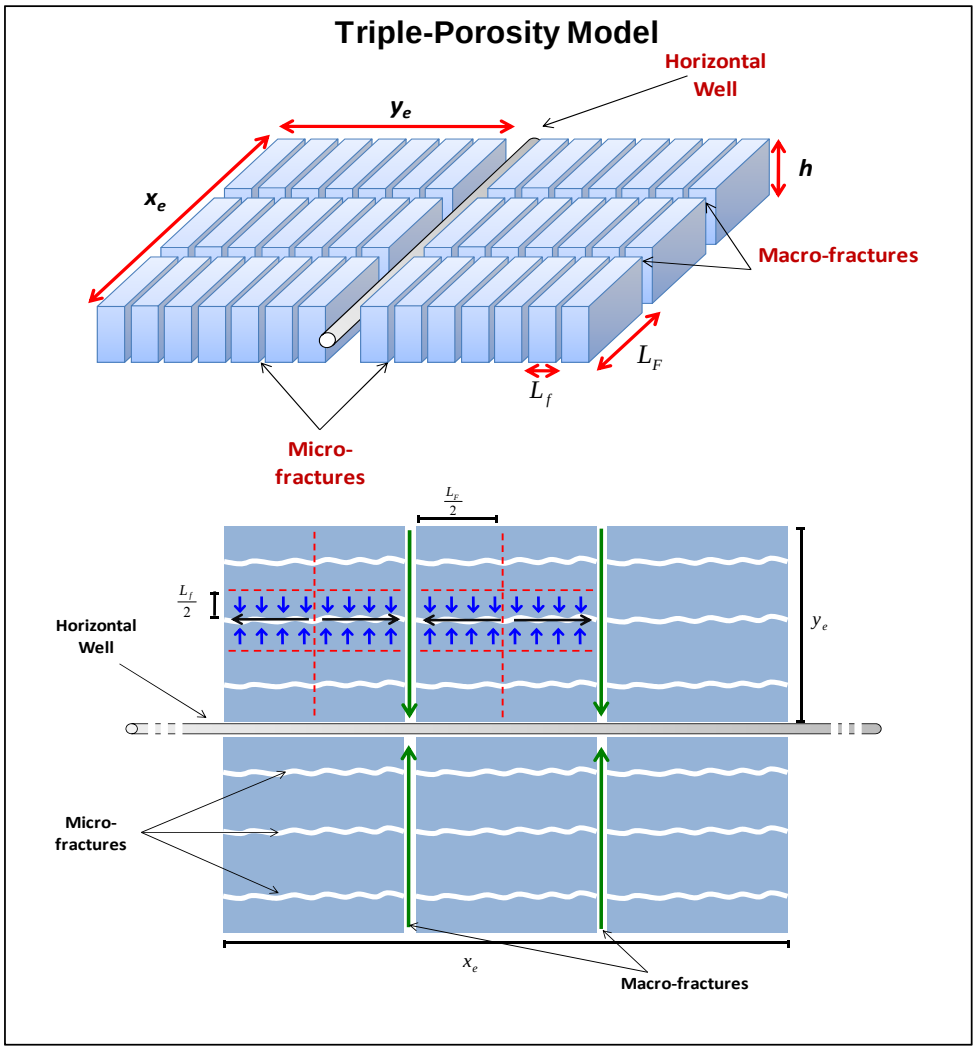

Fig. 4.1—Sketch of Triple Porosity model

4.3 Dimensionless Variables

Following are dimensionless variables for triple porosity model.

$$t_{DA_{cw}} = \frac{0.00633\, k_F\, t}{\phi \mu c_t A_{cw}} \quad \text{..... (4.1)}$$

$$\frac{1}{q_{DL}} = \frac{k_F \sqrt{A_{cw}} \left[m(p_i) - m(p_{wf}) \right]}{1422\, q_g T} \quad \text{..... (4.2)}$$

$$\frac{1}{q_{DL}} = \frac{k_F \sqrt{A_{cw}} \left[p_i - p_{wf} \right]}{141.2 q_o B \mu} \quad \text{..... (4.3)}$$

$$\lambda_{A_{cw},Ff} = \frac{12}{L_F^2} \frac{k_f}{k_F} A_{cw} \quad \text{..... (4.4)}$$

$$\lambda_{A_{cw},fm} = \frac{12}{L_F^2} \frac{k_m}{k_F} A_{cw} \quad \text{..... (4.5)}$$

$$\omega_F = \frac{\left[\phi V c_t \right]_F}{\left[\phi V c_t \right]_t} \quad \text{..... (4.6)}$$

$$\omega_f = \frac{\left[\phi V c_t \right]_f}{\left[\phi V c_t \right]_t} \quad \text{..... (4.7)}$$

$$y_{eD} = \frac{y_e}{\sqrt{A_{cw}}} \quad \text{..... (4.8)}$$

4.4 Asymptotic Equations

Al-Ahmadi (2010) showed six different regions that can happen in Linear Dual Porosity Model which is shown in Fig. 2.5. However, no asymptotic equations were presented for those regions. Moreover, during this research it was concluded that actually, more than 6 regions can occur with linear triple porosity model. In the following sections those different flow regions will be shown and asymptotic equations will be presented for each of them. All in all, twelve different regions were detected with linear triple porosity where 6 of them are linear, 4 bilinear, 1 trilinear, and 1 boundary dominated flow (Table 4.1). First six regions are the same as Al-Ahmadi (2010) showed but asymptotic equations were added. The rest of the regions are new and have been developed in this research (Figs. 4.2, 4.3, 4.4, 4.5, 4.6).

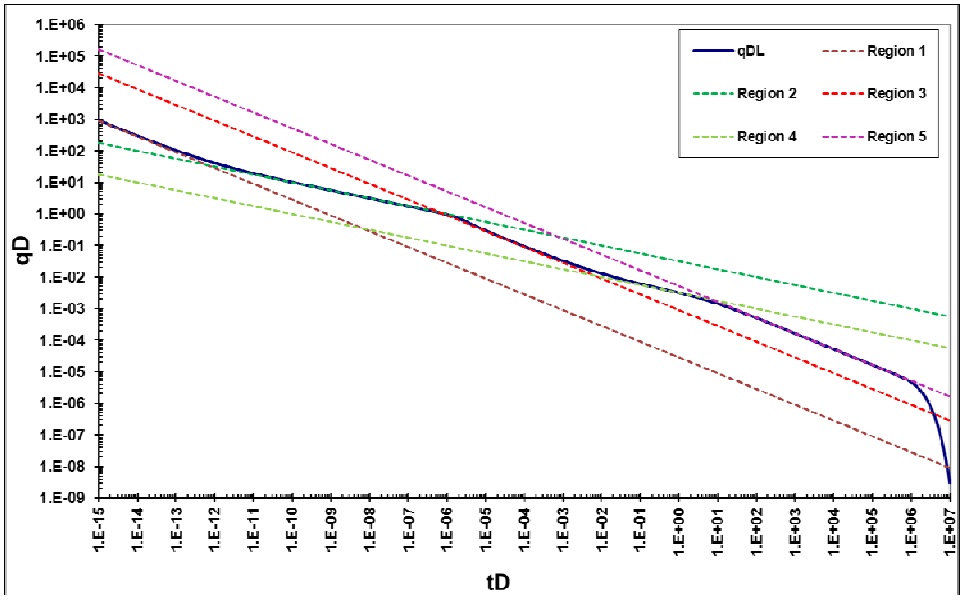

Fig. 4.2— q_{DL} vs t_{DAcw} plot. Asymptotic equations in Triple Porosity model for Regions 1, 2, 3, 4, and 5. Parameters: $\lambda_{Acw,Ff}$ =100, $\lambda_{Acw,fm}$ =1.0E-6, ω_F =1.0E-7, ω_f =1.0E-4, and y_{eD} =100

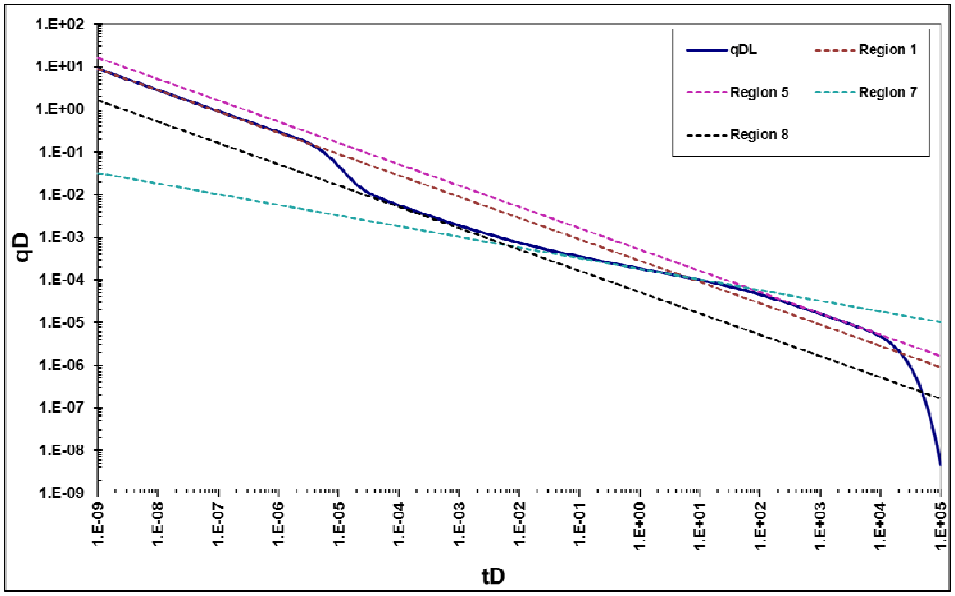

Fig. 4.3— q_{DL} vs t_{DAcw} plot. Asymptotic equations in Triple Porosity model for Regions 1, 2, 3, 4, and 5. Parameter: $\lambda_{Acw,Ff}$ =1.0E-3, $\lambda_{Acw,fm}$ =1.0E-4, ω_F =1.0E-5, ω_f =1.0E-3, and y_{eD} =1.

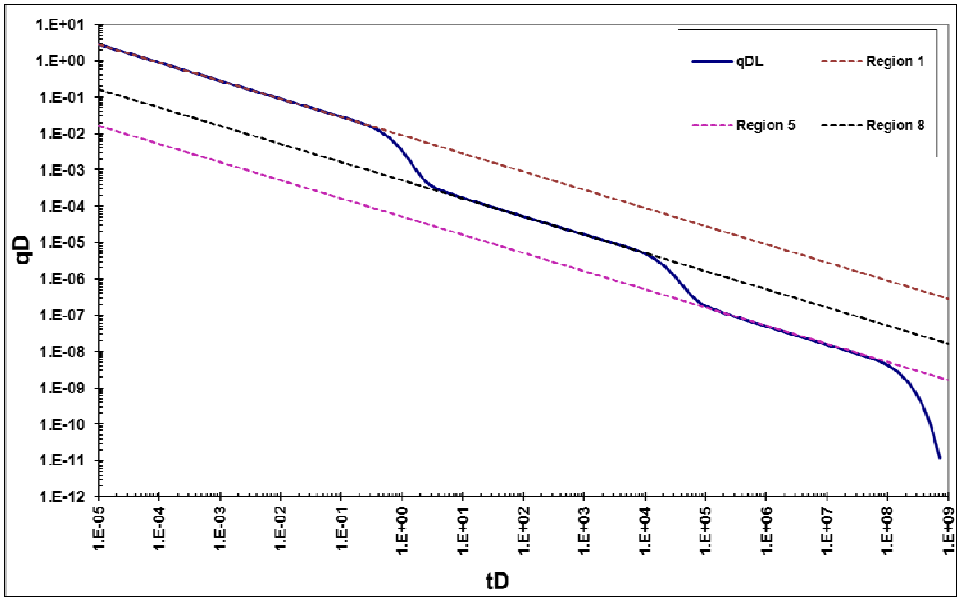

Fig. 4.4— q_{DL} vs t_{DAcw} plot. Asymptotic equations in Triple Porosity model for Regions 1, 2, 3, 4, and 5. Parameters: $\lambda_{Acw,Ff}$ =1.0E-5, , $\lambda_{Acw,fm}$ =1.0E-8, ω_F =1.0E-2, ω_f =1.0E-1, and y_{eD} =10.

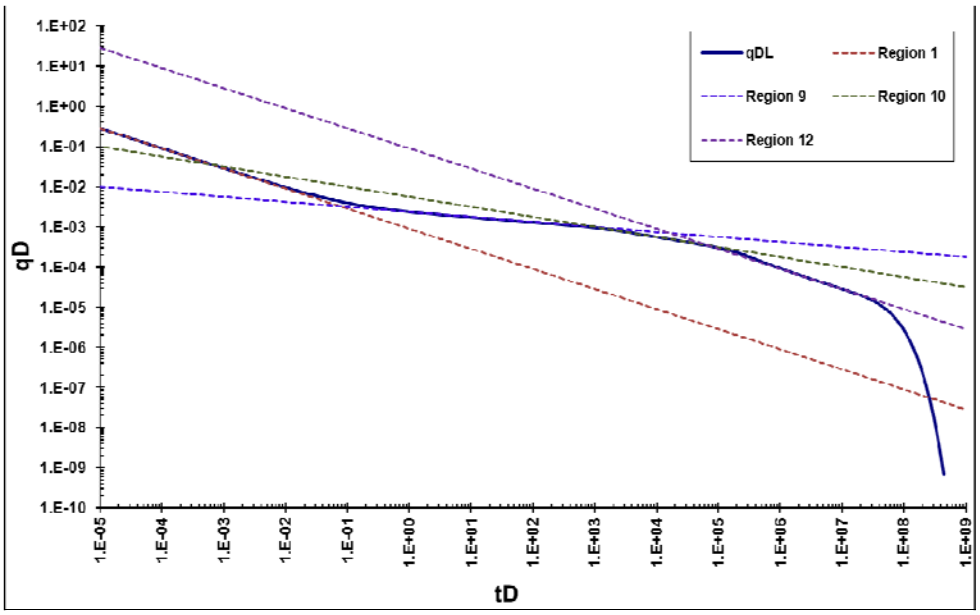

Fig. 4.5— q_{DL} vs t_{DAcw} plot. Asymptotic equations in Triple Porosity model for Regions 1, 2, 3, 4, and 5. Parameters: $\lambda_{Acw,Ff}$=1.0E-5, $\lambda_{Acw,fm}$ =1.0E-3, ω_F =1.0E-4, ω_f =1.0E-5, and y_{eD} =10000.

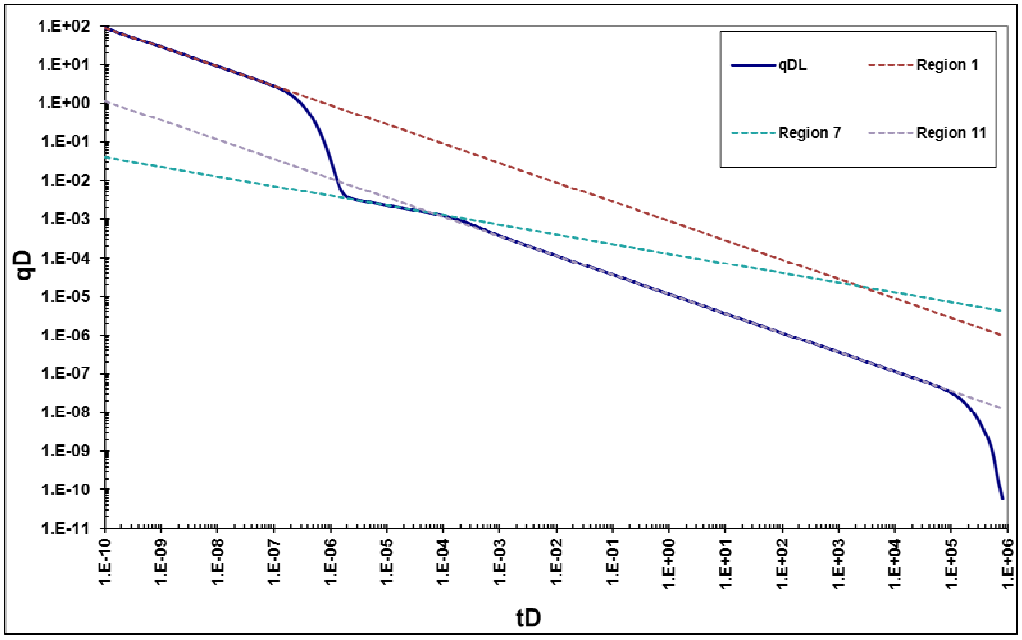

Fig. 4.6— q_{DL} vs t_{DAcw} plot. Asymptotic equations in Triple Porosity model for Regions 1, 2, 3, 4, and 5. Parameters: $\lambda_{Acw,Ff}$ =1.0E-5, $\lambda_{Acw,fm}$ =1000, ω_F =1.0E-4, ω_f =1.0E-5, and y_{eD} =0.07.

Table 4.1—Summary of analysis equations for the constant p_{wf} inner boundary case (slab matrix, triple porosity).	
Region	Equation
1	$q_{DL} = \frac{\sqrt{\omega_1}}{2\pi\sqrt{\pi}} t_{DA_{cw}}^{-1/2}$
2	$q_{DL} = \frac{(\lambda_{12}\omega_2)^{1/4}}{10.133} t_{DA_{cw}}^{-1/4}$
3	$q_{DL} = \frac{\sqrt{\omega_2}}{2\pi\sqrt{\pi}} t_{DA_{cw}}^{-1/2}$
4	$q_{DL} = \frac{\lambda_{23}^{1/4}}{10.133} t_{DA_{cw}}^{-1/4}$
5	$q_{DL} = \frac{\sqrt{\lambda_{23}/3}\, y_{eD}}{2\pi\sqrt{\pi}} t_{DA_{cw}}^{-1/2}$
6	----------
7	$q_{DL} = \frac{\sqrt{\lambda_{12}/3}\,\lambda_{23}^{1/4} y_{eD}}{10.133} t_{DA_{cw}}^{-1/4}$
8	$q_{DL} = \frac{\sqrt{(\lambda_{12}\omega_2)/3}\, y_{eD}}{2\pi\sqrt{\pi}} t_{DA_{cw}}^{-1/2}$
9	$q_{DL} = \frac{\lambda_{12}^{1/4}\lambda_{23}^{1/8}}{10.133} t_{DA_{cw}}^{-1/8}$
10	$q_{DL} = \frac{\lambda_{12}^{1/4}}{10.133} t_{DA_{cw}}^{-1/4}$
11	$q_{DL} = \frac{\sqrt{\lambda_{12}/3}\, y_{eD}}{2\pi\sqrt{\pi}} t_{DA_{cw}}^{-1/2}$
12	$q_{DL} = \frac{1}{2\pi\sqrt{\pi}} t_{DA_{cw}}^{-1/2}$

4.5 Important Parameter Group for each Region

Like in linear Dual Porosity model, information about different reservoir parameter group is needed to match the production of shale gas/oil wells with linear

Triple Porosity model. For this purpose, each region was analyzed separately and parameters group are found to use in history matching. Below is the brief description of each region is given with rate equation in field units for each of them. Complete derivation of equations is shown in Appendix B.

4.5.1 Region 1

This region is the transient linear flow between natural and hydraulic fractures. Duration of this flow region is not expected to be captured in the field because it occurs very fast. To match this flow region hydraulic fracture effective porosity and permeability is required to be known.

$$q_g = \frac{\left[m(p_i) - m(p_{wf})\right]}{2844\pi\sqrt{\pi}T}\left[\frac{\mu}{0.00633}\right]^{1/2}\left\{\left[\phi Vc_t\right]_F^{1/2} k_F^{1/2}\right\}A_{cw}t^{-1/2} \quad \text{..... (4.9)}$$

$$q_o = \frac{\left[p_i - p_{wf}\right]}{282.4\pi\sqrt{\pi}B}\left[\frac{1}{0.00633\mu}\right]^{1/2}\left\{\left[\phi Vc_t\right]_F^{1/2} k_F^{1/2}\right\}A_{cw}t^{-1/2} \quad \text{..... (4.10)}$$

4.5.2 Region 2

This region is bilinear flow between natural and hydraulic fractures. If it is seen in the field, in order to match it with triple porosity model, natural fractures' effective porosity and permeability, and hydraulic fractures' effective permeability is needed to be known.

$$q_g = \frac{\left[m(p_i) - m(p_{wf})\right]}{14409.13T}\left[\frac{12\mu}{0.00633L_F^2}\right]^{1/4}\left\{\left[\phi Vc_t\right]_F^{1/2} k_f^{1/4} k_F^{1/2}\right\}A_{cw}t^{-1/4} \quad \text{..... (4.11)}$$

$$q_o = \frac{\left[p_i - p_{wf}\right]}{1430.78B}\left[\frac{12}{0.00633L_F^2\mu^3}\right]^{1/4}\left\{\left[\phi Vc_t\right]_F^{1/2} k_f^{1/4} k_F^{1/2}\right\}A_{cw}t^{-1/4} \quad \text{..... (4.12)}$$

4.5.3 Region 3

This region is transient linear flow inside natural fractures. Regression should be done on natural fractures' effective porosity and hydraulic fractures' effective permeability to history match production from shale gas/oil well with triple porosity model.

$$q_g = \frac{\left[m(p_i) - m(p_{wf})\right]}{2844\pi\sqrt{\pi}T}\left[\frac{\mu}{0.00633}\right]^{1/2}\left\{\left[\phi V c_t\right]_f^{1/2} k_F^{1/2}\right\} A_{cw} t^{-1/2} \quad \text{..... (4.13)}$$

$$q_o = \frac{\left[p_i - p_{wf}\right]}{282.4\pi\sqrt{\pi}B}\left[\frac{1}{0.00633\mu}\right]^{1/2}\left\{\left[\phi V c_t\right]_f^{1/2} k_F^{1/2}\right\} A_{cw} t^{-1/2} \quad \text{..... (4.14)}$$

4.5.4 Region 4

This region is bilinear flow between natural fractures and formation matrix. Main parameters needed to be matched for this region are effective matrix and hydraulic fracture peremeabilties.

$$q_g = \frac{\left[m(p_i) - m(p_{wf})\right]}{14409.13T}\left[\frac{12\phi\mu c_t}{0.00633L_f^2}\right]^{1/4}\left\{k_m^{1/4} k_F^{1/2}\right\} A_{cw} t^{-1/4} \quad \text{..... (4.15)}$$

$$q_o = \frac{\left[p_i - p_{wf}\right]}{1430.78B}\left[\frac{12\phi c_t}{0.00633L_f^2\mu^3}\right]^{1/4}\left\{k_m^{1/4} k_F^{1/2}\right\} A_{cw} t^{-1/4} \quad \text{..... (4.16)}$$

4.5.5 Region 5

This region is the transient linear flow from matrix to natural fractures. It is believed that the last linear flow seen in the field should correspond to this region. For successful match of model with field data effective matrix permeability and effective hydraulic fracture half-length should be known.

$$q_g = \frac{\left[m(p_i) - m(p_{wf})\right]}{2844\pi\sqrt{3\pi}T}\left[\frac{12\phi\mu c_t}{0.00633L_f^2}\right]^{1/2}\left\{k_m^{1/2}y_e\right\}A_{cw}t^{-1/2} \quad \text{..... (4.17)}$$

$$q_o = \frac{\left[p_i - p_{wf}\right]}{282.4\pi\sqrt{3\pi}B}\left[\frac{12\phi c_t}{0.00633L_f^2\mu}\right]^{1/2}\left\{k_m^{1/2}y_e\right\}A_{cw}t^{-1/2} \quad \text{..... (4.18)}$$

4.5.6 Region 6

This region is exponential decline in the Triple Porosity Model and mainly depends on hydraulic fracture half-length like in linear Dual Poroisty model (Fig. 3.3). No asymptotic equation is derived for this region.

4.5.7 Region 7

This region is bilinear flow between matrix and natural fractures but compared to Region 4 this happens if transient in hydraulic fractures ends faster and curve bends down after Region 1 in the log-log plot of rate versus time. This would happen in high conductive hydraulic fractures where bilinear flow is not observed after hydraulic fracture linear flow (Region 1). The main parameters to match this region are effective matrix and natural fractures' permeability and effective hydraulic fracture half length.

$$q_g = \frac{\left[m(p_i) - m(p_{wf})\right]}{14409.13T}\left[\frac{12\sqrt{12\phi\mu c_t}}{\sqrt{0.00633}L_F^2L_f}\right]^{1/2}\left\{k_m^{1/4}k_f^{1/2}y_e\right\}A_{cw}t^{-1/4} \quad \text{..... (4.19)}$$

$$q_o = \frac{\left[p_i - p_{wf}\right]}{1430.78B}\left[\frac{12\sqrt{12\phi c_t}}{\sqrt{0.00633}L_F^2L_f\mu^{3/2}}\right]^{1/2}\left\{k_m^{1/4}k_f^{1/2}y_e\right\}A_{cw}t^{-1/4} \quad \text{..... (4.20)}$$

4.5.8 Region 8

This region corresponds to linear flow inside natural fractures. Compared to Region 3 this linear will occur if transient inside hydraulic fractures reaches tip of the fracture before linear flow starts inside of natural fractures. Thus, Region 3 occurs after quarter slope, whereas Region 8 occurs after bend down in the log-log plot of rate versus time.

$$q_g = \frac{\left[m(p_i) - m(p_{wf})\right]}{2844\pi\sqrt{3\pi}T}\left[\frac{12\mu}{0.00633L_F^2}\right]^{1/2}\left\{[\phi Vc_t]_f^{1/2} k_f^{1/2} y_e\right\}A_{cw}t^{-1/2} \quad \text{..... (4.21)}$$

$$q_o = \frac{\left[p_i - p_{wf}\right]}{282.4\pi\sqrt{3\pi}B}\left[\frac{12}{0.00633L_F^2\mu}\right]^{1/2}\left\{[\phi Vc_t]_f^{1/2} k_f^{1/2} y_e\right\}A_{cw}t^{-1/2} \quad \text{..... (4.22)}$$

4.5.9 Region 9

This region refers to trilinear flow where three different transient linear flows occur at the same time. It is expected rarely to see this flow region in field data. The occurrence of this region depends on the extend of the reservoir and physical properties of hydraulic and natural fractures which is difficult to see in nature. Hydraulic fractures should be long but less conductive, having good amount of fluid stored. Natural fractures' conductivity should be similar to matrix and hydraulic fractures, so that three transient linear flows would exist at the same time. The main parameters to match this region with field data are effective matrix, natural fracture, and hydraulic fracture permeabilities.

$$q_g = \frac{\left[m(p_i) - m(p_{wf})\right]}{14409.13T}\left[\frac{12\sqrt{12\phi\mu c_t}}{\sqrt{0.00633}L_F^2 L_f}\right]^{1/4}\left\{k_m^{1/8} k_f^{1/4} k_F^{1/2}\right\}A_{cw}t^{-1/8} \quad \text{..... (4.23)}$$

$$q_o = \frac{\left[p_i - p_{wf}\right]}{1430.78B}\left[\frac{12\sqrt{12\phi c_t}}{\sqrt{0.00633}L_F^2 L_f \mu^{7/2}}\right]^{1/4}\left\{k_m^{1/8} k_f^{1/4} k_F^{1/2}\right\}A_{cw} t^{-1/8} \quad \text{..... (4.24)}$$

4.5.10 Region 10

This region is bilinear flow between hydraulic fractures and natural fractures. Compared to Region 2 this would happen when transient in matrix ends before transient reaches the tip of hydraulic and natural fractures. Thus, matrix is already in boundary dominated flow whereas, hydraulic and natural fractures are dominated by transient flow regimes. The existence of this type of region in actual field data is not expected because in reality, transient flow in matrix would not end before it ends in fractures. If it exists in field data in order to match it with model regression should be done on effective hydraulic and natural fracture permeabilities.

$$q_g = \frac{\left[m(p_i) - m(p_{wf})\right]}{14409.13T}\left[\frac{12\phi\mu c_t}{0.00633L_F^2}\right]^{1/4}\left\{k_f^{1/4} k_F^{1/2}\right\}A_{cw} t^{-1/4} \quad \text{..... (4.25)}$$

$$q_o = \frac{\left[p_i - p_{wf}\right]}{1430.78B}\left[\frac{12\phi c_t}{0.00633L_F^2 \mu^3}\right]^{1/2}\left\{k_f^{1/4} k_F^{1/2}\right\}A_{cw} t^{-1/4} \quad \text{..... (4.26)}$$

4.5.11 Region 11

This region is a transient linear flow inside of natural fractures. It usually followed by boundary dominated flow which means that transient in matrix already ended. Therefore, existence of this type of region in actual field is not realistic. Nevertheless, if this region is suspected in the history of the well, in order to match it

with the model, regression should be done on effective permeability of natural fractures and hydraulic fracture effective half length.

$$q_g = \frac{\left[m(p_i) - m(p_{wf})\right]}{2844\pi\sqrt{3\pi}T}\left[\frac{12\phi\mu c_t}{0.00633L_F^2}\right]^{1/2}\left\{k_f^{1/2}y_e\right\}A_{cw}t^{-1/2} \quad \text{..... (4.27)}$$

$$q_o = \frac{\left[p_i - p_{wf}\right]}{282.4\pi\sqrt{3\pi}B}\left[\frac{12\phi c_t}{0.00633L_F^2\mu}\right]^{1/2}\left\{k_f^{1/2}y_e\right\}A_{cw}t^{-1/2} \quad \text{..... (4.28)}$$

4.5.12 Region 12

This region is a transient linear flow in hydraulic fractures in infinite reservoirs or in closed reservoirs with unrealistically high fracture half length. Therefore, occurrence of this flow region in the field is not expected. However, if match is required with field data then regression should be done only on effective hydraulic fracture half length.

$$q_g = \frac{\left[m(p_i) - m(p_{wf})\right]}{2844\pi\sqrt{\pi}T}\left[\frac{\phi\mu c_t}{0.00633}\right]^{1/2}\left\{k_F^{1/2}\right\}A_{cw}t^{-1/2} \quad \text{..... (4.29)}$$

$$q_o = \frac{\left[p_i - p_{wf}\right]}{282.4\pi\sqrt{\pi}B}\left[\frac{\phi c_t}{0.00633\mu}\right]^{1/2}\left\{k_F^{1/2}\right\}A_{cw}t^{-1/2} \quad \text{..... (4.30)}$$

4.6 Chapter Summary

In this chapter twelve different flow regions were presented for Triple Porosity model where flow between matrix and natural fractures, and natural fractures and hydraulic fractures is transient. Asymptotic equations were derived for each region. Moreover, similar to Dual Porosity model important parameter group affecting each

region is determined and presented. Application of Triple Porosity model on field data is not as easy as Dual Porosity. There are more unknowns to match in Triple Porosity model than Dual Porosity counterpart. Number and spacing of natural fractures are the two important unknowns in application of Triple Porosity model to match field data.

If existence of natural fractures in shale gas/oil well is wells is not suspected, then Dual Porosity model should be used for field applications. Another point which limits the application of triple porosity model is having too many flow regimes. Usually in the field three cases are observed in terms of transient flow regimes: bilinear, bilinear followed by linear, linear. Considering that Triple Porosity model has 6 different linear and 4 different bilinear flow regions it makes it difficult to decide which region needs to be matched. Of course, mathematically each region can be matched with any combinations of parameters. However, this can create too many solutions to one problem. On the other hand Dual Porosity model has only one reasonable linear flow regime which can be related to the linear flow which is observed in the field. This linear flow is the linear flow from matrix to hydraulic fractures. Even if the reservoir is naturally fractured, Dual Porosity can be applied to analyze linear flow from effective permeability matrix to hydraulic fractures. Therefore, instead of finding matrix permeability, effective matrix permeability is found. As it was shown in Chapter III square root of effective matrix permeability with effective fracture half-length gives information about production capacity of the well. Thus, this research is focused on matching production of shale gas/oil wells with Dual Porosity model. However, methodology and algorithm developed for Dual Porosity matching can equally be

applied to Triple Porosity model, too if existence of natural fractures suspected and more than one linear flow regime exists in the field data.

CHAPTER V

HISTORY MATCHING WITH LINEAR DUAL POROSITY MODEL — SYNTHETIC CASES

5.1 Introduction

In this chapter a method for application of linear Dual Porosity model for history matching and forecasting of production of shale gas/oil wells is discussed. Validation of some assumptions is shown with synthetic wells. History matching algorithm is outlined briefly for both oil and gas wells. Correction for adsorbed gas and gas properties change in shale gas wells is discussed in detail. Derivation is done for modified material balance and compressibility equations with adsorbed gas. Different flow regimes are history matched with proposed method on synthetic gas and oil wells. Variable drawdown matching was shown with linear Dual Porosity model. The methodology and algorithm described here are equally applicable to match field data with Triple Porosity model, too. However, the software developed in this research can match with only Dual Porosity model since none of the analyzed shale plays suspected to have network of natural fractures. Moreover, only one linear flow regime is observed in the analyzed wells, which is strongly believed to be Region 4 in Dual Porosity model.

5.2 Validation of SRV Assumption

One of the important assumptions of linear Dual Porosity model is the assumption that well will not drain outside of Stimulated Reservoir Volume (SRV) which is limited to the extent of hydraulic fractures and horizontal wellbore length. This

assumption should be quite good for ultra-low permeability reservoirs where permeability values are in the range of 10-100 Nano-Darcies. On the other hand many authors (Freeman et al. (2009), Luo et al. (2010)) have discussed the importance of Compound Linear Flow (CLF) in horizontal tight/shale gas wells which was initially proposed by Van Kruysdijk and Dullaert (1989). CLF occurs when hydraulic fractures start to interfere and fluid from non-stimulated reservoir drains normal to the vertical well plane. A reservoir simulation model was built with typical shale gas well completion and reservoir parameters to prove this assumption. Table 5.1 shows the summary of these parameters. The main goal of this simulation study was to show the sensitivity of occurrence of CLF to the matrix permeability. The simulation model was run for 30 years to check the occurrence of CLF in the practical life time of the well for different matrix permeability values. Permeability values from 1.00E-3 md to 1.00E-6 md were used in this analysis. It has been proven that CLF would not occur in the practical life time of the horizontally drilled shale gas well for matrix permeability less than 5.00E-5 md. Fig. 5.1 shows the summary for three values of matrix permeability. Upper part of the plot is rate versus time for constant bottomhole pressure production and lower part is derivative of reciprocal rate with respect to square root of the time.

Table 5.1—Model parameters for CLF analysis.			
Hydraulic Fracture	Porosity	0.002	
	Width	0.1	ft
	Spacing	100	ft
Matrix	Porosity	0.06	
	Thickness	200	ft
General	Perforated Length	2500	ft
	Fracture Half-Length	150	ft
	Area of Well Plane	500000	ft2
	# of hydraulic-fractures	25	
	Rock Compressibility	0.000004	1/psi
	Water Compressibility	4.2E-06	1/psi
	Initial Water Saturation	0.3	
	Initial Pressure	2950	psi
	Bottom-hole Pressure	500	psi
	Temperature	160	deg. F
	Gas Gravity	0.635	

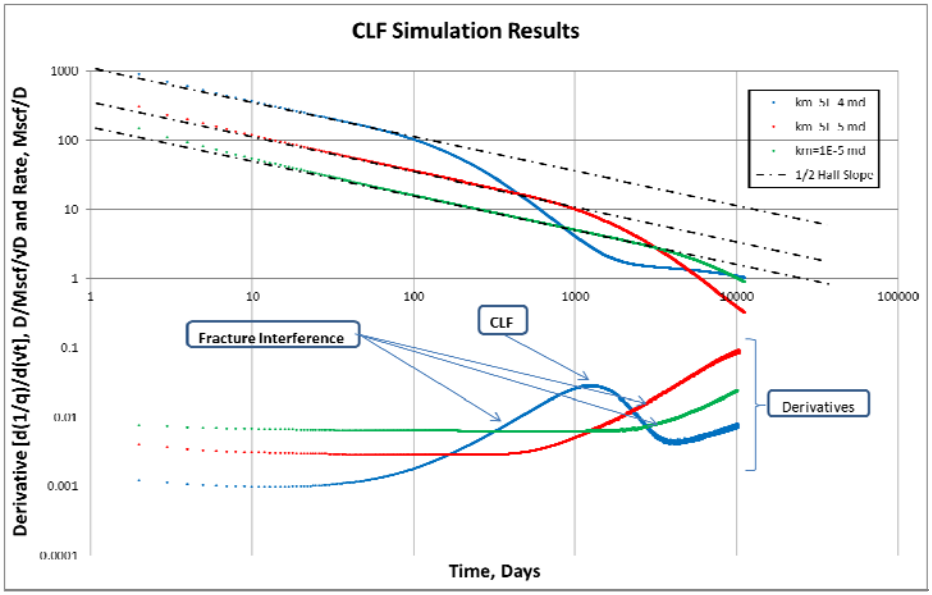

Fig. 5.1—Simulation results for CLF analysis. Upper half of the plot is showing rate versus time for different matrix permeability values simulated. Lower half of the plot is derivative of reciprocal rate with respect to square root of time. Linear flow exhibits flat (constant derivative) in this kind of plots.

From this simulation analysis it is clear that CLF would not occur in the practical life time of the horizontally drilled shale gas/oil well for matrix permeability less than 5.00E-5 md.

5.3 History Matching Algorithm for Shale Gas/Oil Wells

In order to apply linear Dual Porosity solutions proposed by El-Banbi (1998) a history matching algorithm was developed and programmed in Excel's VBA. Constant pressure and constant rate solutions are solved in Laplace domain and converted to real time domain by aid of Stehfest (1968) algorithm. Following are linear Dual Porosity solutions for constant rate (Eq. 5.1) and constant pressure (Eq. 5.2) inner boundary conditions in Laplace domain adopted from El-Banbi (1998). For complete derivation of solutions refer to Appendix C.

$$\overline{p_{wDL}} = \frac{2\pi}{s\sqrt{sf(s)}}\left[\frac{1+\exp(-2\sqrt{sf(s)}y_{eD}}{1-\exp(-2\sqrt{sf(s)}y_{eD}}\right] \quad \text{..... (5.1)}$$

$$\frac{1}{\overline{q_{DL}}} = \frac{2\pi s}{s\sqrt{sf(s)}}\left[\frac{1+\exp(-2\sqrt{sf(s)}y_{eD}}{1-\exp(-2\sqrt{sf(s)}y_{eD}}\right] \quad \text{..... (5.2)}$$

Since constant rate production is difficult to maintain in the field, wells are usually operated either on constant bottomhole flowing pressure or variable bottomhole flowing pressure. Thus, history matching program was designed to analyze data with constant or variable drawdown cases depending on user's preference. *Sthefest* VBA program was used to get semi-analytical solutions for constant pressure solutions. Deconvolution of drawdowns was done to analyze variable drawdown cases with constant pressure solutions which will be described in the following sections.

5.3.1 Correction for Time and Adsorbed Gas

Analytical solutions cannot be used to history match the production of shale gas wells without correction of time for gas properties change. Moreover, if one would like to include desorption of gas at low pressures another correction is required to the compressibility equation. Fraim and Wattenbarger (1987) presented a method to normalize the time to correct the gas properties change.

$$t_n = \int_0^t \frac{(\mu c_t)_i}{\mu(\bar{p})c_t(\bar{p})} d\tau \quad \text{..... (5.3)}$$

In order to apply this correction average pressure in the reservoir for particular time step is needed to be known. The average pressure is calculated from material balance equation which makes time normalization iterative process. Since constant volume reservoir is assumed, volumetric material balance equation for gases can be used to calculate average pressure for each time step.

It is well known that coal beds and organic rich shales have gas adsorbed at matrix surface. In shale gas reservoirs there are two types of fluid flow. The first flow is obeying Darcy's law (Eq. 5.4) and is migration of fluid in the pore space. The second flow is the diffusion of adsorbed gas which is following Fick's first law (King 1990) (Eq. 5.5).

$$q_g = \frac{0.00633kA}{2T} \frac{dm(p)}{dx} \quad \text{..... (5.4)}$$

$$q_g = \frac{-DAz_{sc}RT_{sc}}{p_{sc}} \frac{dC_M}{dx} \quad \text{..... (5.5)}$$

King (1990) also discusses how to modify material balance equations to account for adsorbed gas in the matrix. However, no one in the literature showed explicit equation for adsorbed gas in place at initial conditions.

One of the important equations to calculate average pressure at each time step is the modified material balance equation. In this work, modified material balance and total gas in place equations are derived explicitly by using initial work of King (1990). In conventional reservoirs material balance for gas reservoir without water drive is as following.

$$G_p = \frac{G\left(B_g - B_{gi}\right)}{B_g} \quad \text{..... (5.6)}$$

In explicit form it would be;

$$G_p = \frac{z_{sc}T_{sc}}{p_{sc}T}\left\{\frac{\left(1-S_{wi}\right)p_i V_b \varphi}{z_i} - \frac{\left(1-S_w\right)pV_b\varphi}{z}\right\} \quad \text{..... (5.7)}$$

which becomes

$$\frac{p}{z} = \frac{p_i}{z_i}\left[1 - \frac{G_p}{G}\right] \quad \text{..... (5.8)}$$

for conventional reservoirs without water drive.

In coal bed methane and shale reservoirs adsorbed gas also is added to material balance equation. Bumb and McKee (1986) show Langmuir isotherm for adsorption;

$$V_E = V_L \frac{p}{\left(p_L + p\right)} \quad \text{..... (5.9)}$$

where V_E is the volume of the adsorbed gas per ton of the rock. V_L and p_L stand for Langmuir volume and pressure, respectively. The unit of Langmuir volume is also

standard cubic feet of adsorbed gas per ton of the rock. In the lab it is always reported as standard cubic feet of adsorbed gas per ton of the rock. However, to calculate adsorbed gas in place standard cubic feet per cubic feet of the rock is required. Thus, we define a new Langmuir volume in following way.

$$V_{Lcuft} = 0.031214\rho_m V_L \quad \text{..... (5.10)}$$

where ρ_m is the matrix density in grams per cubic centimeters. On the other hand, densities of formation are usually measured as bulk densities, especially from well logs which can also be used in calculations. The bulk density of the formation is defined as;

$$\rho_b = \rho_m(1-\phi) + \rho_f\phi \quad \text{..... (5.11)}$$

Considering that matrix porosity in shales is low and the fluid density is much smaller than the bulk density (because gas will saturate the most part of the pore space which has very small density compared to matrix), matrix density can be approximated with known bulk density and matrix porosity in following way;

$$\rho_m = \frac{\rho_b}{(1-\phi)} \quad \text{..... (5.12)}$$

$$V'_{Lcuft} = 0.031214\rho_b V_L \quad \text{..... (5.13)}$$

Following these equations Adsorbed gas in place at any pressure *p* will be;

$$AGIP = V_b(1-\phi)V_{Lcuft}\frac{p}{(p+p_L)} = V_b(1-\phi)(0.031214\rho_m V_L)\frac{p}{(p+p_L)} \quad \text{..... (5.14)}$$

$$AGIP = V_b V'_{Lcuft}\frac{p}{(p+p_L)} = V_b(0.031214\rho_b V_L)\frac{p}{(p+p_L)} \quad \text{..... (5.15)}$$

Depending on which density is available, either equation can be used for calculation of adsorbed gas in place.

Modified material balance equation uses total gas in place which is the summation of free gas stored in pore space and adsorbed gas at the surface of matrix.

$$OGIP_T = V_b\left[\frac{\phi(1-S_{wi})}{B_{gi}} + V'_{Lcuft}\frac{p_i}{(p_i+p_L)}\right] \quad \text{..... (5.16)}$$

Therefore modified material balance equation will be;

$$G_p = V_b\left\{\left[\frac{\phi(1-S_{wi})}{B_{gi}} + V'_{Lcuft}\frac{p_i}{(p_i+p_L)}\right] - \left[\frac{\phi(1-S_w)}{B_g} + V'_{Lcuft}\frac{p}{(p+p_L)}\right]\right\} \quad \text{.... (5.17)}$$

$$G_p = \frac{V_b\phi}{T}\left(\frac{T_{sc}}{p_{sc}}\right)\left\{\begin{array}{l}\left[\frac{p_i(1-S_{wi})}{z_i} + \frac{T}{\phi}\left(\frac{p_{sc}}{T_{sc}}\right)V'_{Lcuft}\frac{p_i}{(p_i+p_L)}\right] - \\ -\left[\frac{p(1-S_w)}{z} + \frac{T}{\phi}\left(\frac{p_{sc}}{T_{sc}}\right)V'_{Lcuft}\frac{p}{(p+p_L)}\right]\end{array}\right\} \quad \text{..... (5.18)}$$

By introducing new compressibility factor (King, 1990); modified material balance equation looks much like a conventional material balance equation.

$$z^* = \frac{z}{(1-S_w) + \frac{zT}{\phi}\left(\frac{p_{sc}}{T_{sc}}\right)V'_{Lcuft}\frac{1}{(p+p_L)}} \quad \text{..... (5.19)}$$

$$G_p = \frac{V_b\phi}{T}\left(\frac{T_{sc}}{p_{sc}}\right)\left[\frac{p_i}{z_i^*} - \frac{p}{z^*}\right] \quad \text{..... (5.20)}$$

$$\frac{\bar{p}}{z^*} = \frac{p_i}{z_i^*}\left[1 - \frac{G_p}{OGIP_T}\right] \quad \text{..... (5.21)}$$

Eq. 5.20 is the modified material balance equation used to calculate average pressure iteratively.

Another important change that is required to make is the compressibility equation. Bumb and McKee (1986) show the effect of adsorption on compressibility of the rock. According to their work, following changes needs to be done on the compressibility equation.

$$c_t^* = c_f + c_w S_w + c_g\left(1 - S_w\right) + c_{gd} \quad \text{..... (5.22)}$$

$$c_{gd} = \frac{\rho_{gsc} V_{Lcuft}^{'} p_L}{\varphi_m \overline{\rho}_g \left(\overline{p} + p_L\right)^2} = \frac{\overline{B}_g V_{Lcuft}^{'} p_L}{\varphi_m \left(\overline{p} + p_L\right)^2} \quad \text{..... (5.23)}$$

Normalized time equation (Eq. 5.3) is also modified with new compressibility equation.

$$t_n = \int_0^t \frac{\left(\mu c_t\right)_i}{\mu\left(\overline{p}\right) c_t^*\left(\overline{p}\right)} d\tau \quad \text{..... (5.24)}$$

Please see Appendix D for complete derivation of equations.

5.3.2 Variable Bottomhole Pressure History Matching

One of the assumptions initially used for history matching of shale gas wells early in this work was constant bottomhole pressure assumption. This assumption worked quite well for gas wells because of "square effect" of pseudo pressure function. Since pseudo pressure function takes the square of the pressure, up to one or two hundreds of psi error in bottomhole pressure would not affect the difference of $m(p_i) - m(p_{wf})$. However, if more accurate match is desired and bottmhole flowing pressure for each rate is available then deconvolution theorem can be used to do superposition of

pressure drawdowns to calculate rate for each time step. Eq. 5.25 shows how to do superposition of drawdowns by using rate response function [$F_q(t)$].

$$q(t) = \sum_{i=1}^{n} (\Delta p_i - \Delta p_{i-1}) F_q (t_n - t_{i-1}) \quad \text{..... (5.25)}$$

Superposition of drawdown is not common in petroleum industry. Most of the time superposition of rates is used to calculate pressure drops for varying rates in well test analysis (Eq. 5.26).

$$\Delta p(t) = \sum_{i=1}^{n} (q_i - q_{i-1}) F_p (t_n - t_{i-1}) \quad \text{..... (5.26)}$$

Pressure response function [$F_p(t)$] is used from constant rate inner boundary condition solution for diffusivity equation. However, rate response function [$F_q(t)$] is calculated from constant bottomhole flowing boundary condition.

5.3.3 History Matching Algorithm

A program was written in Excel's VBA to history match the production of shale gas/oil wells with linear dual porosity model. A Least Absolute Value (LAV) regression was used in the algorithm. Two options are available for fluid type; oil and gas. History matching can be done either assuming constant pressure production by inputting average bottomhole pressure, or variable pressure production by inserting measured bottomhole pressures for each rate in the matching period. For linear Dual Porosity model there will be three unknowns to match as it was discussed in above sections; k_m, k_F, and y_e. However, sometimes k_m can be known from core reports or previously matched well which is close to analyzed one. In that case only two unknowns will be matched.

Therefore, there will be two options to select at the beginning of history matching, one is two unknowns matching, and the other one is three. Following are the steps to code the program in different languages.

1. Input daily rates and pressure (if available and variable pressure history match is preferred) to the program.
2. Input all necessary well completion and reservoir parameters in to yellow cells.
3. Identify flow regimes by using quarter (green) and half (black) slope lines.
4. Decide on date range that is desired to match and paste them to "*Selected Data for Analysis*" table.
5. Click on "Run History Matching" button and select fluid type (oil or gas), number of unknowns (two or three), and matching type (Constant pressure or variable pressure)
6. Programs reads inputs and initializes the first step.
7. If it is constant pressure matching then for each time step *Stehfest VBA* program is called and rates are calculated for dimensionless times. In case of gas, time is normalized before it is converted to dimensionless form
8. If it is variable drawdown matching then at the beginning of each calculation *Stehfest VBA* program is called to calculate rate response function [$F_q(t)$]. Then for each time step superposition is used to calculate rates. In case of gas, time is normalized before calling superposition subroutine.
9. Objective function is calculated in following way;

$$ObjFunc = \sum_{i=1}^{n} \left| q_{meas,i} - q_{calc,i} \right| \quad \text{..... (5.27)}$$

10. Regression is run for first iteration unknown variables are updated.
11. Objective function is checked again given tolerance. If satisfied, program terminates and variables giving the minimum objective function are used as a solution. If not, then steps 6-10 are repeated until satisfactory match is obtained.

5.4 Validation of Adsorption Modeling – Synthetic Cases

A reservoir simulation model was generated in CMG's GEM to validate equations derived for adsorption. A simple reservoir model, 10x10x1 (equal grid spacing with 5 ft) grid size, was built with dual permeability model to model desorption of gas from matrix surface to natural fractures. Table 5.2 shows important input and outputs used in comparison of modeling with and without including the adsorbed gas.

Table 5.2—Reservoir simulation results for modeling gas wells with adsorption		
Reservoir Property	No Adsorption	With Adsorption
Initial Pressure, psi	2500	2500
Langmuir Volume, gmole/lb	N/A	0.2
Langmuir Pressure, psi	N/A	500
Rock Matrix density, lb/cuft	120	120
Total Bulk Volume, res cuft	1.25000E+07	1.25000E+07
Total Pore Volume, res cuft	3.81513E+06	3.81513E+06
Total HC Pore Volume, res cuft	3.04197E+06	3.04197E+06
Formation Volume Factor, res cuft/scf	6.24043E-03	6.24043E-03
Free Gas in Place, scf	4.87461E+08	4.87461E+08
Adsorbed Gas in Place, scf	0	1.44966E+08
Total Gas in Place, scf	4.87461E+08	6.32425E+08

Hand calculation of free and adsorbed gas in place was done to validate analytical equations derived in above section with simulation results. Below is the explicit calculation of free and adsorbed gas in place.

$$FGIP = \frac{HCPV}{B_{gi}} = \frac{3.04\text{E}+06}{6.24\text{E}-03} = 4.87\text{E}+08\,\text{SCF}$$

$$V_{Lcuft} = 0.2\frac{gmole}{lb}16.043\frac{gr}{gmole}\frac{1lb}{453.59gr}\frac{SCF}{0.04237lb}\frac{120lb}{ft^3} = 20.03\frac{\text{SCF}}{\text{ft}^3}$$

$$AGIP = V_b(1-\phi)V_{Lcuft}\frac{p}{(p+p_L)} = 1.25\text{E}+07*(1-0.3021)*20.03*\left(\frac{2500}{2500+500}\right) =$$

$$= 1.4497\text{E}+08\,\text{SCF}$$

These values are the same as from simulation which confirms the accuracy and rigorousness of derived equations.

Below is the Fig. 5.2, showing a production of a shale gas well with and without adsorption of gas in matrix surface. As it is clear from the graph significance of adsorption in gas production increase as reservoir depletes. In other words, as the average reservoir pressure is getting close to Langmuir pressure.

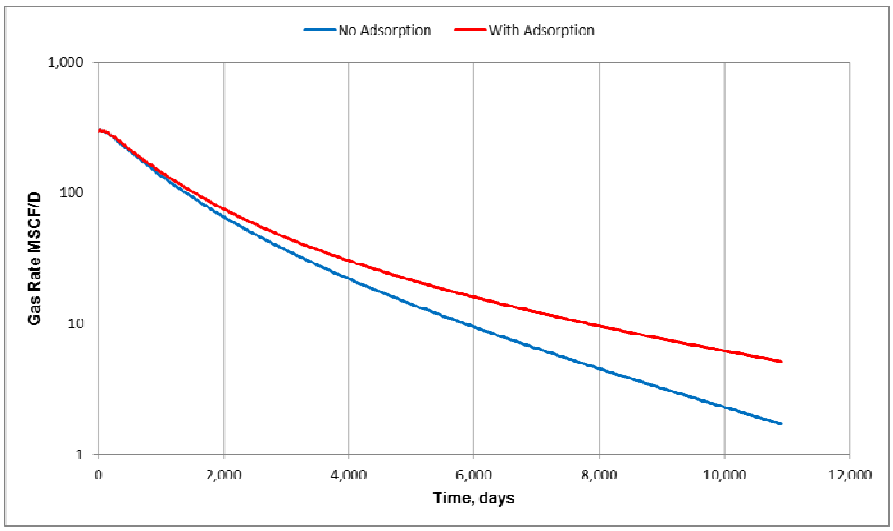

Fig. 5.2—Comparison of gas production from reservoir simulation model with and without adsorption.

5.5 Validation of Dual Porosity History Matching Program – Synthetic Cases

As it was discussed in above sections, important parameters group found for each flow regime. Table 5.3 summarizes flow regimes with found parameters group. Usually, in the field maximum of two transient flow regimes are observed – Bilinear and Linear. From Table 5.3 it is clear that to match these two regions at the same time, three unknowns should be found which makes solution non-unique – one degree of freedom. The unknown parameters are k_m, k_F, and y_e. If matrix permeability is known from history match of Well A which was drilled in the vicinity of the Well B which is going to be analyzed then k_m value of that Well A can be used as a known parameter for Well B. In this case solution will be unique. If Boundary Dominated Flow (BDF) region exists in the data then solutions can be unique for three unknowns problem with presence of Bilinear and Linear Flow – 3 equations, 3 unknowns.

Table 5.3—Summary of equations and unknown parameter group needed to be matched for each region		
Regions	Equations	Unknown Parameters
1	$q_g = \frac{\left[m(p_i) - m(p_{wf})\right]}{2844\pi\sqrt{\pi T}} \left[\frac{\mu}{0.00633}\right]^{1/2} A_{cw} \left\{[\phi V c_t]_F^{1/2} k_F^{1/2}\right\} \frac{1}{t^{1/2}}$	$[\phi V c_t]_F^{1/2} k_F^{1/2}$
2	$q_g = \frac{\left[m(p_i) - m(p_{wf})\right]}{14409.126T} \left[\frac{12\phi\mu c_t}{0.00633 L_F^2}\right]^{1/4} A_{cw} \left\{k_F^{1/2} k_m^{1/4}\right\} \frac{1}{t^{1/4}}$	$k_F^{1/2} k_m^{1/4}$
3	$q_g = \frac{\left[m(p_i) - m(p_{wf})\right]}{2844\pi\sqrt{\pi T}} \left[\frac{\phi\mu c_t}{0.00633}\right]^{1/2} \left\{k_m^{1/2} A_{cm}\right\} \frac{1}{t^{1/2}}$	$k_m^{1/2} A_{cm}$
4	$q_g = \frac{\left[m(p_i) - m(p_{wf})\right]}{2844\pi\sqrt{3\pi T}} \left[\frac{12\phi\mu c_t}{0.00633 L_F^2}\right]^{1/2} A_{cw} \left\{k_m^{1/2} y_e\right\} \frac{1}{t^{1/2}}$	$k_m^{1/2} y_e$
5	----------	

Three well models were generated in simulator with following flow regimes; Bilinear Flow + BDF, Linear Flow + BDF, Bilinear Flow + Linear Flow +BDF. Table 5.4 summarizes general input parameters used in generation of simulation models.

Table 5.4— Model parameters for synthetic data.			
Hydraulic Fracture	Porosity	0.002	
	Width	0.04	ft
	Spacing	400	ft
Matrix	Porosity	0.06	
	Thickness	300	ft
General	Perforated Length	10000	ft
	Fracture Half-Length	500	ft
	Area of Well Plane	6000000	ft2
	# of Macro-fractures	25	
	Rock Compressibility	0.000004	1/psi
	Water Compressibility	4.2E-06	1/psi
	Initial Water Saturation	0.3	
	Initial Pressure	2950	psi
	Bottom-hole Pressure	500	psi
	Temperature	160	deg. F
	Gas Gravity	0.635	

5.5.1 Two Unknowns History Matching

First, two unknown problem was checked to confirm uniqueness of solutions with simulated data. In this case regression was done only on k_F and y_e. Table 5.5 summarizes the results of this analysis.

Case-1:

This well exhibits Bilinear flow for 400 days followed by boundary dominated flow (Fig. 5.3). The first 100, 200, 300 and 400 days of production were used in History Matching program to calculate effective fracture permeability and fracture half length. Since all four cases gave approximately same results, only results of 400 days case is shown in Fig. 5.4.

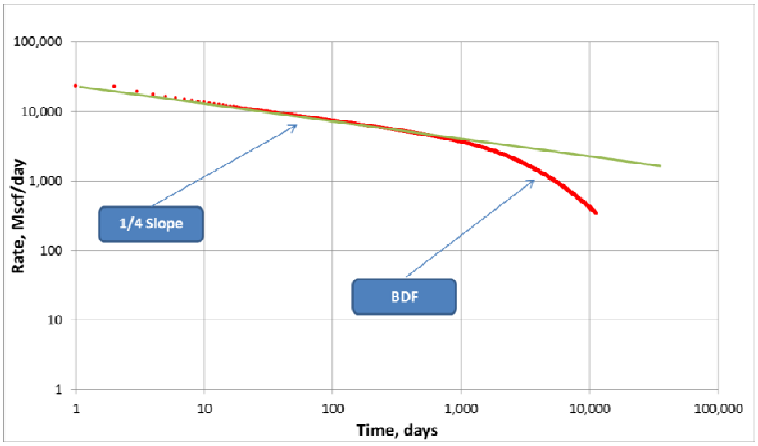

Fig. 5.3—Production history of Case-1. Bilinear flow (1/4 Slope) followed by BDF.

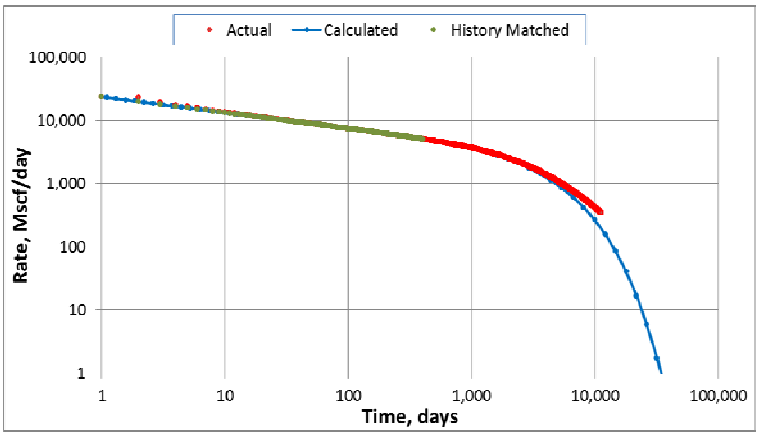

Fig. 5.4— History matching results for Case-1. Only 400 days (green points) were used in history matching program as an input.

Besides calculating the fracture permeability with less than 1.5% error, fracture half-length also was estimated as good as with 6% error. On the other hand, asymptotic equation for Bilinear flow clearly shows that rates in Bilinear flow do not depend on fracture half length. Does it mean that Bilinear flow can be matched with any fracture half length? This was the next thing that was checked. Two cases , y_e=100 ft and y_e=2500 ft were run in linear Dual Porosity model and it was observed that Bilinear flow

can be matched with any y_e as a guess as long as this guess is higher than actual value (Fig. 5.5). This result, actually, is not a surprise. If we look at the theory of Bilinear flow we will see that it lasts as long as the flow inside the fracture is transient. Once the transient flow ends Bilinear flow terminates. Longer the fracture half length, with constant values for other parameters, longer should be the transient flow inside the fractures.

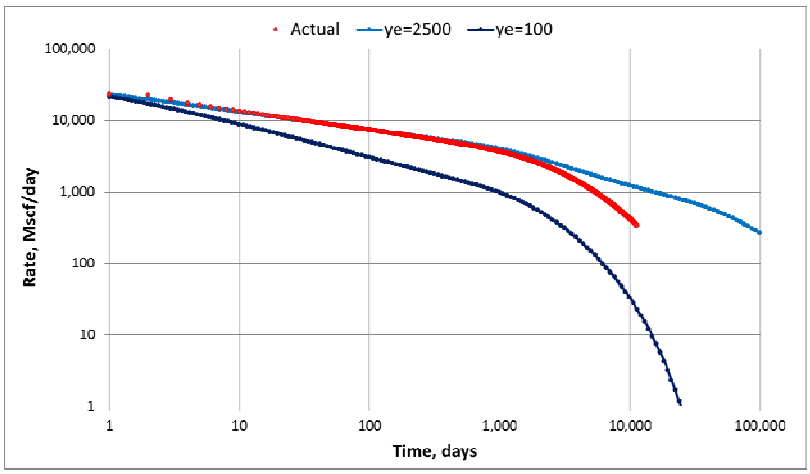

Fig. 5.5—Sensitivity analysis of y_e on Bilinear flow. Bilinear flow will be matched with any y_e as long as guess is greater than actual value.

Case-2:

In this case Linear flow is observed for 3000 days which is followed by BDF (Fig. 5.6). The first 500, 1000, 2000, and 3000 days were analyzed and all of them gave approximately same results for fracture half length. Fig. 5.7 shows history matching results for 3000 days case. However, values of fracture permeability were different in each case. This is expected result since from asymptotic equation for Region 4 we know

that linear flow depends on matrix permeability and fracture half length. On the other hand, same question is rising again – Does it mean that Linear flow can be matched with any fracture permeability? In order to check this two cases, k_F=50 md and k_F=1200 md were run in the program (Fig. 5.8). It was observed that Linear flow will match regardless of k_F as long as guess for k_F is higher than actual value. This is also not a surprise. Since low values of k_F will result in Bilinear Flow everything else being constant, it will lower the rates compared to Linear Flow and slope will be different.

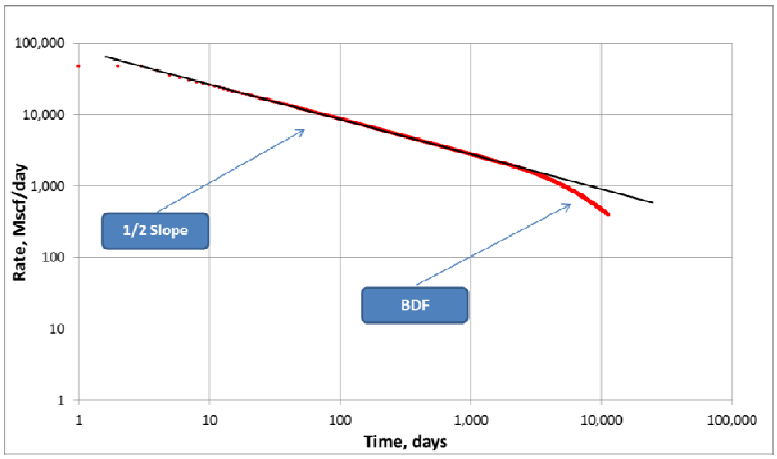

Fig. 5.6—Production history of Case-2. Linear flow (1/2 Slope) followed by BDF.

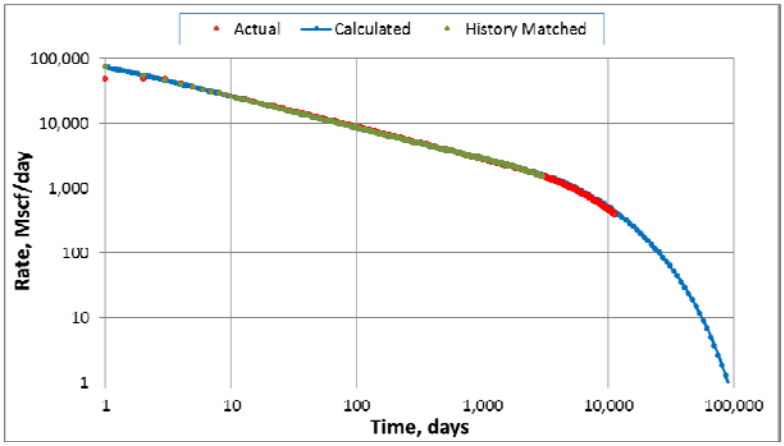

Fig. 5.7—History matching results for Case-2. Only 3000 days (green points) were used in history matching program as an input.

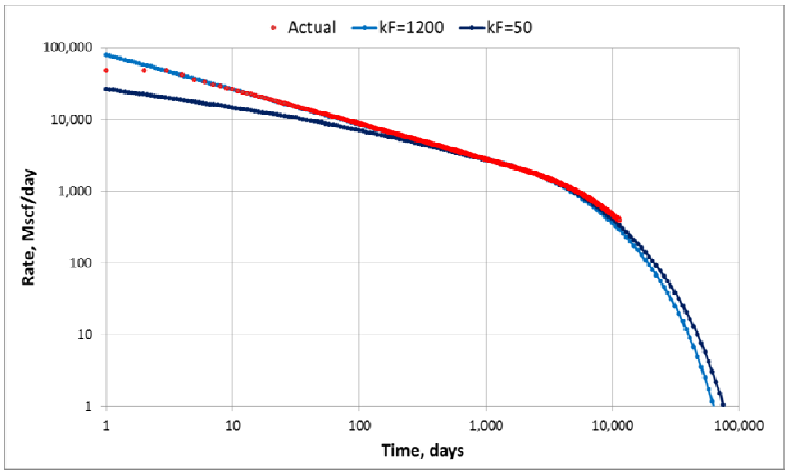

Fig. 5.8—Sensitivity analysis of k_F on Linear flow. Linear flow will be matched with any k_F as long as guess is greater than actual value.

Case-3:

This case was run to analyze the sensitivity of found parameters with wells having Bilinear flow followed by Linear (Fig. 5.9). Late Bilinear and early Linear flow were analyzed in history matching program (Fig. 5.10). Values of fracture permeability and fracture half-length were calculated with 5% and 3 % error, respectively. As it was

discussed earlier, if two flow regimes exist for two unknowns then uniqueness of solution is guaranteed.

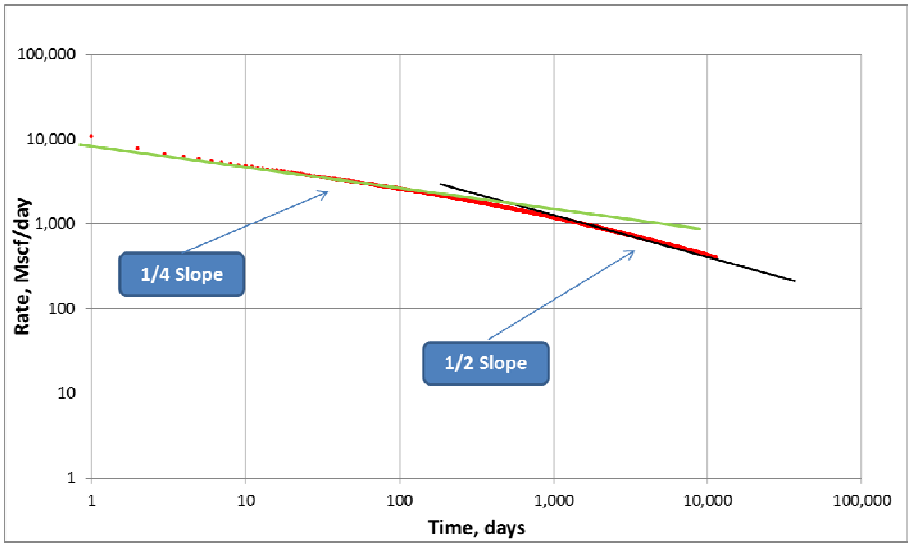

Fig. 5.9—Production history of Case-3. Bilinear flow (1/4 slope) followed by Linear flow (1/2 Slope).

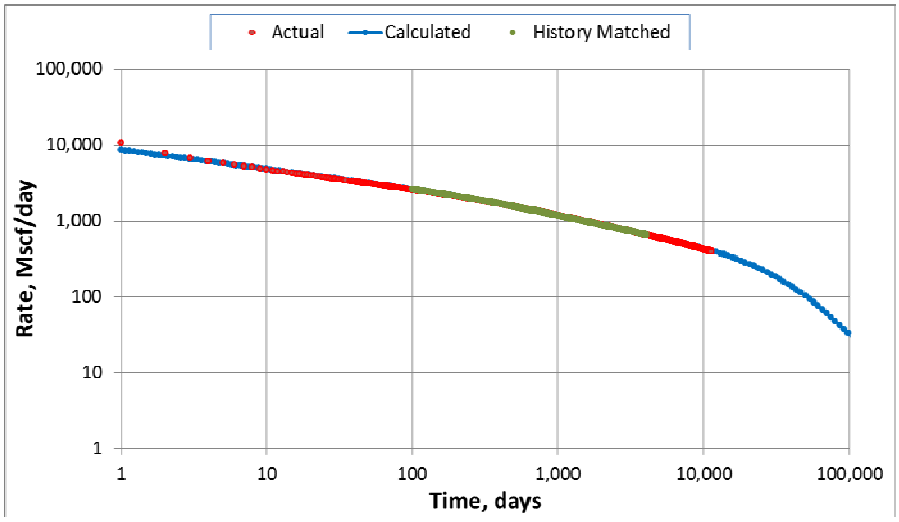

Fig. 5.10—History matching results for Case-3. Only late Bilinear and early Linear (green points) were used in history matching as an input (right).

Table 5.5—Summary of 2 unknown history matching problem					
Case	Period	Calculated		Actual	
		k_F, md	y_e, ft	k_F, md	y_e, ft
Case-1	100	25.74	413	25	500
	200	25.48	458	25	500
	300	25.37	472	25	500
	400	25.31	477	25	500
Case-2	500	490	539	300	500
	1000	539	534	300	500
	2000	643	527	300	500
	3000	790	521	300	500
Case-3	Bilinear	12.16	524	12	500
	Linear	24.8	519	12	500
	Late Bilinear + Early Linear	12.57	515	12	500

5.5.2 Three Unknowns History Matching

What if matrix permeability cannot be estimated with high confidence? In this case regression should be done on matrix permeability, too. According to asymptotic equations, solution to this problem will be non-unique. Now, we will look at the same wells but with three unknowns: k_m, k_F, and y_e. Table 5.6 summarizes the results of this analysis.

Case-1:

History matching program was run for different values of matrix permeability and regression was done on k_F and y_e. Although matrix permeability was wrong, excellent match was obtained with synthetic data. However, values found by regression for fracture permeability were not right answers. For lower values of k_m higher values of k_F were found and vice versa which is obvious from asymptotic equation for Region 4.

Then the program was modified to history match with three unknown variables and regression on k_m, k_F, *and* y_e was done simultaneously. Although the excellent visual match was observed, values found for unknowns were not right answers (Fig. 5.11).

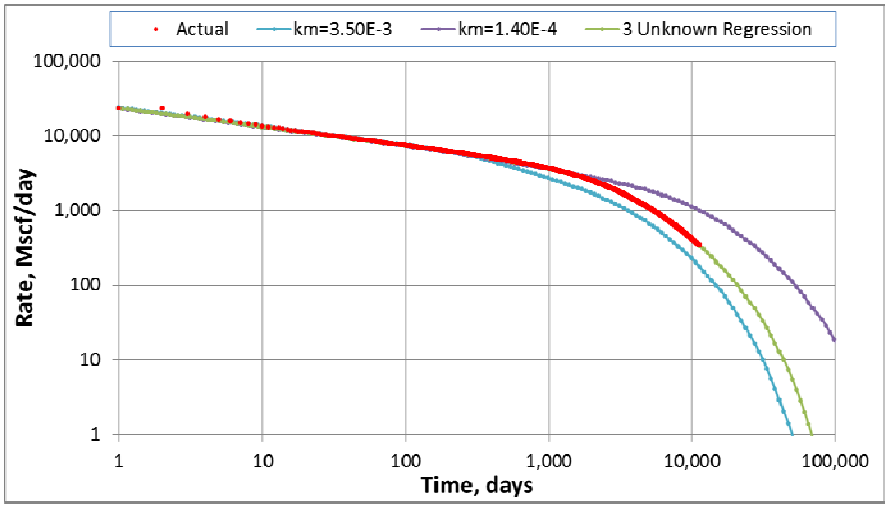

Fig. 5.11—History matching results for Case-1. Regression was done on k_F and y_e for early 400 days by assuming different k_m values (5 times greater and 5 times smaller than actual value). Then regression was done on all 3 parameters to get best match.

Case-2:

Like in previous model, first regression was done on k_F and y_e with different guesses for matrix permeability. Then matrix permeability also was added to unknowns and modified program was run to regress on k_m, k_F, and y_e at the same time. With different guesses for k_m, excellent matches observed with calculated and measured rates for Linear flow. Results of three unknown problem also were good for Linear flow (Fig. 5.12). However, values found for fracture half-length were not right which would affect the evaluation of reserves and estimation of SRV.

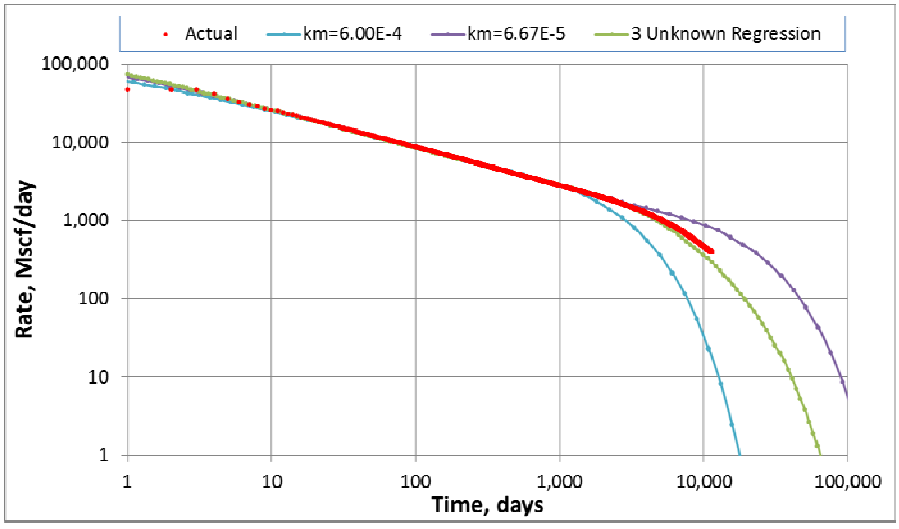

Fig. 5.12—History matching results for Case-2. Regression was done on k_F and y_e for early 3000 days by assuming different k_m values (3 times greater and 3 times smaller than actual value). Then regression was done on all 3 parameters to get best match.

Case-3:

In this case Bilinear and Linear flows were matched at the same time for different guesses for matrix permeability. Then one time regression was done on three parameters to get best estimates for k_m, k_F, and y_e. Like in previous two cases excellent matches were obtained for history matched part (Fig. 5.13). However, model parameters for k_m, k_F, and y_e were not calculated as actual input values.

In all three wells excellent visual match was obtained with actual and history matched rates. However, important parameters such as k_m, k_F, and y_e were not calculated accurate which shows that results are not unique. On the other hand, important parameter group for each region is same regardless of found values. This will be discussed in more detail in the next chapter where actual field data will be analyzed.

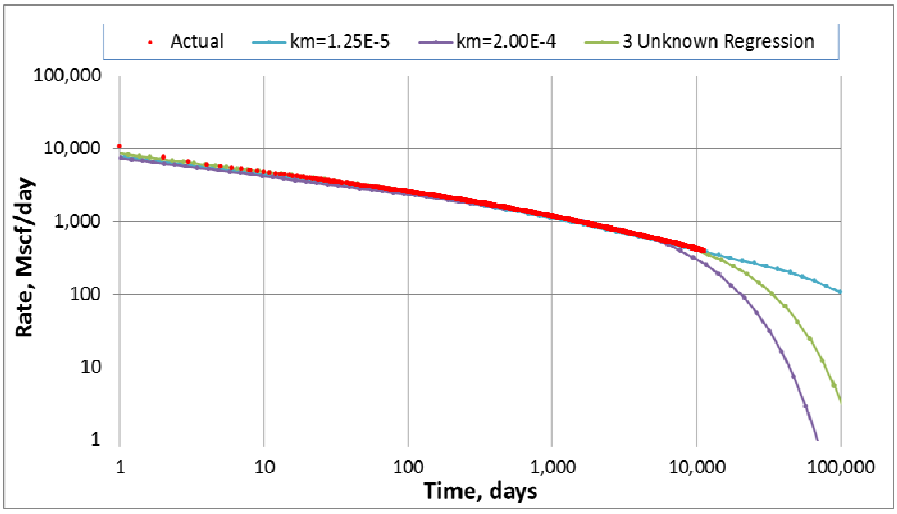

Fig. 5.13—History matching results for Case-3. Regression was done on k_F and y_e for late Bilinear and early linear by assuming different k_m (4 times greater and 4 times less than actual value). Then regression was done on all 3 parameters to get best match.

Table 5.6—Summary of 3 unknown history matching problem

Case	Calculated			Actual		
	k_m, md	k_F, md	y_e, md	k_m, md	k_F, md	y_e, md
Case-1	Assumed = 1.40E-4	50.15	1000	7.00E-04	25	500
	Assumed = 3.50E-3	11.56	348	7.00E-04	25	500
	Regressed = 6.41E-4	26.33	492	7.00E-04	25	500
Case-2	Assumed = 6.00E-4	205	306	2.00E-04	300	500
	Assumed =6.67E-5	923	926	2.00E-04	300	500
	Regressed = 2.89E-4	645	434	2.00E-04	300	500
Case-3	Assumed = 1.25E-5	21.45	999	5.00E-05	12	500
	Assumed = 2.00E-4	4.83	283	5.00E-05	12	500
	Regressed = 7.71E-5	10	411	5.00E-05	12	500

5.5.3 Variable Drawdown History Matching

In Section 5.3.2 a technique was shown to match wells with variable bottomhole pressure production. To check applicability of the method simulation model was built with typical parameters of a shale gas well. To mimic the behavior of shale gas wells, production data and reservoir properties of one Woodford well is used. Table 5.7 summarizes important reservoir and horizontal well properties used in simulation model. After running simulation about 1200 days rates and pressures were recorded to use in variable drawdown history matching (Fig. 5.14).

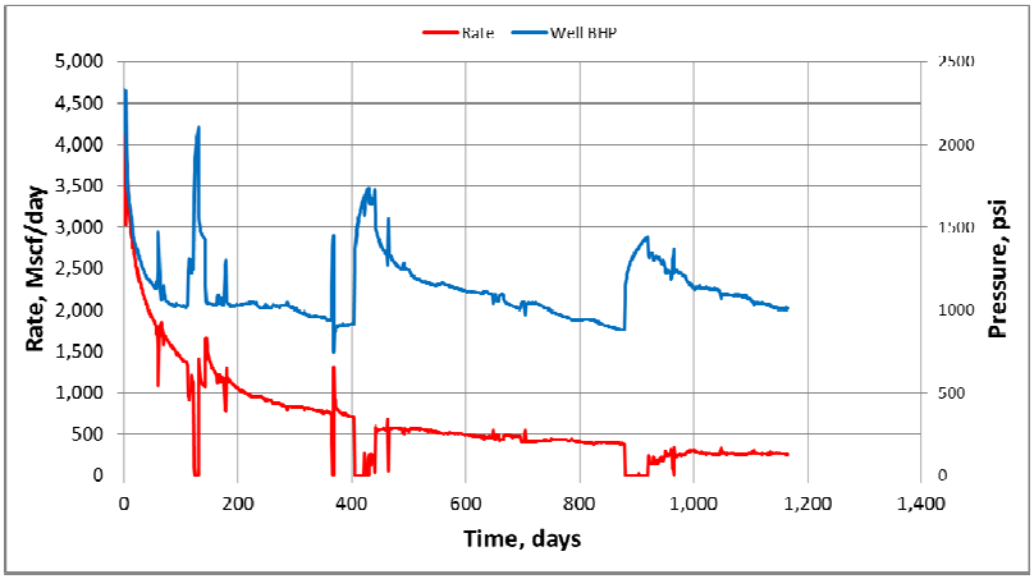

Fig. 5.14—Rates and bottomhole flowing pressures for synthetic well. Production history was simulated for typical well behavior in Woodford shale.

Table 5.7—Completion and reservoir parameters for synthetic well			
Hydraulic Fractures	Porosity	0.002	
	Permeability	50	md
	Width	0.04	ft
	Spacing	110	ft
Matrix	Porosity	0.0425	
	Permeability	0.00002	md
	Thickness	250	ft
General	Perforated Length	2200	ft
	Fracture Half-Length	400	ft
	Area of Well Plane	1100000	ft2
	# of Macro-fractures	20	
	Rock Compressibility	0.000004	1/psi
	Water Compressibility	0.0000042	1/psi
	Initial Water Saturation	0.3	
	Initial Pressure	3850	psi
	Bottom-hole Pressure	1000	psi
	Temperature	210	deg. F
	Gas Gravity	0.62	

Fig. 5.15 is a log-log plot of the rate versus time and a Cartesian plot of normalized reciprocal rate versus square root of time. From the log-log plot it is clear that well was producing under bilinear flow for more than 50 days, followed by Linear flow. Boundary effects are also visible from both plots.

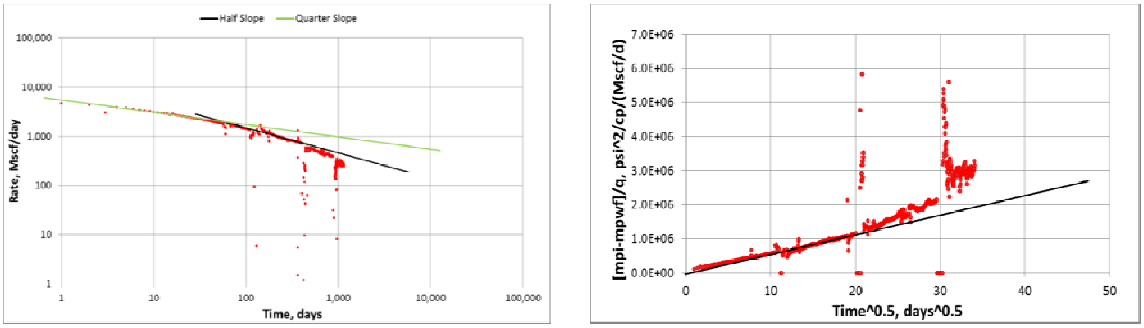

Fig. 5.15—Production history of synthetic well: Bilinear (quarter slope) followed by Linear (half slope) (left). Normalized reciprocal rate versus square root of time plot for synthetic well: Linear flow period shows straight line (right).

First, the two unknown problem was solved with history matching program for both constant drawdown and variable drawdown cases. Fig. 5.16 is showing history matching results. In both cases values for fracture permeability and half-length were found with less than 5% error, but variable drawdown case results are more accurate than constant drawdown case.

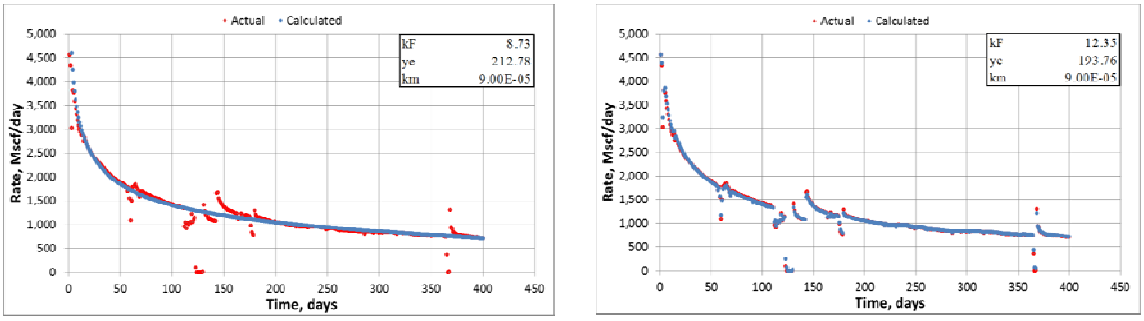

Fig. 5.16—History matching results of synthetic well for constant bottomhole flowing pressure (CP) case with 2 unknowns: k_F and y_e. First 400 days were matched (left). History matching results of synthetic well for variable bottomhole flowing pressure (VP) case with 2 unknowns: k_F and y_e. First 400 days were matched (right).

Then three unknown problem was solved assuming that matrix permeability is also unknown (Fig. 5.17). Although results of constant drawdown case are far away from actual values of parameters, this match should be considered as good because $k_m^{1/2} y_e$ for both constant and variable drawdown cases are the same. The same conclusion can be drawn for Bilinear part of the flow, too where $k_F^{1/2} k_m^{1/4}$ from constant and variable drawdown cases are very similar (Table 5.8).

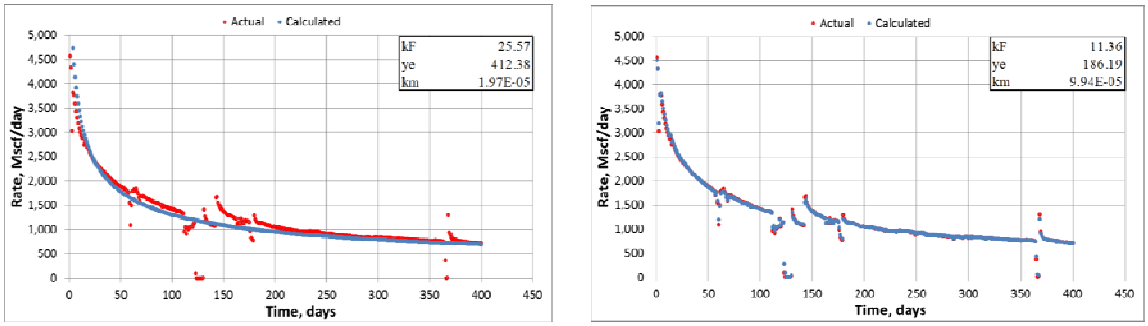

Fig. 5.17—History matching results of synthetic well for constant bottomhole flowing pressure (CP) case with 3 unknowns: k_F, k_m and y_e. First 400 days were matched (left). History matching results of synthetic well for variable bottomhole flowing pressure (VP) case with 3 unknowns: k_F, k_m and y_e. First 400 days were matched (right).

Finally, the whole production period was used in history matching for both cases. Since boundary effects were seen in the life of the well, problem should have more unique solution – 3 unknowns and 3 flow regimes. Fig. 5.18 is showing the results of these cases. An excellent match observed in both cases but values obtained for 3 unknowns from variable drawdown case are more accurate. Table 5.8 summarizes the important results of this analysis. One conclusion can be drawn from these observations: History matching with variable drawdown should give better results than constant

drawdown assumption. However, the difference in accuracy is not significant enough to favor variable drawdown history matching. Since less computation will be done for constant drawdown matching than for the variable drawdown, for practical purposes, the former is recommended. Moreover, accurate and continuous pressure records may not be available for each well which also forces use of the constant drawdown matching.

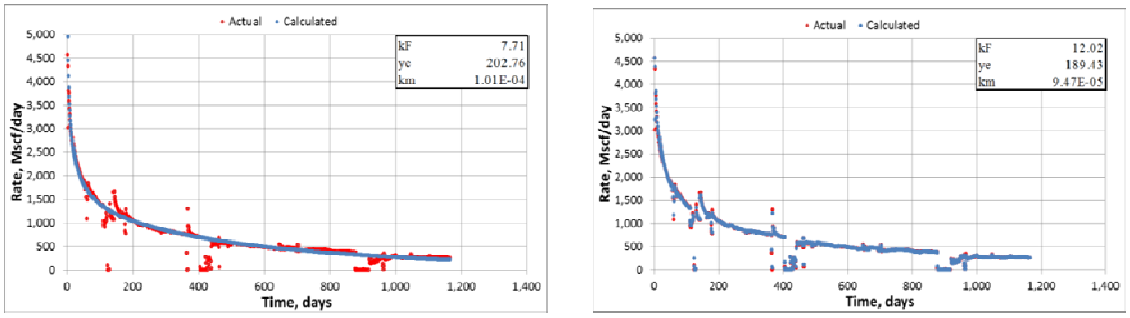

Fig. 5.18—History matching results of synthetic well for constant bottomhole flowing pressure (CP) case with 3 unknowns: k_F, k_m and y_e. The whole production period was matched (left). History matching results of synthetic well for variable bottomhole flowing pressure (VP) case with 3 unknowns: k_F, k_m and y_e. The whole production period was matched (right).

Table 5.8—Summary of history matching results for synthetic well								
Cases	**Initial Guesses**			**Calculated Values**				
	k_F	y_e	k_m	k_F	y_e	k_m	$k_F^{1/2}k_m^{1/4}$	$k_m^{1/2}y_e$
CP 2 unknowns 400 days	50	400	9.00E-5	8.73	212.78	9.00E-5	**2.88E-1**	**2.02**
VP 2 unknowns 400 days	50	400	9.00E-5	12.35	193.76	9.00E-5	**3.42E-1**	**1.84**
CP 3 unknowns 400 days	50	400	9.00E-5	25.57	412.38	1.97E-5	**3.37E-1**	**1.83**
VP 3 unknowns 400 days	50	400	9.00E-5	11.36	186.19	9.94E-5	**3.37E-1**	**1.86**
CP 3 unknowns whole period	50	400	9.00E-5	7.71	202.76	1.01E-4	**2.78E-1**	**2.04**
VP 3 unknowns whole period	50	400	9.00E-5	12.02	189.43	9.47E-5	**3.42E-1**	**1.84**
Actual Values				10	195	9.00E-5	**3.08E-1**	**1.85**

5.5.4 History Matching of Shale Oil Well

In sections above gas wells were used as a synthetic data to validate the robustness of proposed method. The method should be equally applied to oil wells, too as long as average reservoir pressure is above bubble point pressure. In other words, the method works for single phase fluid flow, either gas or oil. A reservoir simulation model was built to show applicability of the method to shale oil wells. It was modeled in a way that fluid flow is always above bubble point pressure, so that assumption of single phase fluid is honored. Table 5.9 summarizes important inputs for the well.

Table 5.9—Completion and reservoir parameters for synthetic shale oil well			
Hydraulic Fractures	Porosity	0.3	
	Permeability	5000	md
	Width	0.05	ft
	Spacing	50	ft
Matrix	Porosity	0.0245	
	Permeability	0.0001	md
	Thickness	300	ft
General	Perforated Length	2200	ft
	Fracture Half-Length	700	ft
	Area of Well Plane	750,000	ft^2
	# of hydraulic-fractures	25	
	Rock Compressibility	0.000008	1/psi
	Water Compressibility	0.000006	1/psi
	Initial Water Saturation	0.2	
	Initial Pressure	3000	psi
	Bottom-hole Pressure	300	psi

Rate history of this well is shown in Fig. 5.19. As it is clear from plot early part of the flow is Linear flow (Half slope on log-log plot) and later part is BDF. First, only linear flow part was put into a program for history matching with known permeability. Then the same period was analyzed assuming matrix permeability is also unknown (Fig. 5.20). Fracture permeability from matching found as 1000 md, where actual one was 5000md. The reason for this is the constraint for upper limit of k_F in the program. It was chosen to utilize the field data application, since nobody expects to have permeability greater than 1000 md in the fracture created in shale formation. From these results it is clear that method is working quite well for oil wells, too.

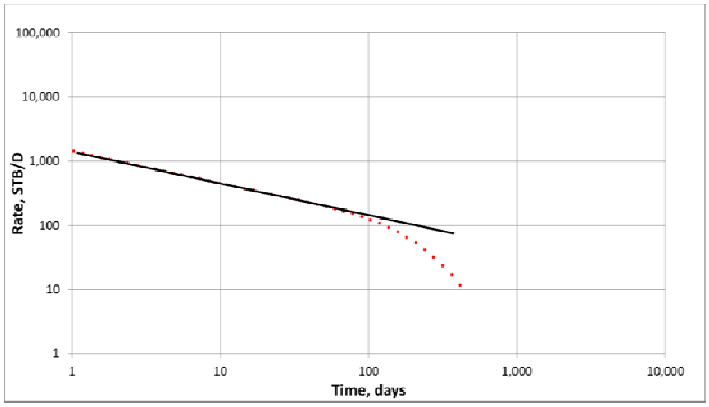

Fig. 5.19—Rate history of simulated horizontal shale oil well with hydraulic fractures on a log-log plot.

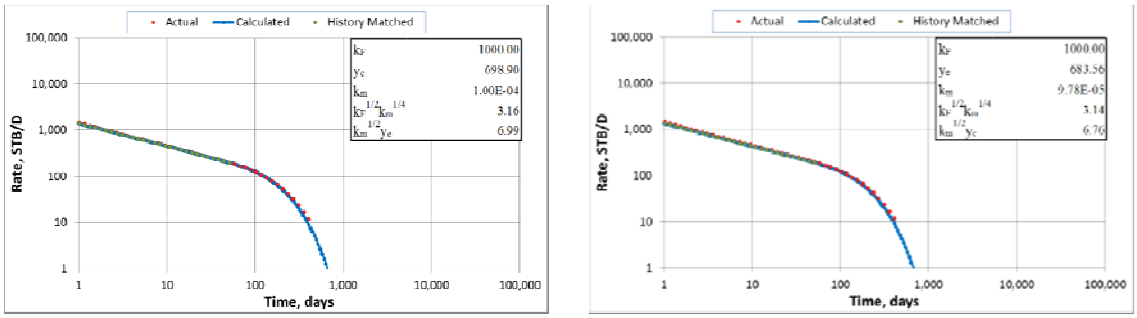

Fig. 5.20—History matching results from known (left) and unknown (right) matrix permeability cases.

5.6 Chapter Summary

In this chapter validation of application of Dual Porosity model on history matching of horizontally drilled shale gas/oil wells was described. First, the most important assumption – assumption of constant drainage volume is validated with the simulation model. Since analytical solutions are used for history matching, correction for gas properties should be done with care not to have errors in rates. Correction for adsorbed gas is also explained in detail and all derivations are outlined in Appendix D. Despite some confusing concepts in the literature about correction of adsorbed gas, right

equations were derived for compressibility and original gas in place. CMG's GEM is used to build simulation model and analytic solutions for adsorbed gas derived in this thesis checked with simulation results.

Different simulation models were built in CMG's IMEX to check robustness of the software developed in this research for history matching and forecasting with Dual Porosity model. Both gas and oil wells used to confirm that method works well with programmed software in Excel's VBA.

Besides constant bottomhole pressure production, variable bottomhole pressure production also was added to program if user wants to match rates with measured pressure drops. It was shown that assumption of constant bottomhole pressure gives results as good as matching with variable drawdowns for gas wells because of the "square effect" in pseudo pressure function. On the other hand, variable bottomhole pressure matching takes more time and uses more CPU than constant pressure assumption. Moreover, if measured pressures are erroneous then it is impossible to get the good match because program will try to match wrong pressure data. Therefore, it was decided to use constant bottomhole pressure production, by taking the mean of measured pressures for matching period.

CHAPTER VI

HISTORY MATCHING AND FORECASTING OF SHALE GAS WELLS—APPLICATION TO THE FIELD DATA

6.1 Introduction

In this chapter field examples from different shale plays will be analyzed with proposed method. Analyzed wells are mainly gas wells from Barnett, Fayetteville, and Woodford shales. The method can be equally applied to oil wells as it was shown in Chapter V on synthetic data. The reason for analyzing gas wells only is the lack of proper field data for oil wells. At the time when this research was started most of the companies were drilling hundreds of gas wells per year in shale plays like Barnett, Fayetteville, Woodford, Marcellus, and Haynesville. However, recently because of huge gap between oil and gas prices most of the companies favoring to drill oil wells. One of the biggest shale play recently discovered is Eagle Ford Shale where many companies acquired leases in condensate and oil zone. This shows that in the future shale oil will attract investors as shale gas did in 2000's.

As it was discussed in Chapter V there are few assumptions to apply the proposed method. If those assumptions are not satisfied then method would not work very well. One of the main assumptions is constant bottomlhole flowing pressure production. It was shown in Chapter V that in the absence of accurate pressure measurements and in case of fairly constant bottomhole pressure (with hundreds of psi

error) a method will give results as accurate as variable drawdown matching in gas wells. Therefore, constant bottomhole pressure is assumed in the analyzed wells below.

Completion data with petrophysical reports are required to apply this method. Completed horizontal well length with number perforation clusters is one of the important inputs. Porosity of hydraulic fractures were assumed to be 0.2 % with fracture with of 0.04 ft. Porosity of matrix and sometimes even permeability (in Fayetteville wells) can be used from core reports. Gas gravity and reservoir temperature are important to calculate pseudo pressure function along with viscosity and compressibility of the gas.

6.2 Forecasting with Dual Porosity Model

Forecasting with proposed method is very simple to apply yet fast and rigorous. First, selected part of the field data is history matched with model and values for k_m, k_F, and y_e is estimated. Once the history matching part is complete program automatically does forecasting with found parameters. Remaining life of the well, expected ultimate recovery (EUR), original gas in place (OGIP) is calculated with given economic limit – abandonment rate.

Normalized time concept is used to convert real times to analytical times for gas well analysis. For a given range of dates program converts times to analytical time, gets dimensionless rates from *Stehfest VBA* code, and finally converts dimensionless rates back to field rates.

6.3 Solving for Exact Values of Unknowns

In this section two gas wells from Barnett Shale will be analyzed with proposed method. Table 6.1 summarizes important reservoir and completion parameters for these wells. Exact values k_m, k_F, and y_e will be showed as a result of history matching. Forecasting is done automatically once the history matching of the rates is finished.

6.3.1 Well B-151

Different authors (Bello and Wattenbarger (2009, 2010), Al-Ahmadi et al., 2010) used matrix permeability, k_m=1.5E-4 md for Barnett wells in their analysis. In our history matching analysis we started as if matrix permeability is known and then showed possible values for it. From Fig. 6.1 it is clear that Well B-151 is showing Bilinear flow followed by Linear. Late data also indicates that BDF or interference between fractures has started.

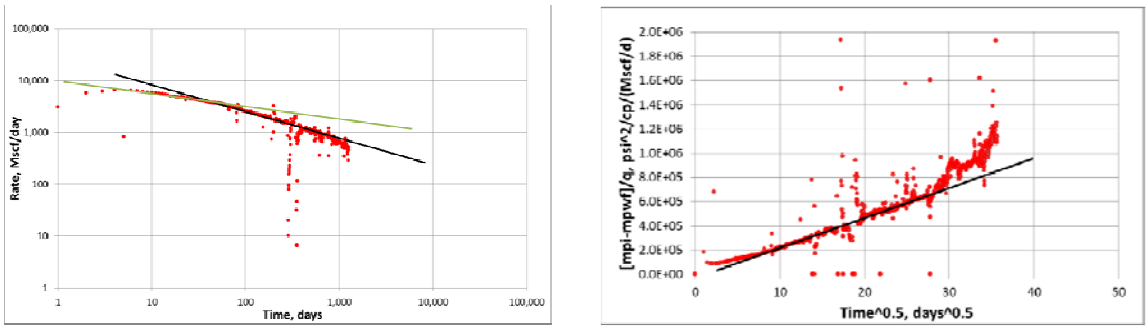

Fig. 6.1—Production history (left) and square root of time plot (right) of Well B-151. Well is in transient Linear flow: half slope on log-log plot and linear behavior on square root of time plot.

First, only Linear flow period is matched with proposed model with "known" permeability. If we look at Fig. 6.2 it is clear that fracture half-length is underestimated.

Asymptotic equation for Region 4 should give us a clue that initial assumption for matrix permeability, k_m=1.5E-5 md is wrong for this well. A multi-parameter regression was done on this well in order to history match the Linear flow period (Fig. 6.3). Although three of the matrix permeability values match linear period quite well only one of them is an actual solution of the problem.

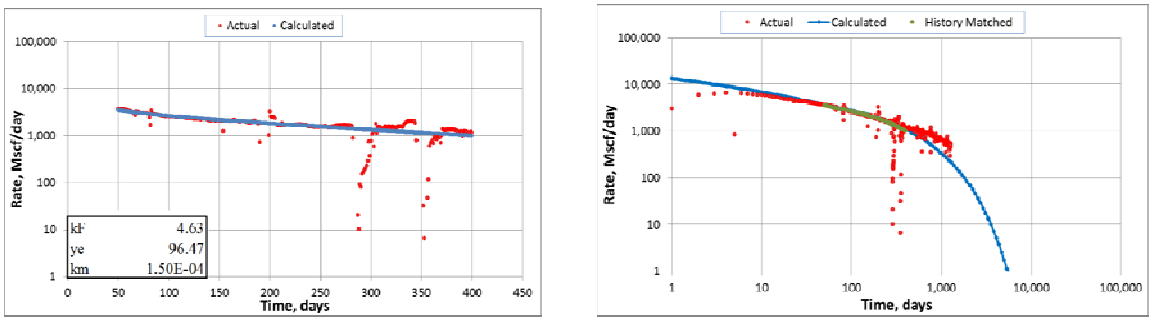

Fig. 6.2—History matching results for Well B-151. Matrix permeability is assumed to be known as 1.5E-4 md and regression was done on k_F and y_e (left). A part of Linear flow (green points) were used in history matching. From figure (right) it is clear that assumed k_m (1.5E-4 md) is overestimated because found y_e is less than actual value (Curve bending down sooner).

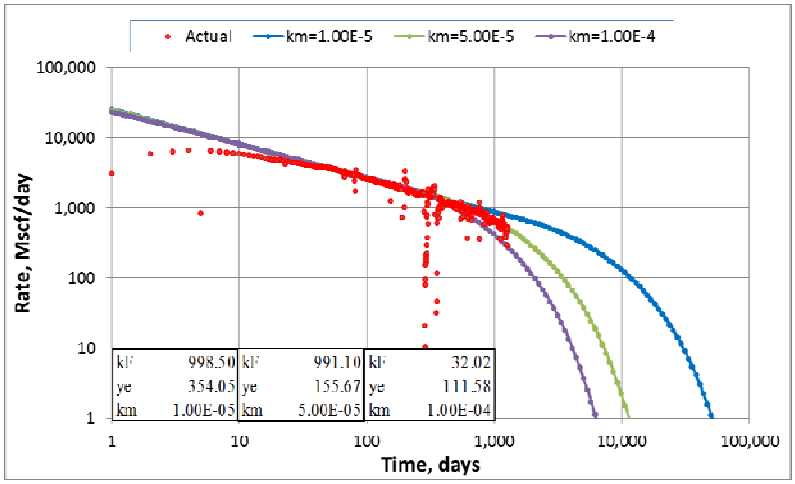

Fig. 6.3—History matching results for Well B-151. Regression was done on k_F and y_e for different assumptions of k_m. Linear period is used in history matching. It was concluded that k_m =5.00E-5 md is giving the best match. Therefore, matrix permeability for this well is estimated as 5.00E-5 md.

Since we have BDF in this well, we know that k_m=5.00E-5 md is the right solution because it correctly determines when curve will bend down. However, usually we do not see the BDF in the production history of the well. In that case there is a range of values for both matrix permeability and fracture half-length which can match Linear flow part. Once the correct solution is obtained, regression can be done on k_F to match the early Bilinear part of the flow. Since the matrix permeability found from this analysis is believed to be actual solution, there is only one k_F value which can match the early few points of Bilinear Flow (Fig. 6.4).

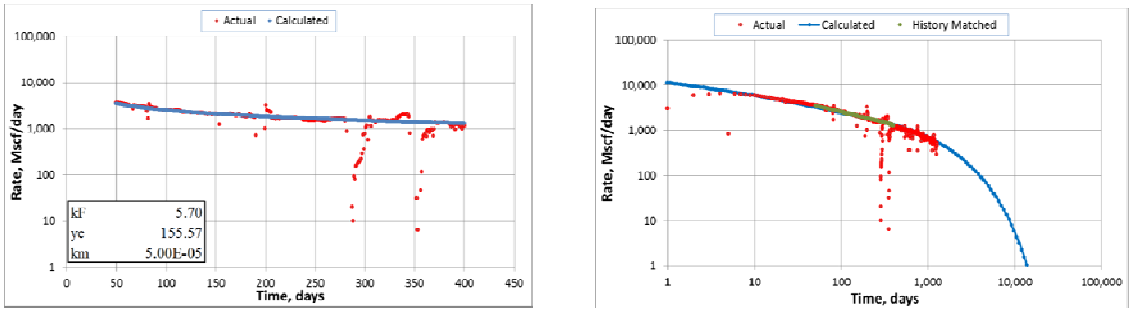

Fig. 6.4—History Matching Results for Well B-151 with known matrix permeability, k_m =5.00E-5 md. Regression also was done on k_F to match the early Bilinear flow.

6.3.2 Well B-130

Well B-130 is from the same county (Johnson County) as B-151 therefore, formation properties of this well are believed to be quite similar. From log-log plot of rate versus time we can see that well exhibits long period of Linear flow (Fig. 6.5). However, at the late times, well has a problem in keeping up the rates stable. After doing analysis for liquid loading it was concluded that most of the data points at the late production of the well are below critical rate. From Fig. 6.5 it is clear that if we ignore rates below critical then the well is still in transient.

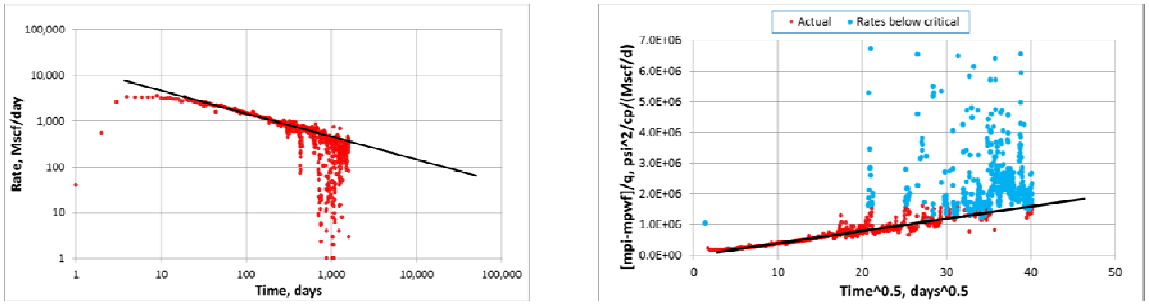

Fig. 6.5—Production history of Well B-130 (left). Square root of time plot for Well B-130 (right). Linear flow is exhibiting linear behavior shown with black line. Blue points are rates below critical value not to have liquid loading.

The period which is showing clearly ½ slope (Linear) in log-log plot was used in history matching program. Since Well B-130 is from the same county as Well B-151 matrix permeability value found for Well B-151 was used as known parameter for Well B-130. Fig. 6.6 shows results of history matching where regression was done only on fracture half length. Although fracture permeability is also shown as a result, it cannot be found exactly because Bilinear flow was not observed in this well. Value of 20 md should be considered as a lower limit for this well. The actual value of fracture permeability can be any number bigger than 20 md. Although excellent match was obtained (Fig. 6.6) it does not mean that parameters found from history matching are exactly same parameters that exist in the reservoir. It should be noted that results are based on the assumption that matrix permeability is known. If matrix permeability is less that the assumed value, then fracture half-length would be bigger which will result in bigger OGIP, too. Therefore, results should be tuned for new production data or any other updates on parameters to decrease the uncertainty as much as possible.

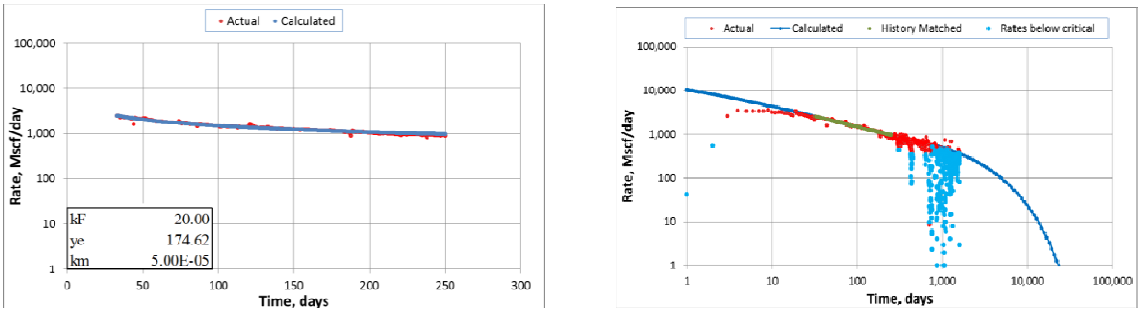

Fig. 6.6—History matching results with known matrix permeability k_m=5.00E-5 md (left). Blue points are showing rates below critical value not to have liquid loading (right). From plot it is clear that assumed value for k_m is good enough not to underestimate y_e or *OGIP*.

Table 6.1—Summary of completion and reservoir properties of wells used as field examples for 2 unknowns problem				
	Parameters	Well B-151	Well B-130	Units
Hydraulic Fractures	Porosity	0.002	0.002	
	Width	0.04	0.04	ft
	Spacing	75	112	ft
Matrix	Porosity	0.06	0.06	
	Thickness	300	300	ft
General	Perforated Length	3,600	2,800	ft
	Area of Well Plane	2,160,000	1,680,000	ft2
	# of Macro-fractures	48	25	
	Rock Compressibility	0.000004	0.000004	1/psi
	Water Compressibility	0.0000042	0.0000042	1/psi
	Initial Water Saturation	0.3	0.3	
	Initial Pressure	2,950	2,950	psi
	Bottom-hole Pressure	500	500	psi
	Temperature	160	160	deg. F
	Gas Gravity	0.635	0.635	
	Langmuir Volume	96	96	scf/ton
	Langmuir Pressure	650	650	psi

6.4 Solving for Important Parameter Group

In this section 1 well from Barnett, 1 well from Fayetteville, and 1 well from Woodford Shale will be analyzed with proposed methods. In section above it was showed that values found for k_m, k_F, and y_e are not unique if three different flow regimes are not observed for the same well. Therefore, instead of looking for exact values of k_m, k_F, and y_e important parameter group found for each flow regime. As it was shown in Chapter V Section 5.5, no matter what values found for k_m, k_F, and y_e, products like $k_F^{1/2}k_m^{1/4}$ and $k_m^{1/2}y_e$ will be same for Bilinear and Linear flow for every match, respectively (Table 5.3).

6.4.1 Well B-15

This well was drilled in Barnett shale. Table 6.2 summarizes important reservoir and completion parameters for this and all other wells which are going to be discussed in this section.

Well B-15 shows Bilinear flow (quarter slope) followed by Linear flow (half slope) in a log-log plot (Fig. 6.7). At late time, well has a problem in keeping up the rates on half slope line. Therefore, boundary dominated flow is suspected when rates deviate from straight line. This is also true for normalized reciprocal rate versus square root of time (Fig. 6.7).

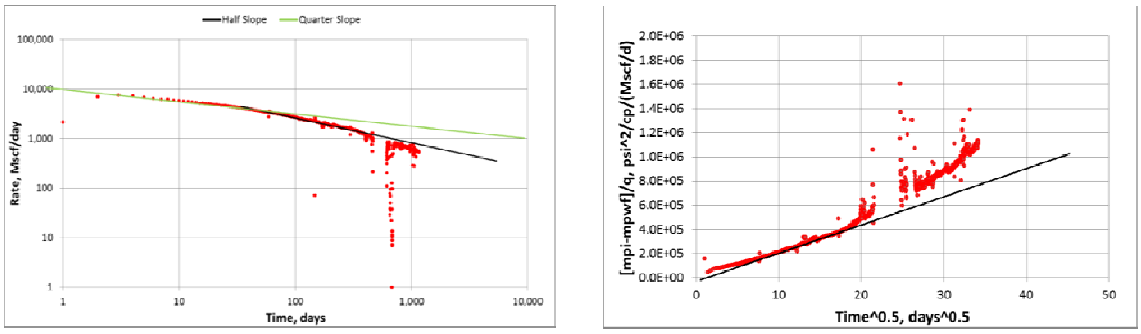

Fig. 6.7—Production history of Well B-15: Bilinear (quarter slope) followed by Linear (half slope) (left). Normalized reciprocal rate versus square root of time plot for Well B-15: Linear flow period shows straight line (right).

During history matching of Bilinear and Linear flow with three unknowns, non-unique results will be obtained. Therefore, rather than getting quantitative numbers for k_F, k_m, and y_e, qualitative results like $k_F^{1/2}k_m^{1/4}$ and $k_m^{1/2}y_e$ are obtained for Bilinear and Linear flow, respectively.

First, only 400 days of production period were matched (Fig. 6.8). Both $k_F^{1/2}k_m^{1/4}$ and $k_m^{1/2}y_e$ values are calculated according to found parameters. Then whole production period was matched by excluding points which are below critical rate not to have liquid loading. New $k_F^{1/2}k_m^{1/4}$ and $k_m^{1/2}y_e$ values found from history matching are in the same range with previous ones however, values found for k_F, k_m, and y_e are different. Since a good match was obtained with the proposed model, forecasting was done for Well B-15 with found parameters (Fig. 6.9).

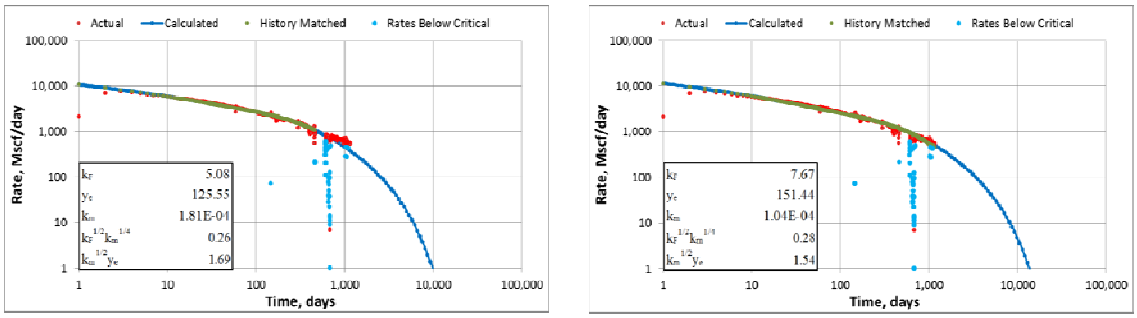

Fig. 6.8—Early part of the production (No shut-ins or rate fluctuation is observed) was matched for Well B-15 (left). The whole production period of Well B-15 was matched for forecasting (right).

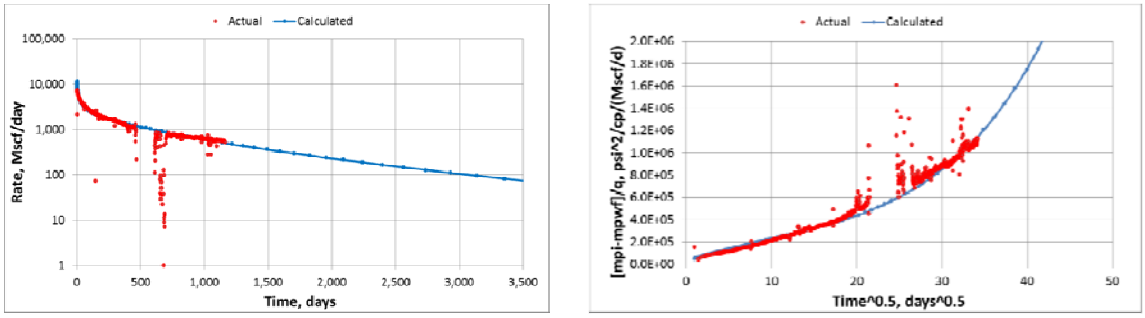

Fig. 6.9—Forecasting for Well B-15 with parameters found from history matching (left). Normalized reciprocal rate versus time plot for Well B-15 with parameters found from history matching (right).

6.4.2 Well W-2-4

This well is a gas well from Woodford shale. From Fig. 6.10 it is obvious that Well W-2-4 is exhibiting Bilinear flow for a long enough time to consider for analysis. Bilinear flow is followed by Linear flow. At late time rate reduction occurs because of liquid loading. The reason for shut-in is not known. It might be a workover or some other maintenance job. Therefore, early parts of production were used in history matching to get an idea about the quality of reservoir and fracture job by estimating $k_F^{1/2}k_m^{1/4}$ and $k_m^{1/2}y_e$ (Fig. 6.11).

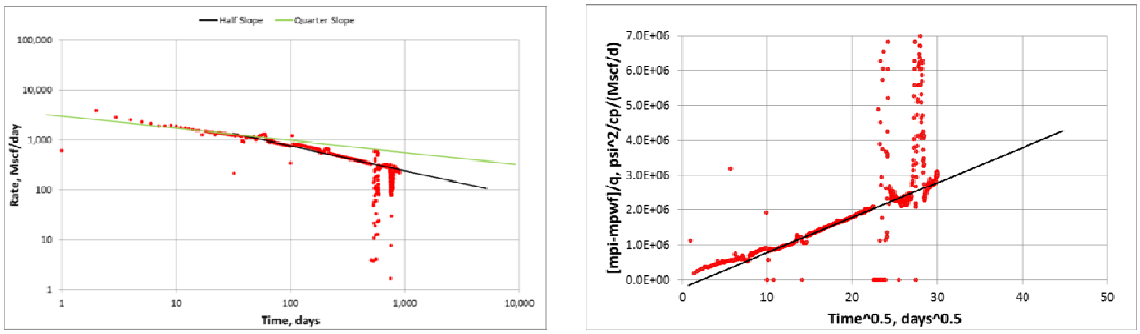

Fig. 6.10—Production history of Well W-2-4: Bilinear (quarter slope) followed by Linear (half slope) (left). Normalized reciprocal rate versus square root of time plot for Well W-2-4 (right).

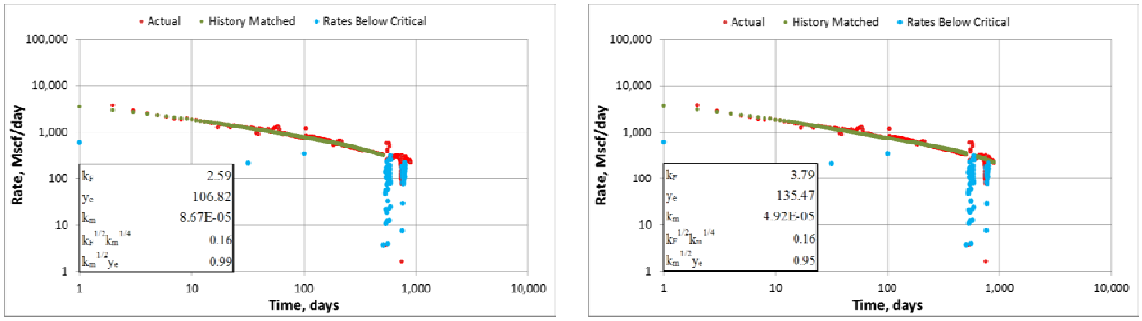

Fig. 6.11—Early part of the production (No shut-ins and less rate fluctuation is observed) was matched for Well W-2-4 (left). The whole production period of Well W-2-4 was matched for forecasting (right).

To do the forecasting, we again matched whole region's production history and found parameters were updated as shown in Fig. 6.11. Like in the previous well, the parameter group found for the early and whole period history matches are equal, with less than 5% error. Long term forecasting was done for this well with economic limit of 30 Mscf/D (Table 6.3). Conventional semi-log plot of rate versus time is shown in Fig. 6.12 for forecasting.

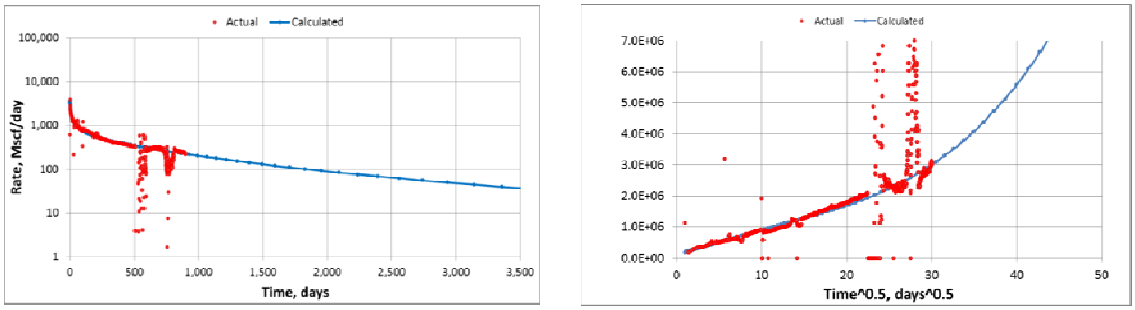

Fig. 6.12—Forecasting for Well W-2-4 with parameters found from history matching (left). Normalized reciprocal rate versus time plot for Well W-2-4 with parameters found from history matching (right).

6.4.3 Well F-3

This well is from Fayetteville Shale where most of the wells show long periods of Bilinear flow. The main distinguishing characteristic of Fayetteville shale from Barnett and Woodford shale is low initial pressure for reservoir. Fig. 6.13 shows characteristic log-log plot for this well, where Bilinear and Linear flow periods are observed.

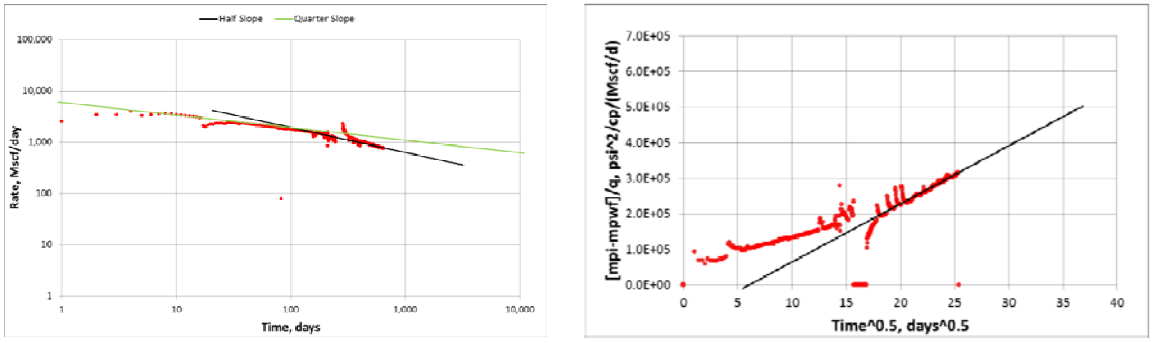

Fig. 6.13—Production history of Well F-3: Bilinear (quarter slope) followed by Linear (half slope) (left). Normalized reciprocal rate versus square root of time plot for Well F-3 (right).

This well is still in transient linear flow, and no sign of BDF was observed. Therefore, the whole production period was used in history matching to get an estimate for $k_F^{1/2}k_m^{1/4}$ and $k_m^{1/2}y_e$ groups of parameters (Fig. 6.14).

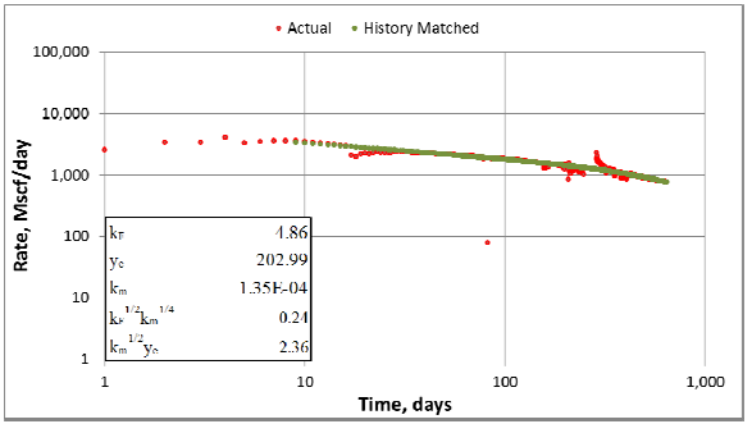

Fig. 6.14—Whole production period of Well F-3 was matched for forecasting. The well is still in transient flow and no effects of BDF were observed.

Long term forecasting was done with found parameters (Fig. 6.15) and the life of the well was calculated with other important parameters for economic limit of 30 Mscf/D as summarized in Table 6.3.

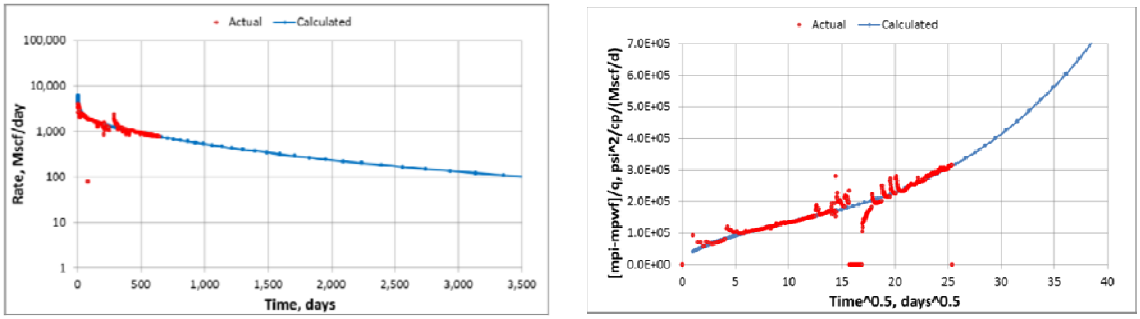

Fig. 6.15—Forecasting for Well F-3 with parameters found from history matching (left). Normalized reciprocal rate versus square root of time plot for Well F-3 with parameters found from history matching (right).

Table 6.2—Summary of completion and reservoir properties of wells used as field examples for 3 unknowns problem

	Parameters	Well B-15	Well W-2-4	Well F-3	Units
Hydraulic Fractures	Porosity	0.002	0.002	0.002	
	Width	0.04	0.04	0.04	ft
	Spacing	82	93	76	ft
Matrix	Porosity	0.06	0.0425	0.092	
	Thickness	300	250	300	ft
General	Perforated Length	2870	2232	3192	ft
	Area of Well Plane	1722000	1116000	1915200	ft2
	# of Macro-fractures	35	24	42	
	Rock Compressibility	0.000004	0.000004	0.000004	1/psi
	Water Compressibility	0.0000042	0.0000042	0.0000042	1/psi
	Initial Water Saturation	0.3	0.3	0.5	
	Initial Pressure	2950	3280	1759	psi
	Bottom-hole Pressure	480	300	200	psi
	Temperature	160	200	119	deg. F
	Gas Gravity	0.635	0.62	0.58	
	Langmuir Volume	96	NA	NA	scf/ton
	Langmuir Pressure	650	NA	NA	psi

Table 6.3—Summary of forecasting results for field examples				
	Well B-15	Well W-2-4	Well F-3	
OGIP (Total)	2.07 (Free) +1.65 (Adsorbed) =3.72	0.85 (Free)	2.18 (Free)	Bscf
Actual Production	1.31	0.40	0.80	Bscf
Economic Limit	30	30	30	Mscf/Day
Actual Production Time	3.24	2.51	1.79	Years
Remaining Life of the Well	12.71	8.40	16.79	Years
Recoverable Remaining	0.65	0.26	0.99	Bscf
EUR	1.96	0.65	1.79	Bscf
Recovery Factor	0.53	0.77	0.82	

6.5 Discussion of Results

Three different wells were analyzed in Section 6.4 from different shale plays. Most shale gas wells show Bilinear flow followed by Linear flow at early life. Considering the low gas prices dominating in the market at the moment, operators try to maintain the well at low costs. Therefore, having good information about the quality of the fracture job and size of the reservoir is crucial. Since running build up test is impractical in low permeability reservoirs, the only way to get information about the formation after fracturing job is production data analysis (PDA). The method described in this research handles this problem in an excellent way. By matching the early undisrupted production data, we can get $k_F^{1/2}k_m^{1/4}$ and $k_m^{1/2}y_e$ which gives us information about quality of the fracturing job and the production capacity of the well, respectively.

In the three wells which were analyzed above, only in Well B-15 the adsorption effect is included, since reliable information about Langmuir volume and pressure is

available only for Barnett shale at the moment. Although, contribution from desorbed gas to total production at the early transient life of shale gas wells is not significant, it is expected that adsorption has started affect the gas production in Barnett shale because of considerable reduction of reservoir pressure from its initial value. Fig. 6.16 shows the total and free gas production for Well B-15 with found parameters. It is clear that at late time adsorbed gas has significant impact on gas production.

Among the analyzed wells, Well W-2-4 has the lowest *OGIP* and obviously shorter life than the others. On the other hand, Well B-15 has the largest *OGIP* because of adsorbed gas. Adsorbed gas also affects the recovery factor. In order to get more gas from matrix surface by desorption, average pressure should be lowered as much as possible.

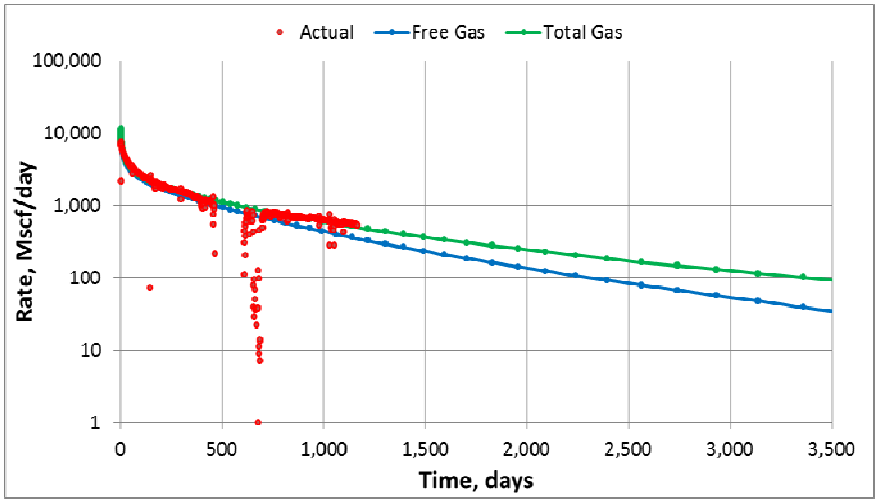

Fig. 6.16—Comparison of total and free gas production for Well B-15.

CHAPTER VII

CONCLUSIONS AND RECOMMENDATIONS

7.1 Conclusions

In this work a new method was proposed to analyze production performance of shale gas/oil wells. The method is based on linear flow equations in dual porosity reservoirs which were initially proposed by El-Banbi (1998). Following are the main conclusions drawn from this research.

- Asymptotic equations were analyzed for Dual Porosity system and important parameter group found for each region.
- It was concluded that there are two main transient flow regimes that can occur in the life of horizontally drilled and multi stage fractured shale gas/oil wells; bilinear and matrix linear flows.
- For both bilinear and linear flows there are two unknowns to be determined in order to match production of shale gas/oil well with Dual Porosity model.
- In case of known matrix permeability unique matches can be obtained if bilinear and linear flows occurred in the life of the shale gas/oil well.
- If boundary dominated flow is observed in the well production history then unique solutions can be obtained for matrix permeability and fracture half length by matching matrix linear and boundary dominated flow regimes at the same time.

- Asymptotic equations were derived for twelve different flow regimes in Triple Porosity model which was initially proposed by Al-Ahmadi (2010)
- Conditions to occur and nature of each flow region described briefly in this research.
- It was concluded that application of Triple Porosity model to match production of shale gas/oil wells will give non-unique solutions because of too many unknowns are needed to be found.
- A mathematical algorithm was developed to match production performance of shale gas/oil wells with Dual Porosity model.
- Desorption of gas at low pressures in shale gas wells is well handled with modified compressibility and material balance equations.
- Software was developed in Excel's VBA to implement the proposed algorithm.
- Different synthetic cases were checked on Software to prove robustness of proposed method.
- The method then applied to field examples. Excellent matches were obtained with field data.
- It was proved that the method proposed in this thesis is powerful tool to analyze the production of shale gas/oil well in short period of time (2-6 minutes in Excel) with high accuracy.

7.2 Recommendations for Future Work

It has been proved that Dual Porosity model is an excellent tool to describe production performance of shale gas/oil wells. Following are recommendation for future work.

- More work should be done on understanding the flow mechanism in Dual Porosity model.
- More synthetic cases should be analyzed to understand application of Dual Porosity model to shale oil wells.
- Type Curves can be generated to match production of shale gas/oil wells with Dual Porosity model.
- Triple Porosity model should be analyzed in detail to understand the occurrence of each flow regime with physical properties of well and reservoir.
- Software can be programmed to match production of shale gas/oil wells with Triple Porosity model once each flow regime is understood well. User should be aware of which flow regime to match with field data.

NOMENCLATURE

A_{cw} = cross sectional area to the flow, ft^2
c_f = formation compressibility, 1/psi
c_g = gas compressibility, 1/psi
c_{gd} = additional compressibility due to adsorbed gas, 1/psi
c_t = total compressibility, 1/psi
c_w = water compressibility, 1/psi
G = original gas in place, Mscf
G_p = cumulative production, Mscf
k_F = effective fracture permeability, md
k_m = matrix permeability, md
L_F = Fracture Spacing, ft
$m(p_i)$ = pseudo initial pressure, psi^2/cp
$m(p_{wf})$ = pseudo bottomhole flowing pressure, psi2/cp
$OGIP$ =original gas in place, Bscf
p = pressure, psi
$\overline{p}$ = average pressure, psi
p_L =Langmuir pressure, psi
p_{sc} = pressure at standard conditions, psi
q_{DL} = dimensionless rate
q_g = gas rate, Mscf/Day
S_{wi} = initial water saturation
SRV = stimulated reservoir volume
$t_{DA_{cw}}$ = dimensionless time
t_n = normalized time, days
T_{sc} = temperature at standard conditions, R
V_E = volume of gas adsorbed, scf/ton
V_L = Langmuir volume, scf/ton
V_{Lcuft} = Langmuir volume – calculated with grain density, scf/ft^3
V'_{Lcuf} = Langmuir volume – calculated with bulk density, scf/ft^3
x_e = perforated length, ft
y_e = fracture half length, ft

y_{eD} = dimensionless fracture half length
z = compressibility factor
z_{sc} = compressibility factor at standard conditions
z_i^* = modified compressibility factor at initial pressure
z^* = modified compressibility factor at average pressure

Greek Symbols

μ_g = gas viscosity, cp
φ = porosity
λ = interporosity coefficient
ρ_{sc} = gas density at standard conditions, gr/cm^3
$\overline{\rho}_g$ = gas density at average pressure, gr/cm^3
ρ_{bulk} = matrix density, gr/cm^3

REFERENCES

Abdassah, D. and Ershaghi, I. 1986. Triple-Porosity Systems for Representing Naturally Fractured Reservoirs. *SPE Formation Evaluation* **1** (2): 113-127. doi: 10.2118/13409-PA

Al-Ahmadi, H.A. 2010. A Triple Porosity Model For Fractured Horizontal Wells. M.Sc. Thesis, Texas A&M University, College Station, Texas.

Al-Ghamdi, A. and Ershaghi, I. 1996. Pressure Transient Analysis of Dually Fractured Reservoirs. *SPE Journal* (March) **1** (1): 93 – 100. doi: 10.2118/26959-PA.

Bello, R.O. and Wattenbarger, R.A. 2008. Rate Transient Analysis in Naturally Fractured Shale Gas Reservoirs. Paper SPE 114591-MS presented at the CIPC/SPE Gas Technology Symposium 2008 Joint Conference, Calgary, Alberta, Canada. doi: 10.2118/114591-MS.

Bello, R. O. and Wattenbarger, R. A. 2009. Modeling and Analysis of Shale Gas Production with a Skin Effect. Paper CIPC 2009-082 presented at the Canadian International Petroleum Conference, Calgary, Alberta, Canada, 16 – 18 June. doi: 10.2118/2009-082.

Bello, R.O. and Wattenbarger, R.A. 2010. Multi-Stage Hydraulically Fractured Horizontal Shale Gas Well Rate Transient Analysis. Paper SPE 126754-MS presented at the North Africa Technical Conference and Exhibition, Cairo, Egypt. doi: 10.2118/126754-MS.

Bumb, A.C., and McKee, C.R. 1986. Gas-Well Testing in the Presence of Desorption for Coal bed Methane and Devonian Shale. Paper SPE 15227-MS presented at SPE Unconventional Gas Technology Symposium, Louisville, Kentucky, 18-21 May. doi: 10.2118/15227-PA.

Cipolla, C.L. 2009. Modeling Production and Evaluating Fracture Performance in Unconventional Gas Reservoirs. *SPE Journal of Petroleum Technology* **61** (9). doi: 10.2118/118536-MS.

Dreier, J., Ozkan, E. and Kazemi, H. 2004. New Analytical Pressure-Transient Models to Detect and Characterize Reservoirs with Multiple Fracture Systems. Paper SPE 92039-MS presented at the SPE International Petroleum Conference in Mexico, Puebla, Mexico, 8 – 9 November. doi: 10.2118/92039-MS.

El-Banbi, A.H. 1998. Analysis of Tight Gas Wells, Ph.D. Dissertation. Texas A&M University, College Station, Texas.

Fraim, M. L. and Wattenbarger, R. A. 1987. Gas Reservoir Decline-Curve Analysis Using Type Curve with Real Gas Pseudopressure and Normalized Time. *SPE Form Eval* (December) **2** (4): 671 – 682. doi: 10.2118/14238-PA.

Freeman, C.M., Moridis, G.J., Ilk, D. et al. 2009. A Numerical Study of Performance for Tight Gas and Shale Gas Reservoir Systems. Paper SPE 124961-MS presented at the SPE Annual Technical Conference and Exhibition, New Orleans, Louisiana. doi: 10.2118/124961-MS.

Ilk, D., Currie, S.M., and Blasingame, T.A. 2010. Production Analysis and Well Performance Forecasting of Tight Gas and Shale Gas Wells. Paper SPE 139118-MS presented at the SPE Eastern Regional Meeting, Morgantown, West Virginia, USA. doi: 10.2118/139118-MS.

Jalali, Y. and Ershaghi, I. 1987. Pressure Transient Analysis of Heterogeneous Naturally Fractured Reservoirs. Paper SPE 16341-MS presented at the SPE California Regional Meeting, Ventura, California. doi: 10.2118/16341-MS.

Jordan, C.L., Smith, C.R., and Jackson, R.A. 2009. A Rapid and Efficient Production Analysis Method for Unconventional & Conventional Gas Reservoirs. Paper SPE 120737-MS presented at the Asia Pacific Oil and Gas Conference & Exhibition, Jakarta, Indonesia. doi: 10.2118/120737-MS.

Kazemi, H. 1969. Pressure Transient of Naturally Fractured Reservoirs with Uniform Fracture Distribution. *SPE Journal* **9** (4): 451– 462. doi: 10.2118/2156-PA.

King, G.R. 1990. Material Balance Techniques for Coal Seam and Devonian Shale Gas Reservoirs. Paper SPE 20730-MS presented at the SPE Annual Technical Conference and Exhibition, New Orleans, Louisiana. doi: 10.2118/20730-MS.

Lee, W.J. and Sidle R.E. 2010. Gas Reserves Estimation in Resource Play. Paper SPE 130102-MS presented at SPE Unconventional Gas Conference, 23-25 February 2010, Pittsburgh, Pennsylvania, USA. doi: 10.2118/130102-MS.

Luo, S., Neal, L., Arulampalam, P. et al. 2010. Flow Regime Analysis of Multi-Stage Hydraulically-Fractured Horizontal Wells with Reciprocal Rate Derivative Function: Bakken Case Study. Paper SPE 137514-MS presented at the Canadian Unconventional Resources and International Petroleum Conference, Calgary, Alberta, Canada. doi: 10.2118/137514-MS.

Mattar, L., Gault B., Morad K. et al. 2008. Production Analysis and Forecasting of Shale Gas Reservoirs: Case History-Based Approach. Paper SPE 119897-MS presented at the SPE Shale Gas Production Conference, Fort Worth, Texas, USA. doi: 10.2118/119897-MS.

Medeiros, F., Kurtoglu, B., Ozkan, E. et al. 2010. Analysis of Production Data from Hydraulically Fractured Horizontal Wells in Shale Reservoirs. *SPE Reservoir Evaluation & Engineering* **13** (3). doi: 10.2118/110848-PA.

Nobakht, M. and Mattar, L. 2010. Analyzing Production Data from Unconventional Gas Reservoirs with Linear Flow and Apparent Skin. Paper SPE 137454-MS presented at the Canadian Unconventional Resources and International Petroleum Conference, Calgary, Alberta, Canada. doi: 10.2118/137454-MS.

Nobakht, M., Mattar, L., Moghadam, S. et al. 2010. Simplified yet Rigorous Forecasting of Tight/Shale Gas Production in Linear Flow. Paper SPE 133615-MS presented at the SPE Western Regional Meeting, Anaheim, California, USA. doi: 10.2118/133615-MS.

Van Everdingen, A. F. and Hurst, W. 1949. The Application of the Laplace Transformation to Flow Problems in Reservoirs. *Trans*., AIME, **186**: 305 – 324.

Valko, P.P. 2010. A Better Way To Forecast Production From Unconventional Gas Wells. Paper SPE 134231-MS presented at SPE Annual Technical Conference and Exhibition, 19-22 September 2010, Florence, Italy. doi: 10.2118/134231-MS.

Van Kruysdijk, C.P.J.W. and Dullaert, G.M. 1989. A Boundary Element Solution of the Transient Pressure Response of Multiple Fractured Horizontal Wells. Paper presented at the 2nd European Conference on the Mathematics of Oil Recovery, Cambridge, England.

Warren, J.E. and Root, P.J. 1963. The Behavior of Naturally Fractured Reservoirs. *SPE Journal* **3** (3): 245 - 255. doi: 10.2118/426-PA.

Watson, A.T., Gatens III, J.M., Lee, W.J. et al. 1990. An Analytical Model for History Matching Naturally Fractured Reservoir Production Data. *SPE Reservoir Engineering* **5** (3). doi: 10.2118/18856-PS

Wattenbarger, R.A. 2001. Long-Term Linear Flow in Tight Gas Wells. Lecture Notes, Texas A&M University, College Station, TX.

APPENDIX A

DERIVATION OF ASYMPTOTIC EQUATIONS IN FIELD UNITS FOR DUAL POROSITY MODEL

Dimensionless Variables

$$t_{DA_{cw}} = \frac{0.00633\, k_F t}{\phi \mu c_t A_{cw}} \quad \text{.....(A-1)}$$

$$\frac{1}{q_{DL}} = \frac{k_F \sqrt{A_{cw}} \left[m(p_i) - m(p_{wf}) \right]}{1422\, q_g T} \quad \text{.....(A-2)}$$

$$\frac{1}{q_{DL}} = \frac{k_F \sqrt{A_{cw}} \left[p_i - p_{wf} \right]}{141.2 q_o B \mu} \quad \text{.....(A-3)}$$

$$\lambda = \frac{12}{L_F^2} \frac{k_m}{k_F} A_{cw} \quad \text{.....(A-4)}$$

$$\omega = \frac{\left[\phi V c_t \right]_F}{\left[\phi V c_t \right]_t} \quad \text{.....(A-5)}$$

$$y_{eD} = \frac{y_e}{\sqrt{A_{cw}}} \quad \text{.....(A-6)}$$

Region 1

$$q_{DL} = \frac{\sqrt{\omega}}{2\pi\sqrt{\pi}} t_{DA_{cw}}^{-1/2} \quad \text{.....(A-7)}$$

By substituting Eqs. A-1, A-2, and A-5 into Eq. A-7 we get equation for gas,

$$q_g = \frac{\left[m(p_i) - m(p_{wf}) \right]}{2844\pi\sqrt{\pi} T} \left[\frac{\mu}{0.00633} \right]^{1/2} A_{cw} \left\{ \left[\phi V c_t \right]_F^{1/2} k_F^{1/2} \right\} \frac{1}{t^{1/2}} \quad \text{.....(A-8)}$$

By substituting Eqs. A-1, A-3, and A-5 into Eq. A-7 we get equation for oil,

$$q_o = \frac{\left[p_i - p_{wf}\right]}{282.4\pi\sqrt{\pi}B}\left[\frac{1}{0.00633\mu}\right]^{1/2} A_{cw}\left\{\left[\phi V c_t\right]_F^{1/2} k_F^{1/2}\right\}\frac{1}{t^{1/2}} \quad \text{.....(A-9)}$$

Region 2

$$q_{DL} = \frac{\lambda^{1/4}}{10.133} t_{DA_{cw}}^{-1/4} \quad \text{..... (A-10)}$$

By substituting Eqs. A-1, A-2, and A-4 into Eq. A-10 we get equation for gas,

$$q_g = \frac{\left[m(p_i) - m(p_{wf})\right]}{14409.126T}\left[\frac{12\phi\mu c_t}{0.00633L_F^2}\right]^{1/4} A_{cw}\left\{k_F^{1/2} k_m^{1/4}\right\}\frac{1}{t^{1/4}} \quad \text{..... (A-11)}$$

By substituting Eqs. A-1, A-3, and A-4 into Eq. A-10 we get equation for oil,

$$q_o = \frac{\left[p_i - p_{wf}\right]}{1430.78B}\left[\frac{12\phi c_t}{0.00633L_F^2\mu^3}\right]^{1/4} A_{cw}\left\{k_F^{1/2} k_m^{1/4}\right\}\frac{1}{t^{1/4}} \quad \text{..... (A-12)}$$

Region 3

$$q_{DL} = \frac{1}{2\pi\sqrt{\pi}} t_{DA_{cw}}^{-1/2} \quad \text{..... (A-13)}$$

By substituting Eqs. A-1 and A-2 (For homogeneous case k_m would be used instead of k_F) into Eq. A-10 we get equation for gas,

$$q_g = \frac{\left[m(p_i) - m(p_{wf})\right]}{2844\pi\sqrt{\pi}T}\left[\frac{\phi\mu c_t}{0.00633}\right]^{1/2}\left\{k_m^{1/2} A_{cm}\right\}\frac{1}{t^{1/2}} \quad \text{..... (A-14)}$$

By substituting Eqs. A-1 and A-2 (For homogeneous case k_m would be used instead of k_F) into Eq. A-10 we get equation for oil,

$$q_o = \frac{\left[p_i - p_{wf}\right]}{282.4\pi\sqrt{\pi}B}\left[\frac{\phi c_t}{0.00633\mu}\right]^{1/2}\left\{k_m^{1/2}A_{cm}\right\}\frac{1}{t^{1/2}} \quad \text{..... (A-15)}$$

Region 4

$$q_{DL} = \frac{\left(\lambda/3\right)^{1/2} y_{eD}}{2\pi\sqrt{\pi}} t_{DA_{cw}}^{-1/2} \quad \text{..... (A-16)}$$

By substituting Eqs. A-1, A-2, A-4 and A-6 into Eq. A-16 we get equation for gas,

$$q_g = \frac{\left[m(p_i) - m(p_{wf})\right]}{2844\pi\sqrt{3\pi}T}\left[\frac{12\phi\mu c_t}{0.00633L_F^2}\right]^{1/2} A_{cw}\left\{k_m^{1/2}y_e\right\}\frac{1}{t^{1/2}} \quad \text{..... (A-17)}$$

By substituting Eqs. A-1, A-3, A-4 and A-6 into Eq. A-16 we get equation for oil,

$$q_o = \frac{\left[p_i - p_{wf}\right]}{282.4\pi\sqrt{3\pi}T}\left[\frac{12\phi c_t}{0.00633L_F^2\mu}\right]^{1/2} A_{cw}\left\{k_m^{1/2}y_e\right\}\frac{1}{t^{1/2}} \quad \text{..... (A-18)}$$

APPENDIX B

DERIVATION OF ASYMPTOTIC EQUATIONS IN FIELD UNITS FOR TRIPLE POROSITY MODEL

Dimensionless Variables

$$t_{DA_{cw}} = \frac{0.00633\, k_F t}{\phi \mu c_t A_{cw}} \quad \text{.....(B-1)}$$

$$\frac{1}{q_{DL}} = \frac{k_F \sqrt{A_{cw}}\left[m(p_i) - m(p_{wf})\right]}{1422\, q_g T} \quad \text{.....(B-2)}$$

$$\frac{1}{q_{DL}} = \frac{k_F \sqrt{A_{cw}}\left[p_i - p_{wf}\right]}{141.2 q_o B \mu} \quad \text{.....(B-3)}$$

$$\lambda_{A_{cw},Ff} = \frac{12}{L_F^2}\frac{k_f}{k_F} A_{cw} \quad \text{.....(B-4)}$$

$$\lambda_{A_{cw},fm} = \frac{12}{L_F^2}\frac{k_m}{k_F} A_{cw} \quad \text{.....(B-5)}$$

$$\omega_F = \frac{\left[\phi V c_t\right]_F}{\left[\phi V c_t\right]_t} \quad \text{.....(B-6)}$$

$$\omega_f = \frac{\left[\phi V c_t\right]_f}{\left[\phi V c_t\right]_t} \quad \text{.....(B-7)}$$

$$y_{eD} = \frac{y_e}{\sqrt{A_{cw}}} \quad \text{.....(B-8)}$$

Region 1

$$q_{DL} = \frac{\sqrt{\omega_1}}{2\pi\sqrt{\pi}} t_{DA_{cw}}^{-1/2} \quad \text{.....(B-9)}$$

By substituting Eqs. B-1, B-2, and B-6 into Eq. B-9, we get equation for gas,

$$q_g = \frac{\left[m(p_i) - m(p_{wf})\right]}{2844\pi\sqrt{\pi}T}\left[\frac{\mu}{0.00633}\right]^{1/2}\left\{\left[\phi Vc_t\right]_F^{1/2} k_F^{1/2}\right\} A_{cw} t^{-1/2} \quad \text{..... (B-10)}$$

By substituting Eqs. B-1, B-3, and B-6 into Eq. B-9, we get equation for oil,

$$q_o = \frac{\left[p_i - p_{wf}\right]}{282.4\pi\sqrt{\pi}B}\left[\frac{1}{0.00633\mu}\right]^{1/2}\left\{\left[\phi Vc_t\right]_F^{1/2} k_F^{1/2}\right\} A_{cw} t^{-1/2} \quad \text{..... (B-11)}$$

Region 2

$$q_{DL} = \frac{\left(\lambda_{12}\omega_2\right)^{1/4}}{10.133} t_{DA_{cw}}^{-1/4} \quad \text{..... (B-12)}$$

By substituting Eqs. B-1, B-2, B-4, and B-7 into Eq. B-12, we get equation for gas,

$$q_g = \frac{\left[m(p_i) - m(p_{wf})\right]}{14409.13T}\left[\frac{12\mu}{0.00633L_F^2}\right]^{1/4}\left\{\left[\phi Vc_t\right]_F^{1/2} k_f^{1/4} k_F^{1/2}\right\} A_{cw} t^{-1/4} \quad \text{..... (B-13)}$$

By substituting Eqs. B-1, B-3, B-4, and B-7 into Eq. B-12, we get equation for oil,

$$q_o = \frac{\left[p_i - p_{wf}\right]}{1430.78B}\left[\frac{12}{0.00633L_F^2\mu^3}\right]^{1/4}\left\{\left[\phi Vc_t\right]_F^{1/2} k_f^{1/4} k_F^{1/2}\right\} A_{cw} t^{-1/4} \quad \text{..... (B-14)}$$

Region 3

$$q_{DL} = \frac{\sqrt{\omega_2}}{2\pi\sqrt{\pi}} t_{DA_{cw}}^{-1/2} \quad \text{..... (B-15)}$$

By substituting Eqs. B-1, B-2, and B-7 into Eq. B-15, we get equation for gas,

$$q_g = \frac{\left[m(p_i) - m(p_{wf})\right]}{2844\pi\sqrt{\pi T}}\left[\frac{\mu}{0.00633}\right]^{1/2}\left\{\left[\phi V c_t\right]_f^{1/2} k_F^{1/2}\right\} A_{cw} t^{-1/2} \quad \text{..... (B-16)}$$

By substituting Eqs. B-1, B-3, and B-7 into Eq. B-15, we get equation for oil,

$$q_o = \frac{\left[p_i - p_{wf}\right]}{282.4\pi\sqrt{\pi B}}\left[\frac{1}{0.00633\mu}\right]^{1/2}\left\{\left[\phi V c_t\right]_f^{1/2} k_F^{1/2}\right\} A_{cw} t^{-1/2} \quad \text{..... (B-17)}$$

Region 4

$$q_{DL} = \frac{\lambda_{23}^{1/4}}{10.133} t_{DA_{cw}}^{-1/4} \quad \text{..... (B-18)}$$

By substituting Eqs. B-1, B-2, and B-5 into Eq. B-18, we get equation for gas,

$$q_g = \frac{\left[m(p_i) - m(p_{wf})\right]}{14409.13T}\left[\frac{12\phi\mu c_t}{0.00633 L_f^2}\right]^{1/4}\left\{k_m^{1/4} k_F^{1/2}\right\} A_{cw} t^{-1/4} \quad \text{..... (B-19)}$$

By substituting Eqs. B-1, B-3, and B-5 into Eq. B-18, we get equation for oil,

$$q_o = \frac{\left[p_i - p_{wf}\right]}{1430.78B}\left[\frac{12\phi c_t}{0.00633 L_f^2 \mu^3}\right]^{1/4}\left\{k_m^{1/4} k_F^{1/2}\right\} A_{cw} t^{-1/4} \quad \text{..... (B-20)}$$

Region 5

$$q_{DL} = \frac{\sqrt{\lambda_{23}/3}\, y_{eD}}{2\pi\sqrt{\pi}} t_{DA_{cw}}^{-1/2} \quad \text{..... (B-21)}$$

By substituting Eqs. B-1, B-2, B-5, and B-8 into Eq. B-21, we get equation for gas,

$$q_g = \frac{\left[m(p_i) - m(p_{wf})\right]}{2844\pi\sqrt{3\pi T}}\left[\frac{12\phi\mu c_t}{0.00633 L_f^2}\right]^{1/2}\left\{k_m^{1/2} y_e\right\} A_{cw} t^{-1/2} \quad \text{..... (B-22)}$$

By substituting Eqs. B-1, B-3, B-5, and B-8 into Eq. B-21, we get equation for oil,

$$q_o = \frac{\left[p_i - p_{wf}\right]}{282.4\pi\sqrt{3\pi}B}\left[\frac{12\phi c_t}{0.00633L_f^2\mu}\right]^{1/2}\left\{k_m^{1/2}y_e\right\}A_{cw}t^{-1/2} \quad \text{..... (B-23)}$$

Region 6

No asymptotic equation for this region was derived.

Region 7

$$q_{DL} = \frac{\sqrt{\lambda_{12}/3}\lambda_{23}^{1/4}y_{eD}}{10.133}t_{DA_{cw}}^{-1/4} \quad \text{..... (B-24)}$$

By substituting Eqs. B-1, B-2, B-4, B-5, and B-8 into Eq. B-24, we get equation for gas,

$$q_g = \frac{\left[m(p_i) - m(p_{wf})\right]}{14409.13T}\left[\frac{12\sqrt{12\phi\mu c_t}}{\sqrt{0.00633}L_F^2L_f}\right]^{1/2}\left\{k_m^{1/4}k_f^{1/2}y_e\right\}A_{cw}t^{-1/4} \quad \text{..... (B-25)}$$

By substituting Eqs. B-1, B-3, B-4, B-5, and B-8 into Eq. B-24, we get equation for oil,

$$q_o = \frac{\left[p_i - p_{wf}\right]}{1430.78B}\left[\frac{12\sqrt{12\phi c_t}}{\sqrt{0.00633}L_F^2L_f\mu^{3/2}}\right]^{1/2}\left\{k_m^{1/4}k_f^{1/2}y_e\right\}A_{cw}t^{-1/4} \quad \text{..... (B-26)}$$

Region 8

$$q_{DL} = \frac{\sqrt{(\lambda_{12}\omega_2)/3}y_{eD}}{2\pi\sqrt{\pi}}t_{DA_{cw}}^{-1/2} \quad \text{..... (B-27)}$$

By substituting Eqs. B-1, B-2, B-4, B-7, and B-8 into Eq. B-27, we get equation for gas,

$$q_g = \frac{\left[m(p_i) - m(p_{wf})\right]}{2844\pi\sqrt{3\pi}T}\left[\frac{12\mu}{0.00633L_F^2}\right]^{1/2}\left\{[\phi Vc_t]_f^{1/2} k_f^{1/2} y_e\right\}A_{cw}t^{-1/2} \quad \text{..... (B-28)}$$

By substituting Eqs. B-1, B-3, B-4, B-7, and B-8 into Eq. B-27, we get equation for oil,

$$q_o = \frac{\left[p_i - p_{wf}\right]}{282.4\pi\sqrt{3\pi}B}\left[\frac{12}{0.00633L_F^2\mu}\right]^{1/2}\left\{[\phi Vc_t]_f^{1/2} k_f^{1/2} y_e\right\}A_{cw}t^{-1/2} \quad \text{..... (B-29)}$$

Region 9

$$q_{DL} = \frac{\lambda_{12}^{1/4}\lambda_{23}^{1/8}}{10.133}t_{DA_{cw}}^{-1/8} \quad \text{..... (B-30)}$$

By substituting Eqs. B-1, B-2, B-4, and B-5 into Eq. B-30, we get equation for gas,

$$q_g = \frac{\left[m(p_i) - m(p_{wf})\right]}{14409.13T}\left[\frac{12\sqrt{12\phi\mu c_t}}{\sqrt{0.00633}L_F^2 L_f}\right]^{1/4}\left\{k_m^{1/8} k_f^{1/4} k_F^{1/2}\right\}A_{cw}t^{-1/8} \quad \text{..... (B-31)}$$

By substituting Eqs. B-1, B-3, B-4, and B-5 into Eq. B-30, we get equation for oil,

$$q_o = \frac{\left[p_i - p_{wf}\right]}{1430.78B}\left[\frac{12\sqrt{12\phi c_t}}{\sqrt{0.00633}L_F^2 L_f \mu^{7/2}}\right]^{1/4}\left\{k_m^{1/8} k_f^{1/4} k_F^{1/2}\right\}A_{cw}t^{-1/8} \quad \text{..... (B-32)}$$

Region 10

$$q_{DL} = \frac{\lambda_{12}^{1/4}}{10.133}t_{DA_{cw}}^{-1/4} \quad \text{..... (B-33)}$$

By substituting Eqs. B-1, B-2, and B-4 into Eq. B-33, we get equation for gas,

$$q_g = \frac{\left[m(p_i) - m(p_{wf})\right]}{14409.13T}\left[\frac{12\phi\mu c_t}{0.00633L_F^2}\right]^{1/4}\left\{k_f^{1/4}k_F^{1/2}\right\}A_{cw}t^{-1/4} \quad \text{..... (B-34)}$$

By substituting Eqs. B-1, B-3, and B-4 into Eq. B-33, we get equation for oil,

$$q_o = \frac{\left[p_i - p_{wf}\right]}{1430.78B}\left[\frac{12\phi c_t}{0.00633L_F^2\mu^3}\right]^{1/2}\left\{k_f^{1/4}k_F^{1/2}\right\}A_{cw}t^{-1/4} \quad \text{..... (B-35)}$$

Region 11

$$q_{DL} = \frac{\sqrt{\lambda_{12}/3}\,y_{eD}}{2\pi\sqrt{\pi}}t_{DA_{cw}}^{-1/2} \quad \text{..... (B-36)}$$

By substituting Eqs. B-1, B-2, B-4, and B-8 into Eq. B-36, we get equation for gas,

$$q_g = \frac{\left[m(p_i) - m(p_{wf})\right]}{2844\pi\sqrt{3\pi}T}\left[\frac{12\phi\mu c_t}{0.00633L_F^2}\right]^{1/2}\left\{k_f^{1/2}y_e\right\}A_{cw}t^{-1/2} \quad \text{..... (B-37)}$$

By substituting Eqs. B-1, B-3, B-4, and B-8 into Eq. B-36, we get equation for oil,

$$q_g = \frac{\left[m(p_i) - m(p_{wf})\right]}{2844\pi\sqrt{3\pi}T}\left[\frac{12\phi\mu c_t}{0.00633L_F^2}\right]^{1/2}\left\{k_f^{1/2}y_e\right\}A_{cw}t^{-1/2} \quad \text{..... (B-38)}$$

Region 12

$$q_{DL} = \frac{1}{2\pi\sqrt{\pi}}t_{DA_{cw}}^{-1/2} \quad \text{..... (B-39)}$$

By substituting Eqs. B-1 and B-2 into Eq. B-39, we get equation for gas,

$$q_g = \frac{\left[m(p_i) - m(p_{wf})\right]}{2844\pi\sqrt{\pi}T}\left[\frac{\phi\mu c_t}{0.00633}\right]^{1/2}\left\{k_F^{1/2}\right\}A_{cw}t^{-1/2} \quad \text{..... (B-40)}$$

By substituting Eqs. B-1 and B-3 into Eq. B-39, we get equation for oil,

$$q_o = \frac{\left[p_i - p_{wf}\right]}{282.4\pi\sqrt{\pi}B}\left[\frac{\phi c_t}{0.00633\mu}\right]^{1/2}\left\{k_F^{1/2}\right\}A_{cw}t^{-1/2} \quad \text{..... (B-41)}$$

APPENDIX C

LAPLACE SPACE SOLUTIONS FOR LINEAR DUAL POROSITY SYSTEM

El-Banbi (1998) showed differential equation after transformation to Laplace domain for linear flow as in Eq. C-1.

$$\frac{\partial^2 \overline{p_{DLF}}}{\partial y_D^2} - sf(s)\overline{p_{DLF}} = 0 \quad \text{.....(C-1)}$$

The *f(s)* function is a fracture function and is equal to unity for homogeneous reservoirs. El-Banbi (1998) showed fracture function for different type of reservoirs having linear flow. Table C-1 summarizes them. Fig. C-1 describes reservoir model for linear flow.

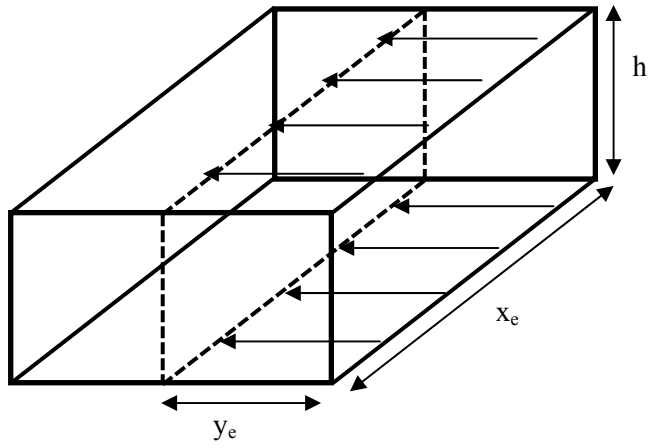

Fig. C-1—A sketch of horizontal well in SRV. The main flow is linear flow perpendicular to well plane.

Table C-1—Fracture function for different linear reservoir models

Model	f(s)
Homogeneous	1
PSS Dual Porosity	$f(s)=\frac{\omega(1-\omega)s+\lambda_{Acw}}{(1-\omega)s+\lambda_{Acw}}$
Transient Dual Porosity (slabs)	$f(s)=\omega+\frac{\lambda_{Acw}}{3s}\sqrt{\frac{3(1-\omega)s}{\lambda_{Acw}}}\tanh\left[\sqrt{\frac{3(1-\omega)s}{\lambda_{Acw}}}\right]$
Transient Dual Porosity (cylinder)	$f(s)=\omega+\frac{\lambda_{Acw}}{4s}\sqrt{\frac{8(1-\omega)s}{\lambda_{Acw}}}\frac{I_1\left[\sqrt{\frac{8(1-\omega)s}{\lambda_{Acw}}}\right]}{I_0\left[\sqrt{\frac{8(1-\omega)s}{\lambda_{Acw}}}\right]}$
Transient Dual Porosity (cubes)	$f(s)=\omega+\frac{\lambda_{Acw}}{5s}\left[\sqrt{\frac{15(1-\omega)s}{\lambda_{Acw}}}\coth\left[\sqrt{\frac{15(1-\omega)s}{\lambda_{Acw}}}\right]\right]$

Initial Conditions:

Initial conditions for both matrix and fracture are uniform pressure distribution throughput the matrix and fracture.

$$p_{DLM}\left(y_D, t_{DA_{cw}}=0\right)=0 \quad \text{.....(C-2)}$$

$$p_{DLF}\left(y_D, t_{DA_{cw}}=0\right)=0 \quad \text{.....(C-3)}$$

Inner Boundary Conditions:

Inner boundary conditions can be either constant rate (Eq. C-4) or constant bottomhole flowing pressure (Eq. C-5).

$$\left.\frac{\partial p_{DLF}}{\partial y_D}\right|_{y_D=0} = -2\pi \quad \text{.....(C-4)}$$

$$p_{DLF}\left(y_D = 0, t_{DA_{cw}}\right) = 1 \quad \text{.....(C-5)}$$

Outer Boundary Conditions:

Outer boundary conditions can be infinite (Eq. C-6), closed (Eq. C-7), and constant pressure boundary (Eq. C-8).

$$p_{DLF}\left(y_D \to \infty, t_{DA_{cw}}\right) = 0 \quad \text{.....(C-6)}$$

$$\left.\frac{\partial p_{DLF}}{\partial y_D}\right|_{y_D=\frac{y_e}{\sqrt{A_{cw}}}} = 0 \quad \text{.....(C-7)}$$

$$p_{DLF}\left(y_D = \frac{y_e}{\sqrt{A_{cw}}}, t_{DA_{cw}}\right) = 0 \quad \text{.....(C-8)}$$

Here constant rate and constant bottomhole flowing pressure conditions inner conditions with closed outer boundary condition problem will be solved in Laplace space.

Constant Rate Solution:

Initial, inner and boundary conditions in Laplace space will be as following, respectively.

$$\overline{p_{DLF}}\left(y_D\right) = 0 \quad \text{.....(C-9)}$$

$$\left.\frac{\partial \overline{p_{DLF}}}{\partial y_D}\right|_{y_D=0} = \frac{-2\pi}{s} \quad \text{..... (C-10)}$$

$$\left.\frac{\partial \overline{p_{DLF}}}{\partial y_D}\right|_{y_D=\frac{y_e}{\sqrt{A_{cw}}}} = 0 \quad \text{..... (C-11)}$$

It is well known that general solution to second order ordinary differential equation of the form like in Eq. A-1 is given by;

$$\overline{p_{DLF}} = A\cosh\left(\sqrt{sf(s)}y_D\right) + B\sinh\left(\sqrt{sf(s)}y_D\right) \quad \text{..... (C-11)}$$

In order to determine exact solution, inner and outer boundary conditions should be applied. By applying inner boundary conditions we get B.

$$\frac{\partial \overline{p_{DLF}}}{\partial y_D}\Big|_{y_D=0} = \frac{-2\pi}{s} = A\sqrt{sf(s)}\cosh\left(\sqrt{sf(s)}y_D\right) + B\sqrt{sf(s)}\sinh\left(\sqrt{sf(s)}y_D\right) \quad \text{..... (C-12)}$$

$$\frac{-2\pi}{s} = B\sqrt{sf(s)} \quad \text{..... (C-13)}$$

$$B = \frac{-2\pi}{s\sqrt{sf(s)}} \quad \text{..... (C-14)}$$

By applying outer boundary condition we get A.

$$\frac{\partial \overline{p_{DLF}}}{\partial y_D}\Big|_{y_D=0} = 0 = \frac{-2\pi}{s} = A\sqrt{sf(s)}\cosh\left(\sqrt{sf(s)}y_D\right) - \frac{2\pi}{s}\sinh\left(\sqrt{sf(s)}y_D\right) \quad \text{..... (C-15)}$$

$$A = \frac{2\pi}{s\sqrt{sf(s)}}\frac{\cosh\left(\sqrt{sf(s)}y_{De}\right)}{\sinh\left(\sqrt{sf(s)}y_{De}\right)} \quad \text{..... (C-16)}$$

Inserting *A* and *B* to Eq. C-11 gives this.

$$\overline{p_{DLF}} = \frac{2\pi}{s\sqrt{sf(s)}}\frac{\cosh\left(\sqrt{sf(s)}y_{De}\right)}{\sinh\left(\sqrt{sf(s)}y_{De}\right)}\cosh\left(\sqrt{sf(s)}y_D\right) + \frac{-2\pi}{s\sqrt{sf(s)}}\sinh\left(\sqrt{sf(s)}y_D\right) \quad \text{..... (C-17)}$$

At the wellbore condition (y_D=0) Eq. C-17 becomes;

$$\overline{p_{wDL}} = \frac{2\pi}{s\sqrt{sf(s)}}\frac{\cosh\left(\sqrt{sf(s)}y_{De}\right)}{\sinh\left(\sqrt{sf(s)}y_{De}\right)} \quad \text{..... (C-18)}$$

El-Banbi (1998) showed that this equation is equivalent to following.

$$\overline{p_{wDL}} = \frac{2\pi}{s\sqrt{sf(s)}}\left[\frac{1+\exp(-2\sqrt{sf(s)}y_{eD}}{1-\exp(-2\sqrt{sf(s)}y_{eD}}\right] \quad \text{..... (C-19)}$$

Constant Bottomhole Flowing Pressure Solution

Van Everdingen and Hurst (1949) showed that in Laplace domain constant rate and constant bottomhole flowing pressure cases are related with Eq. C-20.

$$\overline{p_{wDL}} \times q_{DL} = \frac{1}{s^2} \quad \text{..... (C-20)}$$

Form this solution can be obtained for constant bottomhole flowing pressure condition by using constant rate solution as El-Banbi (1998) showed.

$$\frac{1}{\overline{q_{DL}}} = \frac{2\pi}{s\sqrt{sf(s)}}\left[\frac{1+\exp(-2\sqrt{sf(s)}y_{eD}}{1-\exp(-2\sqrt{sf(s)}y_{eD}}\right] \quad \text{..... (C-21)}$$

APPENDIX D

DERIVATION OF EQUATIONS FOR ADSORBED GAS IN SHALE GAS RESERVOIRS

Derivation of Diffusivity Equation

Continuity equation for any system with "non-reactive rock" assumption is given below.

$$\nabla(\rho\vec{u}) = -\frac{\partial}{\partial t}(\phi\rho) \quad \text{.....(D-1)}$$

However, for coal bed methane and shale gas reservoirs gas is also adsorbed at matrix surface besides storage in pore volume. Thus, total gas volume in place would be;

$$OGIP_T = V_b\phi\rho_g + V_b\rho_{gsc}V_E^{'} \quad \text{.....(D-2)}$$

where $V_E^{'}$ is adsorbed gas volume in scf per cuft of the rock. Assuming that pore volume consists of immobile water with saturation S_{wi} and gas with saturation $(1\text{-}S_{wi})$ continuity equation becomes as following.

$$\nabla(V_b\rho\vec{u}) = \frac{\partial OGIP_T}{\partial t} = V_b\left(\frac{\partial(\phi\rho_g)}{\partial t} + \rho_{gsc}\frac{\partial V_E^{'}}{\partial t}\right) \quad \text{.....(D-3)}$$

$$\frac{\partial(\phi\rho_g)}{\partial t} = \phi(1-S_{wi})\frac{\partial\rho_g}{\partial t} + \rho_g\frac{\partial\phi}{\partial t} = \phi(1-S_{wi})\frac{\partial\rho_g}{\partial t} + \rho_g\left(\frac{\partial\phi}{\partial t} + S_{wi}\frac{\partial\phi}{\partial t}\right) \quad \text{.....(D-4)}$$

Where pore volume reduction is due to water expansion and rock volume expansion.

Darcy's Law:

$$\vec{u} = -\frac{k}{\mu}\nabla p \quad \text{.....(D-5)}$$

Combining Continuity equation (Eq. D-4) with Darcy's law (Eq. D-5) in a gas reservoir with connate water saturation of S_{wi} gives following equation.

$$\frac{1}{r}\frac{\partial}{\partial r}\left(r\frac{k}{\mu}\rho_g\frac{\partial p}{\partial r}\right)=(1-S_{wi})\phi\frac{\partial\rho_g}{\partial t}+\rho_g\frac{\partial\phi}{\partial t}+S_{wi}\rho_g\frac{\partial\phi}{\partial t}+\rho_{gsc}\frac{\partial V_E}{\partial t} \quad \text{.....(D-6)}$$

Given following definitions for density of gas and compressibility equations,

$$\rho_g=\frac{pM}{zRT} \quad \text{.....(D-7)}$$

$$c_g=\frac{1}{\rho_g}\frac{\partial\rho_g}{\partial p} \quad \text{.....(D-8)}$$

$$c_w=\frac{1}{V_p}\frac{\partial V_p}{\partial p} \quad \text{.....(D-9)}$$

$$c_f=\frac{1}{\phi}\frac{\partial\phi}{\partial p} \quad \text{..... (D-10)}$$

Eq. D-6 can be expanded to following.

$$\frac{1}{r}\frac{\partial}{\partial r}\left(r\frac{k}{\mu}\rho_g\frac{\partial p}{\partial r}\right)=(1-S_{wi})\phi\frac{\partial\rho_g}{\partial t}+c_f\phi\rho_g\frac{\partial p}{\partial t}+S_{wi}\phi c_w\rho_g\frac{\partial p}{\partial t}+\rho_{gsc}\frac{\partial V_E}{\partial t} \quad \text{..... (D-11)}$$

$$\frac{1}{r}\frac{\partial}{\partial r}\left(r\frac{k}{\mu}\frac{pM}{zRT}\frac{\partial p}{\partial r}\right)=$$
$$=\left[(1-S_{wi})\phi\frac{pM}{zRT}c_g+c_f\phi\frac{pM}{zRT}+S_{wi}\phi c_w\frac{pM}{zRT}+\rho_{gsc}\frac{V'_{Lcuft}\,p_L}{(p+p_L)^2}\right]\frac{\partial p}{\partial t} \quad \text{..... (D-12)}$$

Where $V'_{Lcuft\ is}$ in scf of gas per cuft of rock. By simplifying Eq. D-12 we get following,

$$\frac{1}{r}\frac{\partial}{\partial r}\left(r\frac{p}{\mu z}\frac{\partial p}{\partial r}\right)=\frac{p\phi}{zk}\left[(1-S_{wi})c_g+c_f+S_{wi}c_w+\rho_{gsc}\frac{V'_{Lcuft}\,p_L}{(p+p_L)^2}\frac{zRT}{Mp\phi}\right]\frac{\partial p}{\partial t} \quad \text{..... (D-13)}$$

Given the definition for pseudo pressure function,

$$m(p) = 2\int_{p_0}^{p} \frac{p}{z\mu} dp \quad \text{..... (D-14)}$$

$$\frac{dm}{d\xi} = \frac{2pdp}{z\mu d\xi} \quad \text{..... (D-15)}$$

and defining compressibility due to adsorbed gas as following,

$$c_{dg} = \rho_{gsc} \frac{V_L p_L}{(p+p_L)^2} \frac{zRT}{Mp\phi} = \frac{\rho_{gsc}}{\rho} \frac{V_L p_L}{(p+p_L)^2} \frac{1}{\phi} = \frac{B_g}{\phi} \frac{V'_{Lcuft} p_L}{(p+p_L)^2} \quad \text{..... (D-16)}$$

Eq. D-13 becomes,

$$\frac{1}{r}\frac{\partial}{\partial r}\left(r \frac{1}{2} \frac{2p}{z\mu} \frac{\partial p}{\partial r} \right) = \frac{\phi\mu}{2k} \frac{2p}{z\mu} \left[(1-S_{wi})c_g + c_f + S_{wi}c_w + c_{gd} \right] \frac{\partial p}{\partial t} \quad \text{..... (D-17)}$$

$$\frac{1}{r}\frac{\partial}{\partial r}\left(r \frac{\partial m(p)}{\partial r} \right) = \frac{\phi\mu}{k} \left[(1-S_{wi})c_g + c_f + S_{wi}c_w + c_{gd} \right] \frac{\partial m(p)}{\partial t} \quad \text{..... (D-18)}$$

By defining total compressibility as following,

$$c_t = (1-S_{wi})c_g + c_f + S_{wi}c_w + c_{gd} \quad \text{..... (D-19)}$$

Final form of diffusivity equation will be as below.

$$\frac{1}{r}\frac{\partial}{\partial r}\left(r \frac{\partial m(p)}{\partial r} \right) = \frac{\phi\mu c_t}{k} \frac{\partial m(p)}{\partial t} \quad \text{..... (D-20)}$$

Derivation of Material Balance Equation

Langmuir isotherm for adsorption is given as following.

$$V_E = V_L \frac{p}{(p_L + p)} \quad \text{..... (D-21)}$$

Unit of V_L in Eq. D-17 is in scf/ton. The useful form would be in scf of gas per cuft of rock. Thus, following conversion is done.

$$V_{Lcuft} = 0.031214 \rho_m V_L \quad \text{..... (D-22)}$$

On the other hand matrix density is usually is not measured. Most of the time bulk density of the rock is measured and reported from core or well log reports.

$$\rho_b = \rho_m (1 - \phi) + \rho_f \phi \quad \text{..... (D-23)}$$

Assuming that porosity in shales is very low (4-15 %), following approximation can be done.

$$\rho_m = \frac{\rho_b}{(1 - \phi)} \quad \text{..... (D-24)}$$

$$V'_{Lcuft} = 0.031214 \rho_b V_L \quad \text{..... (D-25)}$$

Adsorbed gas in place (AGIP) at any pressure p will be;

$$AGIP = V_b (1 - \phi) V_{Lcuft} \frac{p}{(p + p_L)} = V_b (1 - \phi)(0.031214 \rho_m V_L) \frac{p}{(p + p_L)} \quad \text{..... (D-26)}$$

$$AGIP = V_b V'_{Lcuft} \frac{p}{(p + p_L)} = V_b (0.031214 \rho_b V_L) \frac{p}{(p + p_L)} \quad \text{..... (D-27)}$$

Total gas originally in place will be;

$$OGIP_T = V_b\left[\frac{\phi(1-S_{wi})}{B_{gi}} + V'_{Lcuft}\frac{p_i}{(p_i+p_L)}\right] \quad \text{..... (D-28)}$$

Material Balance Equation for volumetric gas reservoirs with adsorbed gas at the surface of matrix will be as below.

$$G_p = V_b\left\{\left[\frac{\phi(1-S_{wi})}{B_{gi}} + V'_{Lcuft}\frac{p_i}{(p_i+p_L)}\right] - \left[\frac{\phi(1-S_w)}{B_g} + V'_{Lcuft}\frac{p}{(p+p_L)}\right]\right\} \quad \text{..... (D-29)}$$

$$G_p = \frac{V_b\phi}{T}\left(\frac{T_{sc}}{p_{sc}}\right)\left\{\begin{array}{l}\left[\frac{p_i(1-S_{wi})}{z_i} + \frac{T}{\phi}\left(\frac{p_{sc}}{T_{sc}}\right)V'_{Lcuft}\frac{p_i}{(p_i+p_L)}\right] - \\ -\left[\frac{p(1-S_w)}{z} + \frac{T}{\phi}\left(\frac{p_{sc}}{T_{sc}}\right)V'_{Lcuft}\frac{p}{(p+p_L)}\right]\end{array}\right\} \quad \text{..... (D-30)}$$

By using the compressibility equation proposed by King (1990) it becomes;

$$z^* = \frac{z}{(1-S_w) + \frac{zT}{\phi}\left(\frac{p_{sc}}{T_{sc}}\right)V'_{Lcuft}\frac{1}{(p+p_L)}} \quad \text{..... (D-31)}$$

$$G_p = \frac{V_b\phi}{T}\left(\frac{T_{sc}}{p_{sc}}\right)\left[\frac{p_i}{z_i^*} - \frac{p}{z^*}\right] \quad \text{..... (D-32)}$$

In order to get equation of a straight line similar to conventional material balance equation following simplifications in equation were done.

$$G_p = \frac{V_b\phi}{T}\left(\frac{T_{sc}}{p_{sc}}\right)\left(\frac{p_i}{z_i^*}\right)\left[1 - \frac{z_i^*}{p_i}\frac{p}{z^*}\right] \quad \text{..... (D-33)}$$

$$G_p = \frac{V_b\phi}{T}\left(\frac{T_{sc}}{p_{sc}}\right)\left(\frac{p_i}{z_I}\right)\left[(1-S_{wi}) + \frac{z_iT}{\phi}\left(\frac{p_{sc}}{T_{sc}}\right)V'_{Lcuf}\frac{1}{(p_i+p_L)}\right]\left[1 - \frac{z_i^*}{p_i}\frac{p}{z^*}\right] \quad \text{..... (D-34)}$$

Free gas in place (*FGIP*) will be;

$$FGIP = \frac{V_b \phi}{T}\left(\frac{T_{sc}}{p_{sc}}\right)\left(\frac{p_i}{z_I}\right)\left(1 - S_{wi}\right) \quad \text{..... (D-35)}$$

Adsorbed gas in place (*AGIP*) will be;

$$AGIP = V_b V'_{Lcuft}\frac{p}{\left(p + p_L\right)} \quad \text{..... (D-36)}$$

Material balance equation will be;

$$G_p = \left(FGIP + AGIP\right)\left[1 - \frac{z_i^*}{p_i}\frac{p}{z^*}\right] \quad \text{..... (D-37)}$$

$$G_p = OGIP_T\left[1 - \frac{z_i^*}{p_i}\frac{p}{z^*}\right] \quad \text{..... (D-38)}$$

Final form of material balance equation which resembles straight line equation will be;

$$\frac{p}{z^*} = \frac{p_i}{z_i^*}\left[1 - \frac{G_p}{OGIP_T}\right] \quad \text{..... (D-39)}$$

VITA

Name: Orkhan Samandarli

Address: Shahbazi kuc. Ev 100 Menzil 10
Yasamal Rayonu, Baki, AZ 1165
AZERBAIJAN

Email Address: orkhan.samandarli@gmail.com

Education: B.S., Petroleum and Natural Gas Engineering, Middle East Technical University, Ankara, TURKEY, 2009

M.S., Petroleum Engineering, Texas A&M University, College Station, USA, 2011